Twenty-Sixth Annual

Daniel T. Watts

Research Poster Symposium

A Scientific Forum for the VCU Community

October 27-29, 2009

Hermes A. Kontos
Medical Sciences Building
Virginia Commonwealth University

In Memory of

Daniel T. Watts
(1917-1994)

The Daniel T. Watts Poster Research Symposium is named in honor of Daniel T. Watts, former Dean of the School of Basic Health Sciences and Graduate Studies who passed away in 1994 at the age of 77. Dean Watts was a nationally recognized pharmacologist. In 1946 and 1947, he worked on projects to determine human tolerance to the acceleration forces experienced in aviators' ejection seats. From 1947 to 1953, he taught pharmacology at the University of Virginia. He served as chair of Pharmacology at West Virginia University from 1953 to 1966 before coming to the Medical College of Virginia in 1966, continuing to serve as Dean as the institution was incorporated into Virginia Commonwealth University in 1968. Dean Watts held interests in intercollegiate athletics as well as biomedical research and graduate education and represented the University in that capacity. He retired as Dean, Basic Health Sciences in 1982.

During his tenure at this institution he established the foundation of the research enterprise in basic health sciences that continues today. His legacy continues both in the breadth of research and educational programs particularly the development of Ph.D. training. The growth of research and graduate training build on the pioneering efforts of John C. Forbes and C.C. Clayton, establishing the traditions which continue today. Shortly after his retirement, the Poster Symposium was initiated as a tribute to Dr. Watts and his effort, serving as an illustration of the research and development for continuing generations of life/health science researchers.

Daniel T. Watts

Session I - Tuesday, October 27, 2009

Presentations: A-01 to A-37

Session II – Wednesday, October 28, 2009

Presentations: B-01 to B-36

Session III - Thursday, October 29, 2009

Presentations: C-01 to C-39

Tuesday, October 27

A-01 Wilm's Tumor-1 Expression In Glioblastoma Cells Fosters Cell Survival: Identifying Underlying Mechanisms.
Archana Chidambaram, Nitya Moothathu, Catherine Dumur, Helen Fillmore and William C. Broaddus
Anatomy and Neurobiology

A-02 In-Vitro Binding Of 5-Hydroxymethylfurfural (5-HMF) To Human Hemoglobin (Hb) And Serum Albumin (HSA)
Taghrid Obied, M.S., Jürgen Venitz, MD, Ph.D.
Pharmaceutics

A-03 Metabolism Of 5-Hydroxymethylfurfural (5-Hmf) In Human Hepatic Cytosol By Aldehyde Dehydrogenase (Aldh) And Alcohol Dehydrogenase (Adh)
Taghrid Obied, M.S., Jürgen Venitz, MD, Ph.D.
Pharmaceutics

A-04 5-Hydroxymethylfurfural (5-Hmf) Metabolism In Hepatic Cytosol From Mice, Rats, Dogs, And Humans
Taghrid Obied, M.S., Jürgen Venitz, MD, Ph.D.
Pharmaceutics

A-05 Focal Adhesion Kinase (FAK) Regulates Oligodendrocyte Process Dynamics And Remodeling
A.D. Forrest, B. Fuss
Anatomy and Neurobiology

A-06 Tumorigenicity And Angiogenic Protein Profiles Of Glioblastoma Cells With Altered MMP-1 Expression Levels
Nicholas A. Pullen (1), Monika Anand (2), Helen L. Fillmore
The Harold F. Young Neurosurgical Center and (1) Department of Anatomy & Neurobiology, (2) Department of Biochemistry & Molecular Biology

A-07 Glioblastoma Cell Motility Is Mediated Through A Nitric Oxide-MMP-1 Axis
Nicholas A. Pullen (1) and Helen L. Fillmore, Ph.D.
The Harold F. Young Neurosurgical Center and (1) Department of Anatomy & Neurobiology

A-08 Identification Of A Two Component Regulatory System Of The Periodontal Pathogen, *T.Denticola*: Insight Into The Molecular Mechanisms Of Environmental Adaptation During The Development Of Periodontal Disease
Juni Sarkar[1], Jesse Frederick[2] and Dr. Richard Marconi[2,]
Integrative Life Sciences

A-09 Second Hand Smoke Induced Molecular Effects In Pup Rat Brain
Brian F. Fuller and Andrew K. Ottens
Anatomy and Neurobiology

A-10 Rescue Of Visual Cortex Plasticity Deficits In A Mouse Model Of Fetal Alcohol Syndrome Using A Phosphodiesterase Type 1 Inhibitor
Crystal Lantz
Anatomy and Neurobiology

A-11 Effects Of Stimulating Innate Immune Receptors In Ovarian Cancer Cell Lines
Danielle N. Schramm, Sandrine Lépine, Jessica K. Bell
Biochemistry and Molecular Biology

A-12 The Role Of Threonine 260 In Mycobacterium Tuberculosis Lanosterol 14α-Demethylase Catalysis
Gareth K. Jennings1, Anuja Modi1, James Terner2 and John C Hackett1
Medicinal Chemistry

A-13 Biochemical And Structural Characterization Of Innate Immunity Kinase Complex Proteins
R. Jason Call, R. Ghirlando, J.K. Bell
Biochemistry and Molecular Biology

A-14 The Role Of Stat1 In Regulation Of Mitochondrial Gene Expression
Jennifer D Sisler, Magdalena Szelag, Dr. Andrew Larner
Biochemistry and Molecular Biology

A-15 Investigating Genetic And Environmental Contributions To The Relationship Between Church Attendance And Alcohol Dependence
Jia Yan, Fazil Aliev, Kenneth S. Kendler, Steven H. Aggen, Laura Bierut, and Danielle M. Dick, with SAGE collaborators
Human and Molecular Genetics

A-16 A Calcineurin-Dependent Loss And An Overgrowth Of Dendritic Spines Following Lateral Brain Injury In Rat
John N. Campbell(1), Brian Low(2), David Register(3), & Severn B. Churn(1-4)
Anatomy & Neurobiology(1), Physiology & Biophysics(2), Neurology(3), and Pharmacology & Toxicology(4)

A-17 Production And Charecterization Of Silencer Of Ikk-Epsilon
Jonathan L. Forbes, R. Jason Call & Dr. Jessica Bell
Biochemistry and Molecular Biology

A-18 Potential Of Mean Force Reconstruction For High-Selectivity Substrate Binding At Human Aromatase.
Justin E. Elenewski and John C Hackett
Medicinal Chemistry

A-19 Theoretical Studies Of Lanosterol 14α-Demethylase Catalysis: Mechanistic Insight Into P450-Catalyzed C-C Bond Cleavage
Kakali Sen and John C Hackett
Medicinal Chemistry

A-20 Autotaxin (Atx) Regulates The Appearance Of Mbp-Positive Oligodendrocytes In The Hindbrain Of The Zebrafish
Larra M. Yuelling1, Kevin R. Lynch3, James A. Lister2, Babette Fuss1 1Department of Anatomy and Neurobiology and 2Human and Molecular Genetics, and 3Department of Pharmacology, University of Virginia Medical Center
Anatomy and Neurobiology

A-21 Dynamics Of Substrate Interactions In Trna (M1g37) Methyltransferase; Implications For Drug Discovery
Maria Palesis, John Hackett, and Walter M. Holmes
Pharmacology and Toxicology

A-22 Is Tyk2 A Critical Regulator Of Obesity?
Derecka Marta, Gornicka A, Larner A
Biochemistry and Molecular Biology

A-23 Synthesis, Screening And Cocrystalization Of Adenosine-Based Inhibitors For Ermc' And Ksga
Mr. Matthew R. Baker, Dr. Keith C. Ellis, Dr. Fiek N. Musayev, and Dr. Jason P. Rife
Medicinal Chemistry

A-24 Epidermal Growth Factor Mediated Up-Regulation Of Mmp-1 In Glioma
Monika Anand(1) and Helen L Fillmore (2)
Biochemistry and Molecular Biology

A-25 Investigation Of Various Endogenous Blood Plasma Phospholipids, Glycerides And Cholesterols That Contribute To Matrix Effects In Lc/Ms/Ms
Omnia A. Ismaiel, Tianyi Zhang, Rand G. Jenkins, H. Thomas Karnes
Pharmaceutics

A-26 Expression Of AMP-Activated Kinase (AMP Kinase) And Inactivation Of Myosin Light Chain (MLC) Kinase By AMP Kinase Determines The Magnitude Of Smooth Muscle Contraction In Different Regions Of The Stomach.
O. Al-Shboul, S. Mahavadi, C. Strane and K.S. Murthy
Physiology and Biophysics

A-27 Acute Ethanol-Responsive Gene Expression In Fyn Kinase Knockout Mouse Prefrontal Cortex And Nucleus Accumbens
Sean P. Farris and Michael F. Miles
Pharmacology and Toxicology

A-28 Adam10 Transgenic Mice Serve As A Novel Model For Studying The Role Of Mdscs In Tumor Metastasis
Sheinei Saleem, David Gibb, Daniel Conrad, Laura Graham, Harry Bear
Microbiology and Immunology

A-29 Expression Of Matrix Metalloproteinase-2 After Olfactory Nerve Transection
Bakos, S.R. Costanzo, R.M.
Physiology and Biophysics

A-30 Cotranslational Folding And Oligomerization Of HSV Gb In The Endoplasmic Reticulum
S.J. Dollery, M.G. Delboy, A.V. Nicola
Microbiology and Immunology

A-31 Expression Pattern Of High Molecular Weight- Melanoma Associated Antigen (HMW-MAA) In Breast Cancer Stem Cells
Stuti Agarwal, Maciej Kmieciak, Soldano Ferrone, Masoud H. Manjili
Microbiology and Immunology

A-32 Substrate Specificity Of Arm/Rmt Methyltransferases
Tamara Zarubica, H. Tonie Wright, Jason P. Rife
Biochemistry and Molecular Biology

A-33 Bioluminescent Osteoclasts: Characterization Of Mtrap-Luciferase Transgenic Mice In Vivo And In Vitro
Tamer M. Hadi, Mark A. Subler, Greg E. Campbell, Christina Boykin, Jolene J. Windle
Human and Molecular Genetics

A-34 In Vitro Manipulation Of Adult Human Neural Stem/Neural Progenitor Cells Isolated From Neurosurgical Resection For Use In Cell Replacement Therapy Following Traumatic Brain Injury.
Wendy Reid, Martin Graf, Kathryn Holloway, Helen Fillmore, Dong Sun.
Neurosurgery

A-35 Tissue Specific Microrna Target Prediction In Humans
William T. Budd Zendra Zehner Nihar Sheth
Center for the Study of Biological Complexity

A-36 Opposing Roles For Lyn And Fyn Kinases In Mast Cell, Basophil And Macrophage Igg Receptor Signaling
Yves T. Falanga and John J. Ryan
Biology (Integrative Life Sciences)

A-37 Design Synthesis And Interaction Studies Of Dual, Direct, Non-Saccharide, Allosteric Modulators Of Factor Xa And Thrombin
Preetpal Singh Sidhu*, Qibing Zhou, and Umesh R. Desai.
Medicinal Chemistry

Wednesday, October 28

B-01 KLF2 Is Required For Normal Heart Development In Mice
Aditi Chiplunkar, Tina Lung, Dr. Jack Haar, Dr. Joyce Lloyd
Human and Molecular Genetics

B-02 Effects Of Hemoglobin-Based Oxygen Carriers (Hbocs) On Nitric Oxide (NO) Levels In The Spinotrapezius Muscle And Mesentery Of The Rat
Andrew T. Yannaccone, Helena Carvalho and Roland N. Pittman
Physiology and Biophysics

B-03 The Anaplasma Phagocytophilum-Occupied Vacuole Selectively Recruits Rab Gtpases
Bernice Huang, Marci A. Scidmore and Jason A. Carlyon
Microbiology and Immunology

B-04 Regulation Of Pre-Mrna Splicing By Group VIA Phospholipase A2 (Ipla2)
Bhargavi Emani, Xiaoyong Lei, Sasanka Ramanadham, and Suzanne E. Barbour
Biochemistry and Molecular Biology

B-05 Microcirculatory Effects Of Hemorhage And Rescucitation On Tissue Oxygenation Using A Hemoglobin-Based Oxygen Carrier
Bjorn K Song, Michael D Connery1, P. Moon-Massat, Aleksander S. Golub, Roland N Pittman.
Physiology and Biophysics

B-06 ADAM10 Critically Regulates B Cell Development By Activating Notch2 Signaling
David R. Gibb, Mohey El Shikh, Dae-Joong Kang, Warren J. Rowe, Rania El Sayed, Joanna Cichy, Hideo Yagita, John G. Tew, Peter J. Dempsey*, Howard C. Crawford*, Daniel H. Conrad*
Microbiology and Immunology

B-07 Opioid Tapering In Children: A Critical Review Of The Literature
Deborah Fisher
Pediatric Nursing

B-08 Bacterial Cpgs Synergize With Il-15 To Enhance Cd8+ T Cell Function
Derek Hambright, Dustin Cobb, Siqi Guo, and Ronald B. Smeltz
Microbiology and Immunology

B-09 T-Bet Dependent Regulation Of Cd4 Th17 Cells During Trypanosoma Cruzi Infection
Drew Cobb, Derek Hambright, and Ronald B. Smeltz
Microbiology and Immunology

B-10 Computational Studies: Binding Mode Of Alpha2A-Adrenoceptors
Genevieve S. Alley, Philip D. Mosier, Malgorzata Dukat
Medicinal Chemistry

B-11 Evidence For Genes On Chromosome 2 Contributing To A Variety Of Psychiatric Outcomes
Jacquelyn Meyers, Danielle M. Dick, Fazil Aliev, John Nurnberger Jr., John Kramer, Sam Kuperman, Bernice Porjesz, Jay Tischfield, Howard Edenberg, Tatiana Foroud, Marc Schuckit, Alison Goate, Victor Hesselbrock & Laura Bierut
Human and Molecular Genetics

B-12 Adjuvant Potential Of Double Stranded RNA
James D. Marion and Jessica K. Bell
Biochemistry and Molecular Biology

B-13 CB1 Agonist-Like CNS Effects Following Prolonged Inhibition Of Monoacylglycerol Lipase (MAGL) Undergo Tolerance
Joel E. Schlosburg, Divya Ramesh, James J. Burston, Steven G. Kinsey, Lamont Booker, Rehab A. Abdullah, Jonathan Z. Long, Dana E. Selley, Benjamin F. Cravatt and Aron H. Lichtman
Pharmacology and Toxicology

B-14 Faah Inhibition Reverses Lipopolysaccharide-Induced Mechanical Allodynia
Lamont Booker1, Steven G. Kinsey1, Kay Ahn2, Benjamin F. Cravatt3, Aron H. Lichtman1
1Department of Pharmacology and Toxicology, 2Pfizer Global Research and Development, Groton, CT, USA 3The Skaggs Institute, The Scripps Research Institute, La Jolla, CA, USA

B-15 Adenovirus Infection Alters Metabolism In Adipose And Hepatic Tissues
Marianna Sukholutsky, W. Palmer Wilkins III, and Suzanne E. Barbour
Biochemistry and Molecular Biology

B-16 Properties Of The Icp0 Tegument Protein Of Hsv-1
Mark G. Delboy, Carlos R. Siekavizza-Robles, and Anthony V. Nicola
Microbiology and Immunology

B-17 Inside-Out Signaling Of Estradiol-Mediated S1p Export From Breast Cancer Cells
Masayuki Nagahashi(1,2), Roger H. Kim(1), Jeremy C. Allegood(2), Poulami Mitra(2), Subramaniam Ramachandran(1,2), Kuzhuvelil B. Harikumar(2), Nitai C. Hait(2), Sheldon Milstien(2), Sarah Spiegel(2) and Kazuaki Takabe(1,2)
(1) Division of Surgical Oncology, (2) Department of Biochemistry and Molecular Biology and the Massey Cancer Center

B-18 Effect Of Serum On Staphylococcus Aureus Biofilm Formation
Nabil Abraham, Kimberly Jefferson
Microbiology and Immunology

B-19 The Application Of Luminescent In Vivo Imaging Using 4t1-Luc2 Cells To Determine The Best Model For Breast Cancer Progression And Metastasis
Omar Rashid1, Masayuki Nagahashi1,2, Subramaniam Ramachandran1,2, Sheldon Milstien2, Sarah Spiegel2, and Kazuaki Takabe1,2
1Division of Surgical Oncology, 2Department of Biochemistry and Molecular Biology and the Massey Cancer Center
Surgical Oncology

B-20 Quantitative Structure - Pharmacokinetic Relationships (Qspkr) Of Beta-Adrenergic Receptor Ligands (Barl) In Humans
Prajakta Badri, Ph.D. Candidate, Jürgen Venitz, MD, Ph.D.
Pharmaceutics

B-21 In Vitro Prediction Of Regional Drug Deposition From Dry Powder Inhalers
Renish R Delvadia1, Peter R Byron1, P. Worth Longest2, and Michael Hindle1
Pharmaceutics

B-22 On The Association Of Body Mass Index And Depression In A Population Based Sample Of Twins.
Roseann E. Peterson, B.A., Hermine H. Maes, Ph.D., Lindon J. Eaves, Ph.D., D.Sc.
Human and Molecular Genetics

B-23 Fullerene C70 Derivatives Inhibit Mast Cell Mediated Airway Inflammation And Eosinophilia Associated With Chronic Asthma
Sarah K. Norton*, Anthony Dellinger#, Robert Lenk#, Zhiguo Zhou#, Daniel H. Conrad*, Christopher L. Kepley# *Department of Microbiology and Immunology #Luna Innovations Incorporated, Danville, VA 24541
Microbiology and Immunology

B-24 Molecular Basis Of Reduced Pyridoxine 5'-Phosphate Oxidase Catalytic Activity In Neonatal Epileptic Encephalopathy Disorder
Sayali S. Karve, Faik N. Musayev, Mohini S. Ghatge, Martin K. Safo
Medicinal Chemistry

B-25 Novel Substrates For The Human Serotonin Transporter: Search For A New Class Of Antidepressants Based On The Channel Properties Of Hsert.
Stefania Averaimo, Hideki Iwamoto, Ernesto Solìs, Lynette Daws and Louis J DeFelice
Physiology and Biophysics

B-26 Scribble As A Possible MAP Kinase Binding Partner
Steven Christofakis, Hiroshi Miyazaki, M.D., Ph.D.
Philips Institute, School of Dentistry

B-27 LPA-Induced Gastric Cancer Cell Proliferation Is Mediated By Sphingosine Kinase-1.
Subramaniam Ramachandran1,2, Dai Shida2, Masayuki Nagahashi1,2, Sheldon Milstien2, Sarah Spiegel2 and Kazuaki Takabe1,2
Surgery

B-28 Restoration Of Chemo/Radioresistance And Double-Strand Break Repair Proficiency By Wild-Type But Not Endonuclease-Deficient Artemis
Susovan Mohapatra, Lawrence F. Povirk, Imran Khan, Misako Kawahara-Stillion and Steven M. Yannone
Pharmacology and Toxicology

B-29 Investigation Of A Solvent/Anti-Solvent Crystallization Process For Albuterol Sulfate
Swati Agrawal, Michael Hindle
Pharmaceutics

B-30 Association Of Chromosome 20 Loci With Categorical Diagnoses And Clinical Dimensions Of Schizophrenia In The Irish Study Of High Density Schizophrenia Families
Bigdeli TB et al
Human and Molecular Genetics

B-31 Tie1-Tie2 Interactions Mediate Functional Differences Between Angiopoietin Ligands
Tom C.M. Seegar, Becca Eller, Dorothea Tzvetkova-Robev, Momchil V. Kolev, Scott C. Henderson, Dimitar B. Nikolov, and William A. Barton
Biochemistry and Molecular Biology

B-32 Elucidating The Sources Of Enhanced Oxygen Consumption During Early Reperfusion Following Skeletal Muscle Ischemia In The Rat Spinotrapezius Muscle
William Nugent, Aleksander Golub, and Roland Pittman
Physiology and Biophysis

B-33 Roles Of Krüppel Like Factors Klf1, Klf2, And Klf4 In Embryonic Beta-Globin Gene Expression
Yousef Alhashem, Divya Vinjamur, Gabriel Eades, Joyce Lloyd
Human and Molecular Genetics

B-34 Single Neucleotide Polymorphism In The Pdxk Gene Coding For Pyridoxal Kinase: Studying Its Effect On The Protein Structure And Its Possible Implications In Human Health
Jigar V. Desai, Faik Musayev, Mohini Ghatge, Martin K. Safo
Medicinal Chemistry

B-35 Crystal Structure Of E. Coli L-Threonine Aldolase (Eta): Evidentiary Support For Mechanism Of Reactions Catalyzed By The (E TA) And Comparison With Other PLP-Dependent Enzymes
Soumya G. Remesh
Medicinal Chemistry

B-36 Camk-II Mediates Non-Canonical Wnt-Dependent Morphogenic Events During Zebrafish Gastrulation
Jamie McLeod, Sarah C. Rothschild, Ludmila Francescatto, Alexandra Myers and Robert M. Tombes
Biology

B-37 HIV Protease Inhibitors Activate The ER Stress Response And Disrupt The Lipid Metabolism In 3T3-L1 Adipocytes.
Beth S Pecora, Lixin Sun, Xudong Wu, Weibin Zha, Emily Gurley, Elaine Studer, Phillip B Hylemon, William M. Pandak, Luyong Zhang, Guangji Wang, Huiping Zhou.
Microbiology and Immunology

Thursday, October 29

C-01 The Impact Of Lack Of Access To Health Care On Health Status
Allison A. Wellman
Epidemiology and Community Health

C-02 Analysis Of Microrna Data
Andre Williams, MS Kellie Archer, PhD
Biostatistics

C-03 Fabrication Of 3-D Nerve Guides Using Electrospinning For Nerve Reconstruction
Balendu Shekhar Jha, Raymond J. Colello and David G. Simpson
Anatomy and Neurobiology

C-04 Novel Cinnamic Acid-Based Dehydropolymers For Emphysema: Triple Inhibitors Of Elastase, Inflammation And Oxidation
B. Saluja1, J. Thakkar2, U.R. Desai2, M. Sakagami1
Pharmaceutics

C-05 Development Of A Second Generation, Canine Lyme Vaccine: Identification Of The Predominant Ospc Types Found In Canine Lyme Borreliosis
DeLacy V. LeBlanc, Christopher G. Earnhart, and Richard T. Marconi
Microbiology and Immunology

C-06 Acute Elevation Of Endocannabinoids Attenuates The Precipitated Opioid Withdrawal Syndrome
Divya Ramesh1, Scott T. O'Neal1, Jonathan Z. Long2, Benjamin F. Cravatt2 and Aron H. Lichtman1 1 Department of Pharmacology and Toxicology, Virginia Commonwealth University, Richmond, VA 23298 2The Skaggs Institute for Chemical Biology and Department of Chemical Physiology, The Scripps Research Institute, La Jolla, California 92037
Pharmacology and Toxicology

C-07 The Absence Of Synaptically Evoked Plateau Potentials In Dlgn Relay Cells Leads To A Failure In Retinogeniculate Refinement.
Dilger, E.K., Morhardt, D. R., Shin, H. S. and Guido, W
Anatomy and Neurobiology

C-08 Functional Effects Of Fluorescent Hsert Ligands Validated By Homology-Based Docking Studies
Ernesto Solís, Jr., Igor Zdravkovic, Ian D. Tomlinson, Sergei Y. Noskov, and Louis J. De Felice
Physiology and Biophysics

C-09 Snon Regulates Transcriptional Activation Or Repression Of TGF-Beta Signaling By Preventing Recruitment Of CBP And HDAC1 In Esophageal Cancer Cells
Eugene Y. Kim, Anna V. Miller, Amy C. Ladd, Catherine I. Dumur, David C. Williams, and Deborah A. Lebman
Biochemistry and Molecular Biology

C-10 Entry Of Herpes Simplex Virus Requires Cholesterol In The Virion Envelope And Plasma Membrane Of Host Cells
Frances M. Saccoccio and Anthony V. Nicola
Microbiology and Immunology

C-11 New Cellular Accumulation Pathway For Tri-Platinum Compounds Using Heparan Sulfate
Heveline Silva, John B. Mangrum, John J. Ryan and Nicholas P. Farrell
Chemistry

C-12 Anaplasma Phagocytophilum Infects Murine Mast Cells In Vitro
I. Nore Ojogun, Bernice Huang, Daniel Miller, Brian Barnstein, John J. Ryan, and Jason A. Carlyon
Microbiology and Immunology

C-13 Platelet Function Is Impaired Immediately Following Resuscitation From Cardiac Arrest In A Swine Model
Jessica Brueckner, Nathan White MD, Erika J. Martin MT, Donald Brophy PharmD, Kevin Ward MD, Robert Diegelmann PhD
Departments of Emergency Medicine, Pharmacy, and Biochemistry

C-14 Analysis Of The Diguanylate Cyclase Rrp1 And Its Role In Borrelia Burgdorferi Pathogenesis
Jessica L. Kostick, Elizabeth A. Rogers, & Richard T. Marconi
Microbiology and Immunology

C-15 Diffuse Axonal Injury Within The Optic Nerve Following Fluid Percussion Brain Injury: A New Approach For The Comprehensive Evaluation Of Diffuse Axonal Injury
Jiaqiong Wang John E. Greer Susan A. Walker John T. Povlishock
Anatomy and Neurobiology

C-16 Interaction And Function Of Sphingosine-1-Phosphate And Prohibitin-2 In Mitochondria
Graham M. Strub, Jie Liang, Melanie Paillard, Ludovic Gomez, Nitai C. Hait, Qun Chen, Edward J. Lesnefsky, Sheldon Milstien, Sarah Spiegel
Departments of Biochemistry and Molecular Biology and Medicine, Division of Cardiology

C-17 A Transgenic Approach To The Study Of The Consequences Of Diffuse Axonal Injury
Greer JE, McGinn MJ, Povlishock JT
Anatomy and Neurobiology

C-18 tgf-beta suppresses mast cell function in vivo and in vitro
Fernando Josephine and Ryan John
Biology

C-19 AN Organotypic Hippocampal Slice Culture Model Of Acquired Seizures
J.M. Ziobro, D.S. Carter, R.E. Blair, L.S. Deshpande, R.J. DeLorenzo
Neurology

C-20 Identification Of A Novel Mitochondrial Isoform Of DNA Methyltransferase 1
Lisa Sale Shock, Prashant V. Thakkar, Erica J. Peterson, Shirley M. Taylor
Microbiology and Immunology

C-21 Tissue Oxygenation During Experimental Arterial Gas Embolism Using Intravital Microscopy
Luciana Torres, PhD1,2, Ivo Torres Filho, MD,PhD2,3 and Bruce Spiess, MD1,3
Anesthesiology

C-22 Sphingosine-1-Phosphate Accelerates The Development Of Functionally Mature Chymase-Expressing Human Mast Cells
Price MM, Kapitonov D, Allegood J, Milstien S, Oskeritzian CA, and Spiegel S.
Biochemistry and Molecular Biology

C-23 Electrochemical Profiling Of The Ascorbic Acid Redox System During Cardiac Arrest
Melissa Rich, Nathan White, Maryanne Collinson, Kevin Ward
Emergency Medicine and Chemistry

C-24 The Impact Of Low Consumption Of Vegetables And Fruits On Incidence Of Overweight And Obesity In Adults
Dr. Monica R. Gaidhane
Epidemiology and Community Health

C-25 Zeta Potential Measurements For Contact-Antimicrobial Coatings
Murari L. Gupta*, Kennard Brunson*, Asima Chakravorty*, Julio C. Alvarez**, Fernando Luna-Vera**, ThuTrang T. Nguyen** and Kenneth J. Wynne*
Chemical and Life Science Engineering

C-26 Activated Neutrophils Enhance Vascular Reactivity To Angiotensin II Via Rhoa Kinase Activation By Reactive Oxygen Species.
Nikita Mishra, MBBS Scott W. Walsh, PhD
Physiology and Biophysics

C-27 Sphingosine Kinase 2 And S1P In The Nucleus Regulate Histone Acetylation By Inhibition Of Histone Deacetylases
Nitai C. Hait, Jeremy Allegood, Michael Maceyka, Graham M. Strub, Kuzhuvelil B. Harikumar, Tomasz Kordula, Sheldon Milstien, and Sarah Spiegel
Biochemistry and Molecular Biology

C28 Adenovirus-5 Infection Induces Hepatic Lipid Synthesis And Hypertriglyceridemia In C57bl/6 Mice
W. Palmer Wilkins III, Rachael Griffiths, Jin-Woo Choi, Richard L. Atkinson, Philip B. Hylemon, Gregorio Gil, and Suzanne E. Barbour
Biochemistry and Molecular Biology

C-29 Regulation Of Platelet-Activating Factor Acetylhydrolase By Oxidized Phospholipids
Rachael Griffiths, Minkyeong Son, Muralikrishna Mukkamala, Norbert Leitinger and Suzanne E. Barbour
Biochemistry and Molecular Biology

C-30 Morphologically Distinct Classes Of Relay Neurons Reside In Different Regions Of The Mouse Dorsal Lateral Geniculate Nucleus (Dlgn)
Rana N. Eldanaf, Thomas E. Krahe, Emily K. Dilger, Tania A. Seabrook, And W. Guido
Anatomy and Neurobiology

C-31 Prostate Cancer Screening: Addressing Racial And Ethnic Disparities
Sameer Arora
Epidemiology and Community Health

C-32 Regulation And Role Of YKL-40, A Novel Molecule, During Astrocyte Differentiation: Implications For Reactive Gliosis And Glioma Invasiveness
Sandeep K Singh, Katarzyna Wilczynska, Lauren Bryan, Catherine Dumur, and Tomasz Kordula
Biochemistry and Molecular Biology

C-33 Regulation Of Vascular Smooth Muscle Contraction
Silvina M. Alvarez, Ph.D., Amy S. Miner and Paul H. Ratz, Ph.D.
Pediatrics, Biochemistry and Molecular Biology

C-34 Delineation Of The Critical Region For Brachydactyly-Mental Retardation Syndrome By Array Comparative Hybridization: New Candidate Genes For Sleep Disturbance And Albright's Hereditary Osteodystrophy-Like Phenotypes
Stephen Williams, Santhosh Girirajan, Helga Toriello, Ellen Magenis, David Tegay, Eli Hatchwell, Norma Nowak, and Sarah Elsea
Human and Molecular Genetics

C-35 Intensity Exercise On Reducing Coronary Artery Disease Among Smokers
Susan Cha
Epidemiology and Community Health

C-36 Coordinated Innervation Of Retinogeniculate And Corticogeniculate Porjections In The Dlgn Of The Mouse
T. A. Seabrook, T. E. Krahe, E. K. Dilger, D. R. Morhardt, W. Guido
Anatomy and Neurobiology

C-37 Cannabinoid Receptor Interacting Protein (Crip1a) Attenuates Constitutive Cb1 Receptor Signaling And Cb1 Downregulation
Tricia H. Smith, Maurice R. Elphick, Deborah L. Lewis, Ching-Kang Jason Chen, Dana E. Selley
Pharmacology and Toxicology

C-38 Specific Recruitment Of RNA Pol II By NFI-X3 Induces GFAP Expression In Glial Cells
Sandeep K Singh, Katarzyna Wilczynska, Adrian Grzybowski, Lauren Bryan, Tomasz Kordula
Biochemistry and Molecular Biology

C-39 Molecular Pathogenesis Of Wolfram Syndrome Different In Different Causal Genes
Sami S. Amr & Rita Shiang
Human and Molecular Genetics

A-01 Wilm's Tumor-1 Expression In Glioblastoma Cells Fosters Cell Survival: Identifying Underlying Mechanisms.

Archana Chidambaram, Nitya Moothathu, Catherine Dumur, Helen Fillmore and William C. Broaddus
Anatomy and Neurobiology

Wilm's Tumor-1 (WT-1), a zinc-finger transcription factor, is expressed by cancer cells arising from several different tissue types. Previous studies in our laboratory have established the aberrant expression of this protein in approximately 80% of glioma cells from primary tumor specimens and glioma cell lines, and have also proven its necessity for maintaining cellular proliferation in vitro and in vivo. This study was undertaken to determine the presence of WT-1 in two hitherto unexamined glioblastoma cell lines- GBM-6 and -12 and, if present, to ascertain the importance, if any, of WT-1 in these cells, and finally, to study the mechanism(s) by which WT-1 generally mediates its effects in gliomagenesis. **Results:** a) WT-1 was observed to be expressed in both the GBM-6 and -12 xenograft cell lines. Furthermore, its importance in cell survival was underscored by the finding that WT-1 silencing led to a striking decrease in cell viability, seen with Phase Contrast Microscopy (qualitative) and ATP viability assay (quantitative). b) We assessed the changes wrought by WT-1 silencing, in the expression levels of two of its known target genes- Insulin-like Growth Factor-1 Receptor and Platelet-Derived Growth Factor-A- and found an increase and decrease, respectively, of both mRNA and protein (using real time RT-PCR and western blotting respectively). Our current efforts are focused on further characterizing the roles of IGF-1R and PDGF-A in mediating the effects of WT1 in gliomas, and identifying other gene targets for this complex transcription factor using the gene-array technique. **Conclusions**: WT-1 over-expression in the majority of gliomas suggests an important role for this protein in promoting the glial tumor phenotype. Identifying the downstream factors that help this protein promote oncogenesis, which constitutes the scope of this study, will provide important insights for the development of a multi-molecular targeting strategy against these aggressive tumors.

A-02 In-Vitro Binding of 5-Hydroxymethylfurfural (5-HMF) to Human Hemoglobin (Hb) and Serum Albumin (HSA)

Taghrid Obied, M.S., Jürgen Venitz, MD, Ph.D.
Pharmaceutics

BACKGROUND/AIMS. 5-HMF, an aldehyde present in food, is investigated as potential treatment for sickle cell disease through formation of a transiently covalent Schiff adduct with Hb, leading to increased oxygen affinity.

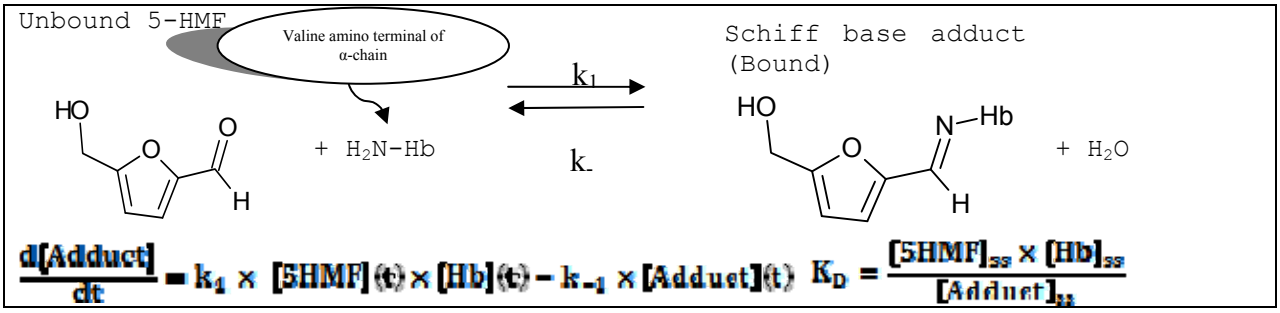

In-vitro studies characterized the binding kinetics with human Hb and HSA. **METHODS.** Time- and concentration-dependency studies were conducted with 5-HMF (5 µM - 54 mM), incubated in Hb (217 µM) and HSA (63 µM) solutions, respectively, at 37 C. Serial samples for up to 30 hrs were ultrafiltered, and unbound 5-HMF concentrations were measured by a validated HPLC-UV assay. After correction for nonspecific binding, the forward rate constant (k1) and backward rate constant (k-1) along with steady-state binding affinity (KD) and capacity (Bmax) were estimated by nonlinear regression. **RESULTS.** Time-dependent binding of 5-HMF was demonstrated for Hb (saturable) and HSA (non-saturable): **1.** Hb binding was characterized by a bimolecular reaction with k1 of 414 (35) M-1hr-1 and k-1 of 0.11 (0.03) hr-1 and KD of 0.26 (0.07) mM; resulting in an equilibration half-life (t1/2eq) of 3.5 hrs at low 5-HMF concentrations. **2.** Steady-state Hb binding revealed a similar KD of 0.59 (0.04) mM and Bmax of 1.7 (0.04) mol 5-HMF/mol Hb. The affinity of Hb for 5-HMF was much higher than for glucose (367 mM) upon glycosylation to form Hb1AC (Higgins, 1981). **3.** HSA binding at low concentration was negligible and less time-dependent than Hb. **CONCLUSIONS.** At physiological Hb concentrations in whole blood, presumed effective concentrations of 5-HMF (0.8-1.6 mM) are expected to show fast association with, but slow dissociation from its drug target, Hb, resulting in prolonged persistence of the adduct (t1/2eq of 0.7 hrs), as shown in-vivo by Abdulmalik (2004). This unique drug-receptor interaction may lead to a prolonged in-vivo PD effect.

A-03 Metabolism Of 5-Hydroxymethylfurfural (5-Hmf) In Human Hepatic Cytosol By Aldehyde Dehydrogenase (Aldh) And Alcohol Dehydrogenase (Adh)

Taghrid Obied, M.S., Jürgen Venitz, MD, Ph.D.
Pharmaceutics

Purpose. In-vitro studies were designed to identify the metabolic pathways of 5-HMF in human hepatic cytosol in order to support clinical studies as a possible treatment of sickle cell disease. The chemical structure of 5-HMF and its known human oxidative metabolites suggest involvement of ALDH and ADH. Methods. Studies were done with human hepatic cytosol, monitoring NAD+ reduction at 340 nm, after incubation with 4-methylpyrazole (4-MP, ADH inhibitor) and disulfiram (DS, ALDH inhibitor) and addition of 26.3 mM of 5-HMF, ethanol (ADH substrate, 1.8 mM) or 4-dimethylamino-1-naphthaldehyde (DN), acetaldehyde (ALDH substrates). Initial reaction rate-substrate concentration profiles were fit by the Michaelis Menten (MM) model. Competitive inhibition models were fit to the reaction rate-inhibitor concentration profiles. **Results.** The tables below summarize the MM parameter (± SD) estimates and the maximum % inhibition, respectively:

	5-HMF	Ethanol	DN	Acetaldehyde
K_m (mM)	218 (74)	1.3 (0.2)	[3.8 (1.4)]·10^{-6}	[149 (123)]·10^{-3}
v_{max} (nmoles/min/mg)	33 (8)	0.70 (0.03)	3.6 (0.3)	2.8 (0.6)

	5-HMF	Ethanol	Acetaldehyde
4-MP	33.6 (5.1)	84.9 (6.9)	
DS	59.9 (7.8)	40.7 (2.3)	92.4 (7.8)

• 5-HMF had the lowest apparent affinity and metabolic efficiency (Clintin-vitro) of all substrates.
• ALDH-selective substrates were cleared more efficiently than the ADH-selective substrate.
• The ADH- and ALDH-substrates had Km values similar to published values.
• 5-HMF metabolism was inhibited by DS and to a lesser extent by 4-MP.

Conclusions. ALDH and ADH activity in human hepatic cytosol was validated using selective substrates and inhibitors. 5-HMF, a low-affinity ALDH/ADH substrate, appears to be metabolized primarily by ALDH, at least at low (< Km) concentrations.

A-04 5-Hydroxymethylfurfural (5-Hmf) Metabolism In Hepatic Cytosol From Mice, Rats, Dogs, And Humans

Taghrid Obied, M.S., Jürgen Venitz, MD, Ph.D.
Pharmaceutics

Purpose. 5-HMF is a compound that is currently investigated as an allosteric hemoglobin modifier in the possible treatment of sickle cell disease.In-vitro studies were designed to identify quantitative differences in ADH/ALDH-mediated metabolism of 5-HMF in hepatic cytosol as a possible source of inter-species differences in in-vivo PK. Methods. Hepatic cytosolic preparations from the four species (protein concentration of 0.2 mg/ml), 1.4 mM nicotinamide adenine dinucleotide (NAD+), and 5-HMF concentrations ranging from 1.5 to 193 mM were mixed in Tris-HCl buffer (pH 7.4). After incubation for 5 minutes at 37oC, the reaction was initiated by the addition of cytosol. NAD+ reduction was monitored using spectrophotometry at 340 nm. Under these optimized conditions, initial reaction rate vs. 5-HMF concentration profiles were fit by the Michaelis Menten (MM) model; Km, vmax, and CLintin-vitro were estimated. CLintin-vivo, ERhep, and CLhep were scaled up using the well-stirred model, assuming negligible plasma protein binding (fu=1) and absence of other metabolic pathways. **Results.** The table below summarizes the MM parameter estimates (± SD) and extrapolated in-vivo PK parameters:

	V_{max} (nmoles/min/mg)	K_m (mM)	$CL_{int}^{in\text{-}vitro}$ (µl/min/mg)	$CL_{int}^{in\text{-}vivo}$ (ml/min/kg)	ER_{hep} (%)	CL_{hep} (ml/min/kg)
Mouse	16.2 (1.0)	37 (6)	0.44	2.3	0.8	2.2
Rat	27.7 (6.8)	77 (32)	0.36	1.9	2.1	1.9
Dog	14.9 (2.3)	18 (8)	0.81	1.7	5.0	1.6
Human	33.2 (8.0)	218 (74)	0.15	0.2	0.8	0.2

• 5-HMF was subject to ADH/ALDH-mediated degradation in all four species.
• 5-HMF had low (millimolar) enzyme affinity in all species.
• As a result of the low Km value, body-weight-corrected CLhep in humans is expected to be about ten-fold lower than in any other species.
• At observed in-vivo murine plasma concentrations, 5-HMF followed first-order PK, as expected, since Cmax was about 15-fold less than the in-vitro Km value.
• The predicted AUC∞ value for a murine oral dose of 794 µmol/kg is 350 mM*min (observed in-vivo AUC∞: 208 mM*min).
• All four species are expected to have low hepatic extraction and high oral bioavailability for 5-HMF.
Conclusions. Despite quantitative species differences in cytosolic ADH/ALDH-mediated metabolism, 5-HMF is expected to be a low-hepatic-extraction-ratio drug with likely high oral bioavailability in all four species.

A-05 Focal Adhesion Kinase (FAK) Regulates Oligodendrocyte Process Dynamics And Remodeling

A.D. Forrest, B. Fuss
Anatomy and Neurobiology

The formation of the myelin sheath is a crucial step during development allowing for efficient conduction velocities to occur in the limited space of the mammalian central nervous system (CNS). During this event, oligodendrocytes, the myelinating cells of the CNS, send out numerous processes that associate with axonal segments and ultimately enwrap them forming the myelin sheath. Previously we had demonstrated that focal adhesion kinase (FAK), a known regulator of cell-extracellular matrix (ECM) interactions, plays a critical role during the initial stages of myelination in vivo. More specifically, our data demonstrated that conditional and inducible knockout of FAK can cause a reduction in the number of myelinated fibers. Here, we present data further investigating the role of FAK during morphological remodeling of post-migratory premyelinating oligodendrocytes. In these studies we used primary oligodendrocyte cultures derived from the brains of three day-old rat pups in combination with siRNA treatment. Our data demonstrate that siRNA-mediated knock-down of FAK expression affects process remodeling and dynamics in a way that is unique to the ECM substrate present. More specifically, our data suggest that FAK confines the expansion of the oligodendrocyte process network in the presence of fibronectin, an ECM substrate that favors the formation of a complex process network. This regulatory role of FAK involves the specific control of dynamic process extension and retraction events. Conversely, FAK appears to promote the expansion of the oligodendrocyte process network in the presence of laminin2/merosin, an ECM substrate that has previously been shown to support membrane sheet formation. Taken together, our findings suggest that FAK regulates oligodendrocyte process dynamics and remodeling in a complex manner that is dependent on the composition of the extracellular environment.

A-06 Tumorigenicity And Angiogenic Protein Profiles Of Glioblastoma Cells With Altered MMP-1 Expression Levels

Nicholas A. Pullen (1), Monika Anand (2), Helen L. Fillmore
The Harold F. Young Neurosurgical Center and (1) Department of Anatomy & Neurobiology, (2) Department of Biochemistry & Molecular Biology

Glioblastoma Multiforme (GBM) is the most common malignant brain tumor. Unfortunately GBM also presents a most perilous course, and to date the impact of various treatment paradigms (surgery, radiation, chemotherapy) remains marginal with median survival at about one year following diagnosis. Two of the salient features of GBM are (1) the ability of the cancer cells to extensively invade and (2) profuse angiogenesis and vascular expansion associated with the bulk of the tumor. Our studies demonstrate that MMP-1 (interstitial collagenase) is found highly expressed in GBM while not in normal brain (McCready et al., 2005), and that this enzyme is integral to the processes of tumor cell motility and invasion (Pullen and Fillmore, 2009). Furthermore, it is suggested that MMP-1 is a vital component of tumor-associated angiogenesis, however potential targets and downstream proteomic effects have yet to be detailed. Herein we present our recent work with two glioma cell lines: T98G that expresses a detectable, basal level of MMP-1, and U251 that does not produce MMP-1 under standard in vitro conditions. We have altered the expression of MMP-1 in each cell line: knockdown in T98G, and over-expression in U251. Our observations in vivo suggest that MMP-1 may be vital to tumor cell establishment. Only 40% of knockdown inoculates become palpable within the same time as all controls. In addition, we observed a stimulation of tumor growth in over-expressers greater than control through two weeks post-inoculation. Preliminary data also demonstrate that MMP-1 expression enhances tumor-stimulated angiogenesis, and that the presence of MMP-1 alters the expression of other angiogenesis related proteins such as TIMP-4 and IGFBP-3 as determined through proteomic profile antibody arrays. These data represent details on a specific MMP and its downstream effects that are common to GBM biology and provide insight for future investigations on focused molecularly targeted interventions for this deadly cancer.

A-07 Glioblastoma Cell Motility Is Mediated Through A Nitric Oxide-MMP-1 Axis

Nicholas A. Pullen (1) and Helen L. Fillmore, Ph.D.
The Harold F. Young Neurosurgical Center and (1) Department of Anatomy & Neurobiology

Work by multiple investigators has demonstrated that constitutive nitric oxide synthase (cNOS) isoforms are associated with high-grade primary CNS tumors. In particular, endothelial (e)NOS is observed with tumor associated endothelial cell foci in GBM. We hypothesize that NO, especially produced from cNOS, fulfills important rolls in maintaining the insidious nature of high-grade gliomas. Previous work from our laboratories as well as other investigators has confirmed the expression of MMP-1 in human GBM, while not in normal brain parenchyma. Herein we present our in vitro NO investigations with regard to MMP-1 in human GBM cell lines considering the overlap of NO and MMP-1 production. We observed significant increases of MMP-1 at the message ($p<0.001$) and mature protein (U-87MG $p<0.001$, T98G $p<0.05$) levels when GBM cell lines were exposed to the NO donor sodium nitroprusside (SNP) at a concentration consistent with constitutive NO production. We recorded no remarkable changes in cell line viability with constitutive-like concentrations. However, as expected inducible-like NO concentration decreased culture viability at least 80% ($p<0.01$), yet a small population of cells remained viable throughout 5-6 day exposure time courses. NO donation resulted in increased cell motility, markedly in T98G ($p<0.001$), while the application of the NOS inhibitor L-NAME produced an opposite effect ($p<0.001$). Furthermore, transient inhibition of MMP-1 production through siRNA resulted in abrogation of the NO-induced motile response ($p<0.05$). These data lead us to conclude that MMP-1 is associated with enhanced glioma cell motility, and that this axis is mediated in part by nitric oxide. We are currently investigating the effects of altered MMP-1 expression in vivo (see Pullen, Anand & Fillmore and Anand, Pullen & Fillmore).

A-08 Identification of a two component regulatory system of the periodontal pathogen, *T.denticola*: insight into the molecular mechanisms of environmental adaptation during the development of periodontal disease

Juni Sarkar[1], Jesse Frederick[2] and Dr. Richard Marconi[2,3].
[1]Department of Life Sciences, [2]Department of Microbiology and Immunology, [3]Center for study of Biological Complexity

Periodontal disease, the most common infection of man, is a progressive disease that initiates with the formation of polymicrobial biofilm. *Treponema denticola*, a spirochete and member of the oral microflora, occurs at elevated levels in periodontal lesions. A complex series of undefined environmental changes result in the relative overgrowth of *T. denticola* over other members of the oral microflora. Little is known regarding the molecular mechanisms associated with the global regulatory networks of oral spirochetes. Two component systems (TCS), which are ubiquitous among bacteria may play central role in transcriptional regulation. In this study, a two component system comprised of ORFs tde1970 (a sensor kinase) and tde1969 (a response regulator) was identified and its components designated as ThkA (treponemal histidine kinase A) and TrrA (treponemal response regulator A). The ThkA- TrrA TCS was determined to be highly conserved and universal among *T. denticola* isolates. Transcriptional analyses revealed that *thkA* and *trrA* are co-transcribed as part of a larger operon and their expression is growth phase dependent. ThkA possesses a PAS domain which has been demonstrated in other bacteria to be involved in the sensing of oxygen, redox potential, energy levels, light, and small ligand. Deletion of the PAS domain from ThkA revealed that in vitro this domain regulates autophosphorylation activity in direct response to environmental conditions. The data suggest that the ThkA-TrrA TCS may be an important sensor of oxygen levels, redox potential, H_2 concentration etc that are associated with disease progression. The functionality of this TCS was demonstrated through the autophosphorylation of ThkA and phosphotransfer to TrrA. This analysis is only the second to demonstrate a functional TCS in an oral spirochete and provides important insight into the molecular mechanisms associated with adaptation of oral spirochetes.

A-09 Second Hand Smoke Induced Molecular Effects In Pup Rat Brain

Brian F. Fuller and Andrew K. Ottens
Anatomy and Neurobiology

Second-hand smoke (SHS) has recently been under intense scientific scrutiny for its deleterious effects to the general population. A recent report by the US Surgeon General reaffirmed that SHS can, in fact, lead to cancer and heart damage. What has yet to be scientifically validated is the effect of SHS on brain development in children. While there have been scattered studies in this area, most lack solid evidence of a connection due to limited and confounded clinical data used in the studies. In this study we utilized a two-dimensional liquid chromatography tandem mass spectrometry (2D-LC MS/MS) to asses differential proteomic changes which occur in the rat pup brain exposed to SHS. Differential changes found in the pup proteome were further explored via immunohistochemistry, and western blotting.

A-10 Rescue Of Visual Cortex Plasticity Deficits In A Mouse Model Of Fetal Alcohol Syndrome Using A Phosphodiesterase Type 1 Inhibitor

Crystal Lantz
Anatomy and Neurobiology

Fetal alcohol spectrum disorder (FASD) is the leading cause of mental retardation. There is growing evidence that deficits in neuronal plasticity underlie cognitive deficits seen in FASD. However, the mechanisms behind these deficits are not clear. Here we test the effect of early alcohol exposure on ocular dominance plasticity in C57/BL6 mice. As well as assess the ability of vinpocetine, a phosphodiesterase type 1 inhibitor, to restore plasticity deficits. Mouse pups were exposed to 5 g/kg of 25% ethanol i.p. every other day from postnatal day (P) 5 to 9. This period is the third trimester equivalent of human gestation, and the brain growth spurt. This regimen resulted in a blood alcohol concentration of ~200 mg/dl for 4 hrs. To assess neuronal plasticity, animals were monocularly deprived (MD) at P21 for 10 days, and tested using optical imaging of intrinsic signals. Beginning one day prior to monocular deprivation and continuing every other day until optical imaging (10 days), some ethanol treated animals were injected with vinpocetine (20mg/kg) or DMSO vehicle (20mg/kg). Monocular deprivation lead to a reduction in the deprived eye responses in controls, but not in alcohol treated animals. Early alcohol exposed animals treated with supplemental vinpocetine exhibited a rescue of ocular dominance plasticity that was not apparent in vehicle treated litter mates. These finding contribute to the development of a mouse model of FASD in our lab, as well as to further the understanding of the causes and possible treatments of FASD.

A-11 Effects Of Stimulating Innate Immune Receptors In Ovarian Cancer Cell Lines

Danielle N. Schramm, Sandrine Lépine, Jessica K. Bell
Biochemistry and Molecular Biology

Pattern recognition receptors (PRRs) function in the innate immune system to alert the host to pathogenic components. Double-stranded RNA (dsRNA), viral genomic material or a viral replication intermediate, trigger the PRRs toll-like receptor 3 (TLR3), retinoic acid-inducible gene I (RIG-I), melanoma differentiation-associated gene 5 (MDA5), and dsRNA-dependent protein kinase receptor (PKR). Previous studies have reported that dsRNA stimulation induced TLR3-dependent apoptosis. Objectives: Examine 786-O, OVCAR-3, OVCA-420, SKOV-3, DOV-13, CAOV-3 cell lines for dsRNA receptor expression and determine dsRNA-induced response. Methods: PRR expression was confirmed via RT-PCR. Expression levels were determined via qPCR. Apoptotic response to dsRNA stimulation was measured by Hoechst staining 48h post-stimulation. Results: RT-PCR analysis showed that cell lines contained mRNA for all dsRNA receptors. qPCR showed a significant increase in PRR expression in those cell lines that underwent dsRNA-induced apoptosis. Conclusions: We have found that at least four dsRNA receptors are present in our cell lines. dsRNA receptor expression does not correlate with dsRNA induced apoptosis, but increased dsRNA receptor expression suggests receptor levels or altered signaling pathways may reduce sensitivity to dsRNA.

A-12 The Role Of Threonine 260 In Mycobacterium Tuberculosis Lanosterol 14α-Demethylase Catalysis

Gareth K. Jennings1, Anuja Modi1, James Terner2 and John C Hackett1
Medicinal Chemistry

In order to understand the underlying mechanisms and confirm the importance of T260 in molecular oxygen activation in lanosterol 14α-demethylase catalysis, mutagenesis and spectroscopic studies were performed on Mycobacterium tuberculosis lanosterol 14α-demethylase. The cyp51 gene was previously cloned into the plasmid pET-17b. Site directed mutagenesis using PCR was performed in order to mutate T260 to A or V. DH5α Escherichia coli were transformed with the pET-17b-CYP51 wild-type or mutated plasmids which were isolated and sequenced to confirm correct mutations. Plasmids were subsequently used to transform BL21 (DE3) E. coli in order to express wild type, T260A or T260V CYP51. Isolation and purification of the proteins were performed using a Ni-NTA agarose column, dialysis and fast protein liquid chromatography. UV/Vis spectral analysis of the enzymes were performed from 350-600 nm of the ferric and ferrous forms as well as binding of CO to the ferrous form. Resonance Raman spectroscopy was used in order to characterize NO binding to the ferric and ferrous forms of the enzymes. UV/Vis spectroscopy gave results consistent with that of literature for ferric and ferrous CYP51 wild-type. Resonance Raman spectroscopy was used to probe the states of the wild-type and mutant CYPs with minor differences between the wild-type and T260A mutant. The T260A mutant gave a shoulder in the υ3 spin state marker at 1488 cm-1 in the ferric form, which is suggestive of a high-spin and low-spin state mixture. Successes were shown in the ability to achieve ferric and ferrous forms of CYP51 as well as binding of diatomic ligands such as CN and NO.

A-13 Biochemical And Structural Characterization Of Innate Immunity Kinase Complex Proteins

R. Jason Call, R. Ghirlando, J.K. Bell
Biochemistry and Molecular Biology

Protein-protein interactions form the communication link from membrane bound receptors to their downstream cellular targets. Our long-term goal is to examine the protein-protein interactions responsible for the activation and regulation of the Toll-like receptor 3 (TLR3) signaling cascade that leads to type I interferon production. In the current study we have targeted the kinase scaffold proteins, TRAF family member-associated NF-κB activator (TANK) and NAK-associated protein 1 (NAP1). Bacterial expression systems have been used to produce recombinant target protein and refolding methods developed for insoluble targets. Initial biochemical characterization of recombinant targets was completed using circular dichroism (CD), gel filtration (GF) and analytical ultracentrifugation (AUC). The protein domain comprising the N-terminal region of NAP1 can be successfully refolded as assessed by CD, while TANK is soluble. Both constructs form homo-oligomers as determined by GF. AUC experiments show that the NAP1 N-term behaves as an elongated dimer in vitro. Gel filtration studies of TANK's kinase interaction site show that it elutes as a dimer species. The scaffold proteins, TANK and NAP1, form stable homo-oligomers via their N-terminal regions.

A-14 The Role Of Stat1 In Regulation Of Mitochondrial Gene Expression

Jennifer D Sisler, Magdalena Szelag, Dr. Andrew Larner
Biochemistry and Molecular Biology

It is well known that Stat1 plays an important role in the activation of interferon-stimulated early response genes. Incubation of cells with type one intereferons (IFNα/β) activates the tyrosine kinases Jak1 and Tyk2 resulting in tyrosine phosphorylation of Stat1 and Stat2. Stat1 and Stat2 form dimers, translocate to the nucleus and binds to IRF9 (p48) forming the heterotrimeric transcription complex ISGF3. ISGF3 binds to interferon stimulated response regions (ISRE) in the promoters of interferon-stimulated genes. Stat1 can also forms homodimers, which bind to the GAS element of early response genes. It has been shown previously that a small fraction of Stat1 is located in the mitochondria. It has also been shown that there is a conserved GAS element located within the mitochondrial genome that is located in the D-loop region where transcription and replication of mitochondrial genes is initiated. Stat1 null cells and mice tissues have much higher levels of mitochondrial mRNAs compared to wild-type samples. This indicates that Stat1 may play a role as a negative regulator of the mitochondrial gene expression. We are examining whether STAT1 plays a direct or indirect role in mitochondrial gene expression. To address this issue we have designed a construct using pcDNA4T0 containing wild-type STAT1 and STAT1 with a mitochondrial localization sequence (MLS STAT1), which targets to the mitochondria; STAT1 with a nuclear localization sequence mutation and a construct that has the MLS with the nuclear localization sequence. We have created stable cell lines using U3A cells and we have looked at mitochondrial gene expression when untreated or treated with IFNβ. Samples will also look at the physiological role of MLS STAT1 in the antigrowth and antiviral responses.

A-15 Investigating Genetic And Environmental Contributions To The Relationship Between Church Attendance And Alcohol Dependence

Jia Yan, Fazil Aliev, Kenneth S. Kendler, Steven H. Aggen, Laura Bierut, and Danielle M. Dick, with SAGE collaborators
Human and Molecular Genetics

Both genetic and environmental factors influence the risk for alcohol dependence (AD). One environment known to be important is religiosity. Religiosity has been shown to have a protective main effect on the risk for substance use disorders and a moderating effect on the extent that genetic effects contribute to alcohol use and other substance use outcomes. We conducted a bivariate analysis to explore the genetic and environmental contributions to the covariance between church attendance (CA) and AD using data from the Virginia Adult Twin Study of Psychiatric and Substance Use Disorders. Religiosity was operationalized by self-reports of frequency of CA, using an ordinal scale. Different response options were used in males and females; accordingly, models were fit separately to male and female data. In males, there was significant shared genetic covariance between CA and AD, with the genetic component shared with CA accounting for approximately 12% of the total genetic variance for AD. In females, although the shared additive genetic and unique environment (AE) and shared common environment and unique environment (CE) models could not be distinguished in females, the shared AE model suggested that ~26% of the variance in AD in females may be shared with CA. With evidence of shared genetic covariance between CA and AD, we are currently testing for specific genes that may be involved in this covariance using data from the Study of Addiction: Genes and Environment (SAGE). SAGE has GWAS data on a sample of 1944 AD cases and 1965 controls, along with information about frequency of CA. Preliminary analyses suggest several loci that may be involved in gene-environment correlation between CA and AD, as well as other loci where the association with AD is moderated by CA. This study represents a first step toward incorporating environmental information into GWAS studies, using twin data to guide these efforts.

A-16 A Calcineurin-Dependent Loss And An Overgrowth Of Dendritic Spines Following Lateral Brain Injury In Rat

John N. Campbell(1), Brian Low(2), David Register(3), & Severn B. Churn(1-4)
Anatomy & Neurobiology(1), Physiology & Biophysics(2), Neurology(3), and Pharmacology & Toxicology(4)

Traumatic brain injury (TBI) causes an acute loss of brain tissue as well as progressive damage through excitotoxicity and inflammation. These progressive processes can alter synaptic circuitry well beyond the focally-damaged tissue, which may play a role in sequelae such as cognitive impairment and post-traumatic epilepsy. One indication of altered synaptic circuitry would be a loss or gain of dendritic spines, specialized protuberances of dendritic membrane on which are formed most of the excitatory synapses in the brain. To investigate the effect of TBI on dendritic spines, a modified Golgi-Cox technique was performed on adult rat brains recovered 1hr, 24hr, and 1wk after lateral fluid percussion injury. Proximal dendrites of principal cells were sampled for dendritic spine density in the following regions of each hemisphere: layer II/III neocortex, hippocampal CA1 and CA3, and the dorsal leaf of the dentate gyrus. At 24hr post-TBI, the density of pedunculated (thin or mushroom-shaped) spines had decreased to 70% of control in ipsilateral neocortex ($p<0.05$; $n=19$), to 71% of control in ipsilateral CA1 ($p<0.01$; $n=18$), and to 77% of control in contralateral CA1 ($p<0.05$; $n=12$). By 1wk post-TBI, dendritic spine density in the hippocampus was significantly greater than control (ipsilateral CA1, 152%, $p<0.001$, $n=14$; contralateral CA1, 143%, $p<0.001$, $n=13$; ipsilateral CA3, 134%, $p<0.01$, $n=14$; contralateral CA3, 125%, $p>0.05$, $n=13$). The spine loss at 24hr post-TBI was prevented by a single, 1hr post-TBI administration of the calcineurin inhibitor, FK506. The data suggest extensive, calcineurin-dependent changes in the synaptic circuitry of the laterally injured brain.

A-17 Production And Charecterization Of Silencer Of Ikk-Epsilon

Jonathan L. Forbes, R. Jason Call & Dr. Jessica Bell
Biochemistry and Molecular Biology

Innate immunity serves as the first line of defense against pathogen challenge. Among the cellular mechanisms of the innate immune response, the recognition of viral dsRNA and subsequent production of type-I interferon (IFN) is, in part, attributed to the Toll-Like Receptor-3 (TLR3) pathway. To control this anti-viral response, a key inhibitor, Suppressor of IKK-epsilon (SIKE), terminates activation of interferon regulatory factor 3 and subsequent production of IFN by an unknown mechanism. Our goal is to decipher the mechanism by which SIKE inhibits the TLR3 pathways. The objective of this project was to produce recombinant SIKE for biochemical characterization. Expression vectors for full-length SIKE and an N-terminally truncated version (SIKE72-207) in bacteria and insect cells were constructed. In bacterial systems, both SIKE constructs were expressed as insoluble material. Target protein was successfully refolded and secondary structure examined by circular dichroism. Size exclusion chromatography of both constructs revealed multiple oligomeric states. For insect cell expression, baculovirus for both constructs has been produced with trial expressions ongoing. From these initial studies, SIKE is a primarily helical protein that forms homo-interactions.

A-18 Potential Of Mean Force Reconstruction For High-Selectivity Substrate Binding At Human Aromatase.

Justin E. Elenewski and John C Hackett
Medicinal Chemistry

Ligand binding and unbinding processes are often regarded strictly by their equilibrium endpoints. Nonetheless, binding and unbinding are inherently nonequilibrium processes, during which the protein-ligand system navigates a manifold of intermediate states through a series of activated barrier crossing events. While frequently neglected, these transient states may contribute to the selectivity of highly substrate-specific systems by precluding the binding of certain agents. That is, it may be requisite for a ligand to induce or contour to certain folding intermediates for the binding process to progress. To characterize this behavior, steered molecular dynamics (SMD) unbinding simulations have been performed using the aromatase / androstenedione complex as a test case. The aromatase / androstenedione system was embedded in a 120A x 120A POPC membrane, solvated, and equilibrated for 25 ns before SMD simulations were initiated. Constant-velocity SMD was repeated with several steering velocities and harmonic restraint forces to explore different regimes of unbinding behavior and provide sufficient sampling of the trajectory space. The resulting force profile was used to reconstruct a thermodynamic potential of mean force along the unbinding reaction coordinate. Intermediates in the unbinding process were analyzed to assess the role of various residues in guiding androstenedione out of the binding pocket. The reported simulations are among the longest of a peripheral membrane protein and the first such simulations of a membrane-associated cytochrome P450. The features and mechanisms implicated in ligand unbinding elucidate the biophysical processes responsible for highly substrate-selective systems. Funding Sources:

A-19 Theoretical Studies Of Lanosterol 14α-Demethylase Catalysis: Mechanistic Insight Into P450-Catalyzed C-C Bond Cleavage

Kakali Sen and John C Hackett
Medicinal Chemistry

The mechanisms of cytochrome P450 (CYP)-catalyzed C-C bond cleavage have been strongly debated and difficult to unravel. In this work we have tried to elucidate the deformylation mechanism of lanosterol 14α-demethylase (CYP51) using hybrid quantum mechanical and molecular mechanical (QM/MM) computational methods. In presence of aldehyde substrate, the proton relay network is apparently diverted from molecular O2 to the lanosta-8,24-dien-32-al carboxyaldehyde oxygen, extending the lifetime of the peroxo species to participate in CYP catalysis. The peroxo species is trapped as peroxohemiacetal without an apparent energetic barrier, allowing peroxo to circumvent the subsequent protonation steps of the catalytic cycle toward O–O bond cleavage. Parallel studies considering the hydroperoxo (Compound 0) disqualify it as an effective nucleophilic oxidant. Concerted 15α-H abstraction followed by fragmentation produced the experimentally observed formate, and unsaturated lanosterol. A stepwise mechanism encountering small energetic barriers producing the observed products was also characterized. These results support competence of the peroxo intermediate in the final catalytic step of CYP51 catalysis and complements numerous experimental investigations supporting a role for this intermediate in the cleavage of C-C bonds by P450 enzymes.

A-20 Autotaxin (Atx) Regulates The Appearance Of Mbp-Positive Oligodendrocytes In The Hindbrain Of The Zebrafish

Larra M. Yuelling1, Kevin R. Lynch3, James A. Lister2, Babette Fuss1
1 Anatomy and Neurobiology and 2Human and Molecular Genetics, 3Department of Pharmacology, University of Virginia Medical Center

Our previous data identified autotaxin (ATX), also known as phosphodiesterase Iα/autotaxin (PD-Iα/ATX), as an oligodendrocyte-secreted protein involved in regulating the developmental progression from a migratory oligodendrocyte progenitor cell to a fully myelinating cell. More specifically, we identified a novel functional domain of ATX, the MORFO domain, which promotes the establishment of a complex process network by premyelinating, post-migratory oligodendrocytes. The majority of research related to ATX, however, is focused on its lysophospholipase D (lysoPLD) activity, which generates the lipid signaling molecule lysophosphatidic acid (LPA). Interestingly, we found that only upon down regulation of ATX expression, LPA induces membrane sheet formation and the expression of the classic isoforms of myelin basic protein (MBP) in differentiating rat oligodendrocytes in culture. Here, we present data using the zebrafish to assess the role of ATX in oligodendrocyte differentiation in vivo. Our findings demonstrate that ATX is expressed in the hindbrain of the developing zebrafish in a similar pattern as other known oligodendrocyte proteins. When ATX expression is down regulated in the zebrafish, the appearance of MBP-positive oligodendrocytes in the hindbrain is decreased. A similar observation is made upon application of VPC8a202, an inhibitor of ATX's lysoPLD activity. Taken together, our data suggest that ATX regulates the appearance of MBP-positive oligodendrocytes at least in part via its lysoPLD active site.

A-21 Dynamics Of Substrate Interactions In Trna (M1g37) Methyltransferase; Implications For Drug Discovery

Maria Palesis, John Hackett, and Walter M. Holmes
Pharmacology and Toxicology

trmD is an essential gene in all eubacteria which encodes the homodimeric enzyme, TrmD. Using S-adenosyl methionine (SAM), the enzyme methylates the G37 nucleotide in all tRNA's which recognize codons beginning with cytosine. A purine must be present at position G36 if methilation is to occur. Methylation of G37 allows for proper codon - anticodon alignment during translation and therefore reduces the occurrence of frame shift mutations. X-ray crystallography of the E. coli enzyme reveals two binding sites for SAM which are deeply buried within the interior of the enzyme. An analysis of the structure suggests that significant conformational changes must occur for substrate binding and catalytic turnover. Molecular dynamics simulations of enzyme and apoenzyme implicate secondary structural elements, namely a flexible loop region and a halo-like loop which may contribute to active site accessibility. Analysis of simulation trajectories indicates an alternating pattern of active site accessibility between the two sides, suggesting a single site mechanism for enzyme activity. This alternating pattern is less synchronous in the apoenzyme simulation however, which may be an indication of a cooperative role for ligand binding. The dynamic contribution of the flexible linker and halo group to enzyme activity is currently being investigated in our laboratory and we have devised a series of experiments that will help elucidate key components of enzyme function. We also are investigating the possibility that these loops are essential for the isomerization (flipping) of tRNA Guanine bases G36 and G37 into the active site. In addition, we are pursuing novel inhibitors for this enzyme using experimental and computational approaches. We have identified two compounds (4,4'-Bis 1-anilinonaphthalene 8-sulfonate and benzidinediazo-bis-1-naphthylamine-4-sulfonic acid) that are potent inhibitors of TrmD activity. Computational ligand docking of one of these compounds suggests that it may interfere with the flexibility of the linker group above the active site. Experimental data indicate an allosteric mode of inhibition as neither the binding of SAM nor tRNA are affected by the addition of this compound. These inhibitors are important lead compounds for the development of new antimicrobials. We are currently testing derivatives of these compounds.

A-22 Is Tyk2 A Critical Regulator Of Obesity?

Derecka Marta, Gornicka A, Larner A
Biochemistry and Molecular Biology

The Jak/Stat pathway is the primary mediator of leptin signaling, which has been implicated in obesity. We found that mice lacking Tyk2, one of the Jak's, become spontaneously obese. Expression of a variety of mRNAs that regulate fatty acid and glucose homeostasis are altered in liver, skeletal muscle and adipose tissue of Tyk2- null mice, which is consistent with metabolic syndrome. Proper energy balance prevents the development of obesity and is dependent on energy expenditure. Brown adipose tissue (BAT) dissipates chemical energy in the form of heat in response to excess of calories and is a natural defence against hypothermia and obesity. Differentiation of BAT is defective in mice that do not express Tyk2, which is one reason that might explain the obese phenotype in these animals. Using an in vitro differentiation model of BAT cells isolated from mice with Tyk2 deletion, we were able to restore the differentiation in Tyk2 -/- preadipocytes by expression of either wild type or kinase inactive Tyk2 (Tyk2KD), as well as constitutively active form of Stat3 (Stat3CA). Recent data provided evidence that PRDM16 is the master regulator controlling brown fat/skeletal muscle switch from the common progenitors. Consistent with severe decrease of PRDM16 expression, we observed up-regulation of muscle-specific RNAs in Tyk2- null cells. Remarkably, differentiation of Tyk2 -/- preadipocytes cannot be rescued by PRDM16. These data suggest that Tyk2 is key player in brown preadipocytes differentiation that works upstream of PRDM16. However, an additional unknown factor is also activated by Tyk2 and Stat3 but its identity remains to be established. Thus Tyk2 appears to be a critical regulator of obesity, which is a major global health and economic problem.

A-23 Synthesis, Screening And Cocrystalization Of Adenosine-Based Inhibitors For Ermc' And Ksga

Mr. Matthew R. Baker, Dr. Keith C. Ellis, Dr. Fiek N. Musayev, and Dr. Jason P. Rife
Medicinal Chemistry

The threat of infectious diseases has risen recent decades largely due to the rampant spread of antibiotic-resistant bacteria, and the lack of new antibiotics. The work being presented here tries to address both these problems by targeting two rRNA methyltransferases, ErmC' and KsgA. ErmC' confers macrolide antibiotic resistance by mono- or di-methylating A2058 (Escherichia coli numbering) in the 23S rRNA of the 50S ribosomal particle. Therefore, inhibitors of ErmC' could renew the effectiveness of macrolide antibiotics against bacterial strains that rely on this specific enzyme for resistance. KsgA, a housekeeping protein, di-methylates both A1518 and A1519 (E. coli numbering) of 16S rRNA in the 30S ribosomal particle, and aids in ribosomal assembly. Catalytically inactive KsgA results in a significant reduction in growth rate for the bacteria. This is caused by inactive KsgA binding to, but not releasing the ribosomal particles, thus blocking the ribosomal assembly process. Therefore, inhibitors to KsgA have the potential to stall ribosome biogenesis by making KsgA catalytically inactive. A series of 22 compounds were synthesized that differed at the N6-position of adenosine. Inhibition of ErmC' and KsgA was measured in vitro with test compounds at 1mM final concentration. The amounts of rRNA methylation were measured using SPA beads that were added to reactions and quenched at the mid-linear time point for that enzyme's typical time course, 32 min for ErmC' and 5 min KsgA. The following test compounds showed the most significant inhibition for ErmC' (in parentheses is the average percent of reduction in methylation compared with the no-inhibitor control, ± the standard deviation); N6-n-butyl adenosine (24.8% ± 10), N6-8-octylamine adenosine (51.1% ± 11), N6-cyclopentyl adenosine (32.2% ± 7), N6-cyclohexyl adenosine (32.2% ± 12), N6-tetrahydropyran adenosine (20.3% ± 12), and N6-phenethyl adenosine (18.5% ± 10). Similarly, compounds that showed significant activity against KsgA were; N6-octyl adenosine (38.9% ± 9), N6-8-octylamine adenosine (25.5% ± 14), N6-cyclopentyl adenosine (16.2% ± 9) and N6-cyclohexyl adenosine (19.2% ± 23). Select compound have been cocrystallized with ErmC' and KsgA in attempts to show how these inhibitors are interacting with ErmC' and KsgA.

A-24 Epidermal Growth Factor Mediated Up-Regulation Of Mmp-1 In Glioma

Monika Anand(1) and Helen L Fillmore (2)
Biochemistry and Molecular Biology

Glioblastoma Multiforme (GBM) is a devastating disease with a median survival rate of approximately 11-13 months. One of the key features underlying the failure of current therapies is the invasive nature of glioma cells. Matrix metalloproteinase-1 (MMP-1) has been implicated in invasion and metastasis in a wide variety of cancers. In addition to their role in invasion, MMPs can also regulate the tumor microenvironment and alter cellular behavior. Previous studies from our laboratory have shown that MMP-1 is over-expressed in GBM and can influence glioma cell invasion in vitro. MMPs are tightly regulated and their biologic function is in part determined by the cell type and cellular environment. The levels of MMP regulation include transcriptional control, post-transcriptional events and interactions at the protein level by activators and inhibitors. Because the epidermal growth factor receptor (EGFR) is amplified in human GBM we wanted to determine the effect of EGFR activation by its ligand, EGF on MMP-1 expression and invasion in human glioma cell lines and determine the signaling mechanisms responsible for such an induction. We stimulated glioma cell lines (T98G and U87MG) with EGF in the presence and absence of the EGFR inhibitor, AG1478. We observed that with EGF (20ng/ml) treatment, in addition to EGFR activation, AKT was phosphorylated, MMP-1 was induced and that in the presence of AG1478, AKT and EGFR phosphorylation was inhibited in a dose dependent manner. Importantly, MMP-1 up-regulation by EGF was abrogated in cells pretreated with AG1478. EGFR has been shown to up-regulate MAPK, PI3K and STAT3 pathways in glioma and other malignancies. To determine which of these downstream signaling pathways are involved in the induction of MMP-1, we first examined MAPK signaling by using the inhibitor, U0126. Only a modest decrease was observed in the conditioned media from cells pretreated with U0126 suggesting potential inputs from other signaling pathways. We are currently examining the involvement of PI3K/AKT and STAT3 pathways in the induction of MMP-1 by EGF.

A-25 Investigation Of Various Endogenous Blood Plasma Phospholipids, Glycerides And Cholesterols That Contribute To Matrix Effects In Lc/Ms/Ms

Omnia A. Ismaiel, Tianyi Zhang, Rand G. Jenkins, H. Thomas Karnes
Pharmaceutics

Matrix effects are a primary challenge in quantitative LC/MS/MS bioanalysis. Glycerophosphocholines (e.g. phosphatidylcholine) are the major phospholipids in plasma and cause significant matrix effects. The purpose of this work is to investigate matrix effects resulting from different phospholipids classes, acylglycerols and cholesterols. The ultimate goal of this work is to build a library for the relative presence of these components in final extracts of commonly used sample preparation techniques. Thirteen compounds were selected which were representatives of eight phospholipids classes, mono, di, triacylglycerols, cholesterol and cholesterol esters. Post-column infusion experiments were carried out to compare relative suppression effects of these compounds. Chlorpheniramine (pKa 9.2) and loratadine (pKa 4.9) were selected as test compounds. A 100 ng/ml solution of each test compound was constantly infused (10 µl/min) into the MS. 25 µg/ml standard solutions of each endogenous compound were injected pre-column (25 µl, n=3). The extractabilities of these components from a plasma pool were compared using liquid-liquid extraction, supported-liquid extraction, solid phase extraction and protein precipitation. Post-column infusion experiments showed that all phospholipids classes resulted in significant ion suppression effects ranged from 54% to 76% and 60% to 92% for chlorpheniramine and loratadine, respectively. Glycerides and cholesterols also resulted in ion suppression effects for both compounds ranging from 29% to 78%. Various phospholipids classes in addition to glycerophosphocholines may result in significant matrix effects; and should be monitored during LC/MS/MS analysis. Endogenous components other than phospholipids such as cholesterol, cholesterol esters triacylglycerols and diacylglycerols may also cause matrix effects. A consideration of the type of matrix and the type of sample preparation procedure may help the scientist anticipate and minimize matrix effects.

A-26 Expression Of AMP-Activated Kinase (AMP Kinase) And Inactivation Of Myosin Light Chain (MLC) Kinase By AMP Kinase Determines The Magnitude Of Smooth Muscle Contraction In Different Regions Of The Stomach

O. Al-Shboul, S. Mahavadi, C. Strane and K.S. Murthy
Physiology and Biophysics

The contractile phenotypes of proximal and distal gastric smooth muscle are distinct with proximal smooth muscle exhibiting tonic characteristics and distal smooth muscle phasic characteristics. Phosphorylation of MLC20 at Ser19 is a prerequisite for initiating and maintaining smooth muscle contraction. The levels of MLC20 phosphorylation during the initial contraction are regulated by a Ca2+/calmodulin-dependent protein kinase. The kinase is rapidly inactivated by the decline in Ca2+ levels and upon phosphorylation by Cam-kinase II and, as shown in studies of airway smooth muscle, by AMP-activated kinase. **Aim.** To determine whether the expression and activity levels of AMP kinase correlate with the contractile phenotypes in proximal versus distal stomach. **Methods.** Protein expression of AMPK was examined in muscle cells isolated separately from distal and proximal stomach. Acetylcholine (ACh)-stimulated MLC kinase and AMP kinase were measured by immunokinase assay using MLC20 and purified MLC kinase as substrates, respectively. Acetylcholine-induced muscle contraction was measured by scanning micrometry in the presence or absence of STO-609, an inhibitor of calmodulin-dependent protein kinase kinase-b, a known upstream kinase of both Cam-kinase II and AMP kinase. **Results.** Expression of AMP kinase, as determined by Western blot, was 3-fold greater in muscle cells from distal stomach. ACh stimulated MLC kinase and AMP kinase activities in muscle cells from both regions, but the activation of AMP kinase was 3-fold higher in muscle cells from distal stomach. ACh stimulated phosphorylation of MLC kinase in muscle cells from distal stomach. ACh-induced MLC kinase activity and contraction were preferentially augmented by STO-609 (10 mM) in muscle cells from distal stomach. Similar results were obtained when muscle contraction was initiated with KCl. The results imply that phosphorylation of MLC kinase by AMP kinase rapidly terminates MLC kinase activity and limits MLC20 phosphorylation and muscle contraction. **Conclusion.** Higher expression and activation of AMP kinase, selective phosphorylation and rapid inactivation of MLC kinase by AMP kinase in muscle cells from distal stomach correlate with the phasic phenotype of muscle in distal relative to proximal stomach.

A-27 Acute Ethanol-Responsive Gene Expression In Fyn Kinase Knockout Mouse Prefrontal Cortex And Nucleus Accumbens

Sean P. Farris and Michael F. Miles
Pharmacology and Toxicology

The molecular mechanisms underlying alcohol abuse and alcoholism are largely unknown, however, changes in gene expression are proposed as important molecular adaptations underlying the development of alcohol abuse and alcoholism. Prior gene expression studies from our laboratory and others have demonstrated reduced myelin-associated gene expression in postmortem alcoholic brain tissue. Acute ethanol differentially regulates myelin-associated gene expression between DBA/2J (D2) and C57BL/6J (B6) mice, two inbred mouse strains that also exhibit divergent behavioral responses to ethanol. Bioinformatic analysis of microarray studies on D2 and B6 mice implicated Fyn kinase as a potential signaling mechanism regulating myelin gene expression. Fyn kinase knockout mice also display altered acute ethanol behaviors, suggesting Fyn may serve a central role in both myelin gene expression and ethanol-related behaviors. Therefore, we conducted expression profiling using microarrays to identify altered basal and ethanol-responsive gene expression patterns in Fyn kinase knockout mice (B6;129S7-Fyntm1Sor/J). Characterizing the corresponding gene networks will test the hypothesis that Fyn kinase is involved in the regulation of myelin gene networks and identify potential signaling mechanisms mediating acute ethanol-related behaviors in Fyn kinase knockout mice. The prefrontal cortex (PFC) and nucelus accumbens (NAC) were chosen because of their role in mediating the rewarding properties of ethanol and prior analysis of microarray data from D2 and B6 mice. Expression profiling revealed 565 genes altered by genotype and 746 genes altered by acute ethanol in the PFC, as well as 1220 altered by genotype, and 1038 genes altered by acute ethanol in NAC (P-value <0.001). Among the genes differently regulated were gene networks related to calcium signaling, GABA-A receptor subunits, and several myelin-associated genes. We believe further characterizing these functional gene networks may have important implications in understanding acute ethanol-mediated behaviors related to Fyn kinase, and interactive neuronal-glial cell signaling mechanisms associated with the neurobiology of alcohol abuse and alcoholism.

A-28 Adam10 Transgenic Mice Serve As A Novel Model For Studying The Role Of Mdscs In Tumor Metastasis

Sheinei Saleem, David Gibb, Daniel Conrad, Laura Graham, Harry Bear
Microbiology and Immunology

Tumor escape and expansion is highly correlated with an increase in immunosuppressive CD11b+Gr-1+ myeloid derived suppressor cells (MDSCs). MDSCs mediate a negative immune response, producing angiogenic factors and inhibiting anti-tumor T cell responses. Thus, characterization of mechanisms underlying MDSC expansion and MDSC-induced T cell suppression is central to understanding and overcoming tumor escape. In previous studies examining MDSCs in tumor-bearing mice, the MDSC induction occurs after tumor initiation. Thus, it is unclear whether MDSC expansion is merely a result of tumor progression or a cause of tumorogenesis. Additionally, results of these studies are confounded by the presence of tumors that secrete multiple factors that may contribute to MDSC expansion and T cell suppression. These issues, therefore, require the evaluation of MDSCs in a tumor-free environment. Here, we describe a novel murine model of MDSC expansion in naïve, untreated, tumor-free mice. Overexpression of a disintegrin and metalloprotease 10 (ADAM10) on B cell progenitors prevented B cell development and resulted in an increase in CD11b+Gr-1+Ly-6G+ and CD11b+Gr-1+Ly-6G− MDSCs in the bone marrow, peripheral blood, and spleen, causing severe splenomegaly. Like MDSCs from tumor-bearing mice, MDSCs from ADAM10 transgenics (Tg) profoundly inhibit T cell proliferation, produce high levels of VEGF, and suppress L-selectin expression on cytotoxic T cells. Additionally, injection of B16 melanoma cells revealed that ADAM10 Tg mice, unlike littermate controls, are unresponsive to adoptive immunotherapy with B16 specific-wild-type T cells. Despite the knowledge gained regarding the role and mechanism of myeloid-derived suppressor cells in anti-tumor immunity, they continue to serve as a confounding and limiting variable in treatment and much remains to be learned. Thus, ADAM10 Tg mice provide a model for examining MDSC expansion and T cell suppression in a tumor-free environment, and elucidating the role of MDSCs in the initiation of tumor growth and tumor escape from immune responses.

A-29 Expression Of Matrix Metalloproteinase-2 After Olfactory Nerve Transection

Bakos, S.R. Costanzo, R.M.
Physiology and Biophysics

The olfactory system is an ideal model for the study of neuronal regeneration. In this study, we investigated changes in Matrix Metalloproteinase-2 (MMP-2) following olfactory nerve transection and subsequent neuronal degeneration, regeneration and recovery in mice. We measured the levels of MMP-2, GAP-43 and olfactory marker protein (OMP) in the olfactory bulb at different recovery time points using Western blot. GAP-43 and OMP are markers for immature neurons and mature olfactory neurons, respectively. In control mice, MMP-2 expression was not observed. MMP-2 levels were observed after nerve transection with a significant peak in expression at day 7. GAP-43 and OMP levels decreased soon after nerve transection, reflecting degeneration of neuron fibers and deinnervation of the bulb. GAP-43 increased rapidly between days 3 and 7, indicating regeneration and growth of new axon fibers reinnervating the bulb. OMP began to increase by day 10, reflecting the maturation of olfactory neurons. This is the first report to demonstrate changes in MMP-2 associated with deinnervation and reinnervation of the olfactory bulb. MMP-2 may serve as a transition event, signifying a switch from degradation to recovery of neurons in the olfactory system.

A-30 Cotranslational Folding And Oligomerization Of Hsv Gb In The Endoplasmic Reticulum

S.J. Dollery, M.G. Delboy, A.V. Nicola
Microbiology and Immunology

Glycoprotein B is conserved among all herpesviruses. HSV-1 gB is a multifunctional protein involved in viral attachment to cell surface heparan sulfate, binding to receptors such as PILRalpha and membrane fusion during entry and egress. The structure of an ectodomain fragment of HSV-1 gB reveals five distinct folded domains and a trimeric conformation (Heldwein et al., 2007). We used a panel of gB-specific conformation-dependent antibodies (Bender et al., 2007) and short (100 sec) radioactive pulses of HSV-infected cells to investigate how gB acquires its native folded state. We determined specifically whether folding occurred on the ribosome concurrent with synthesis. Several co-translational folding events were detected, including folding of the putative fusion domain. The results support the hypothesis that sequential domain folding begins on the nascent polypeptide chain. Notably, co-translational oligomerization of newly synthesized gB was detected on the ribosome within 100 seconds of synthesis. Post-translational domain folding continued up to 60 minutes post-gB synthesis. These data suggest that oligomer formation occurs in the ER prior to termination of translation and that individual monomer subunits continue to fold after oligomerization. Intracellular low pH was required for proper folding of gB domains as detected by confocal microscopy. Treatment of infected cells with bafilomycin A1, which elevates intravesicular pH, increased exposure of an epitope in the putative fusion domain of gB. These results may give insight into why pH-altering agents inhibit syncytium formation by HSV and why there are differences in the pH-dependence of viral entry and cell-cell fusion.

A-31 Expression Pattern Of High Molecular Weight- Melanoma Associated Antigen (Hmw-Maa) In Breast Cancer Stem Cells

Stuti Agarwal, Maciej Kmieciak, Soldano Ferrone, Masoud H. Manjili
Microbiology and Immunology

High Molecular Weight-Melanoma Associated Antigen (HMW-MAA) is expressed in certain tumors as well as in pericytes. Therefore, monoclonal antibody against HMW-MAA can have both anti-tumor and antiangiogenic effects. We examined HER-2/neu positive mouse mammary carcinoma tumor cells (MMC) and a relapse variant of mammary tumors, ANV, for the expression pattern of the HMW-MAA using flow cytometry. Relapsed ANV cells have characteristics of breast cancer stem cells (CD44+CD24-) whereas MMC primary tumors are CD44+CD24+. We showed that MMC had higher expression of HMW-MAA compared to ANV. In fact, we found a direct correlation between CD24 loss and downregulation of HMW-MAA. Despite downregulation of HMW-MAA in ANV, majority of cancer stem cells retained HMW-MAA expression. In vitro culture of the tumor cells with anti-HMW-MAA antibody resulted in the inhibition of tumor growth. These findings suggest that anti-HMW-MAA antibody may have different potency against primary tumors than against breast cancer stem cells.

A-32 Substrate Specificity Of Arm/Rmt Methyltransferases

Tamara Zarubica, H. Tonie Wright, Jason P. Rife
Biochemistry and Molecular Biology

Bacterial resistance to 4,6-type aminoglycoside antibiotics, which target the ribosome, has been traced to the armA family of rRNA methyltransferases. These plasmid-encoded enzymes transfer a methyl group from S-adenosylmethionine to N7 of the buried G1405 of the 16S rRNA in the aminoglycoside binding site of the 30S ribosomal subunit. Neither 16S rRNA alone nor intact 70S ribosome is an efficient substrate for ArmA methyltransferase. To identify the site of interaction between ArmA and the 30S subunit, we used hydroxyl radical cleavage of 16S rRNA mediated by ferrous iron chelated to several sites on the ArmA molecule that were mutated to cysteine. This data suggests that significant conformational changes in 30S structure are involved in productive binding of ArmA. We hypothesized that a precursor intermediate in the biogenesis of the 30S subunit might be the optimal substrate for ArmA enzymes in vivo. To test this, we prepared 30S particles partially depleted of proteins by treatment with increasing concentrations of LiCl and assayed them for ArmA methylation. Even low concentrations of LiCl alter the 30S particles and greatly diminish their susceptibility to methylation. We also tested a previously identified pre-30S particle from E. coli for susceptibility to ArmA methylation and found it to be inferior to intact 30S particles as a methylation substrate. Although G1405 is near the binding site of initiation factor 3 (IF3) and the nucleotides methylated by KsgA, neither the presence of IF3 nor the absence of nucleotide methylation by KsgA affected ArmA activity. However, binding of KsgA does inhibit ArmA methylation. These results support the hypothesis that ArmA methylates a structure of the 30S subunit significantly different from the well-known, translationally active form in which G1405 is inaccessible and that mature 30S ribosomal particle can undergo conformational changes, which are necessary for ArmA methylation.

A-33 Bioluminescent Osteoclasts: Characterization Of Mtrap-Luciferase Transgenic Mice In Vivo And In Vitro

Tamer M. Hadi, Mark A. Subler, Greg E. Campbell, Christina Boykin, Jolene J. Windle
Human and Molecular Genetics

The effective study of bone remodeling, metabolic disease, and potential therapeutics requires careful analysis of changes in osteoclast formation and activity. Bioluminescent imaging represents a quantitative, high resolution tool by which osteoclast induction can potentially be monitored both in vivo and in vitro. Here we describe the generation and characterization of transgenic mice that express luciferase under the control of an osteoclast-selective promoter, and demonstrate potential applications in vivo and in vitro. Specifically, we used the mouse tartrate-resistant acid phosphatase (mTRAP) promoter (which within the bone is osteoclast-specific), to drive expression of a synthetic firefly (Photinus pyralis) luciferase gene, luc2, in transgenic mice. Eight independent mTRAP-Luc founder mice were generated, and lines of mice were established from each. Mice from each line were then characterized with respect to luciferase expression in vivo and in bone marrow-derived osteoclast cell cultures using a Xenogen IVIS® 200 Imaging System. In sum: • Moderate luciferase expression can be detected in the skeleton in vivo, primarily in the tail and paws. The sensitivity of detection of expression in bone may be limited by the relatively low number of luciferase-expressing cells (i.e., osteoclasts) in bone under basal conditions and concomitant expression in numerous other tissues, including kidney, liver, spleen, and thymus. • A modest increase in luciferase expression could be detected in vivo following supracalvarial injection of TNF-alpha for five consecutive days. • Luciferase expression is readily detected in osteoclasts in culture, providing a more sensitive indicator of early osteoclast differentiation than TRAP staining. • The timecourse for induction of luciferase expression during osteoclast differentiation in marrow cell cultures parallels the induction of TRAP expression. • Luciferase activity provides a rapid, safe, nontoxic, non-terminal, repeatable means to monitor osteoclast differentiation longitudinally over time.

A-34 In Vitro Manipulation Of Adult Human Neural Stem/Neural Progenitor Cells Isolated From Neurosurgical Resection For Use In Cell Replacement Therapy Following Traumatic Brain Injury.

Wendy Reid, Martin Graf, Kathryn Holloway, Helen Fillmore, Dong Sun.
Neurosurgery

Neural stem cell and progenitor cell (NS/NPC) transplantation offers a potentially new and promising treatment for repairing the brain following TBI. Adult NS/NPC are especially promising as they could serve as a donor source of autologous cells for brain injured patients. Thus far, we and others have successfully isolated NS/NPC from the human cortex following neurosurgical resection and established protocols for in vitro expansion. Previous studies in our lab demonstrate that adult NS/NPC isolated from the human cortex can survive acutely after transplantation into the injured brain. Although the results of these studies are promising, questions remain of whether the proportions of surviving cells that differentiate and become functional could be increased by transplanting NS/NPC at different developmental stages. In order to achieve the optimal culture conditions before transplantation, human NS/NPC from the neocortex and hippocampus of several patients were cultured in the presence of growth factors for 1, 2 and 3 weeks. Growth factors tested included platelet-derived growth factor-BB (PDGF-BB, 30ng/ml), glial-cell derived neurotrophic factor (GDNF, 20ng/ml), brain-derived neurotrophic factor (BDNF, 50ng/ml) and fibroblast growth factor/epidermal growth factor (bFGF/EGF, 10ng/ml each). The influence of these growth factors on cell proliferation was accessed using a thymidine proliferation assay. We found that compared to all other growth factors tested, cells cultured with PDGF-BB resulted in a significant 5-10 fold elevation in cell proliferation in all cell lines studied and at all time points. Cell differentiation was assessed using immuno-histochemistry and western blot analysis. Although there was some variability in the response of cells from different patients to growth factors, we found nestin-positive progenitor cells to be high in all culture conditions and a general trend towards increased Tuj1, a marker of immature neurons, following PDGF-BB administration. The results provide evidence that priming cells in vitro with PDGF-BB leads to increased proliferation and differentiation of cells into a more neuronal-restricted phenotype. Current studies are exploring the potential of adult human NS/NPC, primed in vitro with PDGF-BB and/or modified via genetic manipulation to secrete PDGF-BB, to survive, differentiate and potentially improve cognitive outcome following transplantation into the injured rat brain.

A-35 Tissue Specific Microrna Target Prediction In Humans

William T. Budd Zendra Zehner Nihar Sheth
Center for the Study of Biological Complexity

MicroRNA molecules are short, endogenous RNAs that play important roles in post translational gene regulation. Mature microRNA molecules are thought to bind to the 3'-untranslated region of the messenger RNA causing translational repression or gene product degradation. MicroRNAs have been shown to be involved in many critical and diverse cellular processes from cellular differentiation, viral defense, and regulation of cellular signaling networks. MicroRNAs have been shown to play a role in the development of several forms of human cancer including breast, prostate, and lung. Elucidating the exact role of microRNA regulation and dysfunction in disease has been and continues to be a complicated undertaking. The past decade has seen the development of many computational methods to predict microRNA targets. The single best tool is only able to achieve 50% sensitivity. In order to accomplish this level of precision, the program must predict nearly 2700 targets per microRNA molecule. It is common for researchers interested in identification of putative microRNA targets to intersect the predictions of multiple target prediction programs. By increasing the sets of predicted targets, researchers are able to increase the sensitivity of the methods, but there is a subsequent increase in the number of predictions per microRNA and a presumed loss of specificity. This work describes the development and utilization of a tissue-specific microRNA target prediction program for use in the identification of human microRNA targets for the prostate tumor suppressing microRNA HSA-miR-17-3p. The purpose of this program is to retain the increased sensitivity achieved by intersecting various microRNA prediction programs, while reducing the overall number of predictions per microRNA. Our approach was able to reduce the list of potential putative targets to two genes.

A-36 Opposing Roles For Lyn And Fyn Kinases In Mast Cell, Basophil And Macrophage Igg Receptor Signaling

Yves T. Falanga and John J. Ryan
Biology (Integrative Life Sciences)

Mast cells are tissue resident cells and are key players of the innate immune system in atopic diseases. They function as effector cells and also have immunorelgulatory roles in infection. Once activated, they degranulate and produce cytokines, resulting in the recruitment of other immune cells and the clearance of the infectious agent. It is mainly known that mast cells are activated via the high-affinity immunoglobulin E (IgE) receptor FcεRI which downstream acti- vates multiple intracellular pathways leading to degranulation and cytokine production. In this study we focus on the mast cell's activation via the immunoglobulin G (IgG) receptor FcγR and the downstream signaling effects of Fyn and Lyn kinases. We use Fyn and Lyn deficient mast cells to elucidate their function in the signaling pathway downstream of FcγR and show that FcγR like FcεRI with IgE, triggers mast cell degranulation and cytokine release after IgG cross-linking and this in a Fyn and Lyn-dependant manner. Lyn deficient mast cells displayed an increase in degranulation (Histamine, Leukotriene C4) and in cytokine release (TNF, MIP-1α and IL-13) whereas the opposite phenomenon is observed when Fyn is knocked out. More importantly and in an extended study, we show that Fyn kinase is required not only for the activation of mast cells but also for the ac- tivation of basophils and macrophages via FcγR and IgG cross-linking. This brings one more element to the understanding of mast cell homeostasis and the hypersensitivity mechanisms in which the previously cited cells are involved.

A-37 Design Synthesis And Interaction Studies Of Dual, Direct, Non-Saccharide, Allosteric Modulators Of Factor Xa And Thrombin

Preetpal Singh Sidhu*, Qibing Zhou, and Umesh R. Desai.
Medicinal Chemistry

To design and synthesizenovel, direct,selective allosteric inhibitors of thrombin and factor Xa and study their interaction at a molecular level with the target enzymes. Specific aims include: I) Chemical synthesis of novel, sulfated and carboxylated benzofuran scaffolds including monomers, dimers and higher oligomers. II) Chemical synthesis of analog of dimer and trimers to perform extensive structure-activity relationship studies. III) Study the inhibition of thrombin, factor Xa and other coagulation enzymes by the synthetic sulfated and carboxylated benzofurans as well as determine the mechanism of inhibition. In this work, a library of small, aromatic molecules based on the sulfated low molecular weight lignin scaffold was synthesized and screened against thrombin and factor Xa. The results reveal that the designed benzofuran derivatives inhibit thrombin well. Factor Xa inhibition is being studied and preliminary results suggests that the IC50 values for factor Xa inhibition are significantly different. Structurally and mechanistically, these molecules are unique and novel. The presence of sulfate group make these molecules water soluble and less toxic.

B-01 KLF2 Is Required For Normal Heart Development In Mice

Aditi Chiplunkar, Tina Lung, Dr. Jack Haar, Dr. Joyce Lloyd
Human and Molecular Genetics

Krüppel-like factor 2 (KLF2) belongs to a family of transcription factors that have 3 C2/H2 zinc finger domains. KLF2 knockout (KO) mice die by embryonic day 14.5 (E14.5) and exhibit heart failure and hemorrhaging. KLF2 is expressed in multiple tissues including erythroid and endothelial cells, and is induced by shear stress. Our preliminary studies indicate that KLF2 KO mice in the FVBN background have abnormal development of the atrioventricular (AV) cushions of the heart. Light microscopy revealed that the E9.5 wild-type (WT, n = 3) AV cushion is lined by a single layer of endothelial cells, with underlying mesenchymal cells. In E9.5 KLF2 KO mice (n = 3), however, there is a 2-fold increase in the number of cells in the AV cushion, and these cells form multiple, disorganized layers in the AV canal. Electron microscopy revealed that compared to the WT, the E9.5 KLF2-/- AV canal appears narrower in some locations, but still allows erythroid cells to pass through. Unlike WT, the KLF2-/- AV canal is lined by endothelial cells having numerous cytoplasmic processes extending toward the lumen. In E10.5 KLF2-/- embryos (n = 3), the AV and outflow tract cushions are hypocellular with respect to mesenchymal cells, and the accumulation of cells in the AV canal persists. These findings further suggest the testable hypothesis that there may be abnormal endothelial to mesenchymal transformation (EMT) in the AV cushions of KLF2 KO embryos. Moreover, the E10.5 KLF2-/- heart has only one atrium, whereas somite-matched WT hearts have a left and right atrium by this time. Additionally, in E10.5 KLF2-/- heart, myocardium is much thinner compared to the WT heart. Based on these observations, KLF2 is required for normal heart development.

B-02 Effects Of Hemoglobin-Based Oxygen Carriers (Hbocs) On Nitric Oxide (NO) Levels In The Spinotrapezius Muscle And Mesentery Of The Rat

Andrew T. Yannaccone, Helena Carvalho and Roland N. Pittman
Physiology and Biophysics

Use of HBOCs has been limited by the side effect of increased mean arterial pressure (MAP). It is thought that HBOCs scavenge NO, leading to decreased [NO], arteriolar vasoconstriction, and increased vascular resistance and arterial pressure. Previous microcirculatory studies investigating effects of HBOC infusion have yielded contradictory results. The aim of this study was to compare responses of tissues with different metabolic activity to HBOC injection. Experiments were conducted in the spinotrapezius muscle or mesentery of anesthetized male Sprague-Dawley rats. Preparations were loaded with 5 uM DAF-2DA for 45 min. Cytosolic esterases convert DAF-2DA to DAF-2 which reacts with an oxygenated derivative of NO to form highly fluorescent DAF-2T. The DAF-2T signal was recorded with a digital CCD camera connected to a Zeiss fluorescence microscope. Vessel diameter, MAP and fluorescence were monitored under control conditions and after bolus i.v. injection of HBOC-201 in 1, 10 and 100 uM plasma concentrations. HBOC-201 increased MAP. There was vasoconstriction and an increase in DAF-2T fluorescence in the spinotrapezius preparation, whereas no vasoconstriction or increase in DAF-2T fluorescence was observed in the mesentery. These results suggest that metabolically active tissues like skeletal muscle have higher [NO] than less metabolically active tissues such as the mesentery.

B-03 The Anaplasma Phagocytophilum-Occupied Vacuole Selectively Recruits Rab Gtpases

Bernice Huang, Marci A. Scidmore and Jason A. Carlyon
Microbiology and Immunology

Anaplasma phagocytophilum is an obligate intracellular bacterium that infects neutrophils to cause human granulocytic anaplasmosis. A. phagocytophilum resides within a host cell-derived vacuole that fails to mature along the endocytic pathway, does not acidify, and does not fuse with lysosomes that facilitate oxidative killing. The molecular basis for the A. phagocytophilum-occupied vacuole's selective fusogenicity is currently unknown. A number of intravacuolar pathogens – including Chlamydia, Legionella, and Salmonella – selectively recruit specific host Rab GTPases to their vacuolar membranes to ensure proper vacuolar maturation and development. Rab family members (>60) coordinate many aspects of endocytic and exocytic cargo delivery and regulate endosomal maturation through lysosomal fusion. To assess whether the A. phagocytophilum-occupied vacuole's altered fusogenicity is attributable to altered Rab recruitment, we monitored localization of a panel of 13 representative Rabs fused to green fluorescent protein (GFP). Only 4 of the 13 Rabs are recruited to the A. phagocytophilum inclusion membrane (AIM). Rab10, Rab11, Rab1 and Rab4A – localize to 51, 43, 6 and 5 percent of inclusions, respectively. Because AIM recruitment of Rabs may be temporally regulated with respect to the Anaplasma developmental cycle we monitored recruitment of Rabs 1, 4, 10, and 11 to the AIM at multiple time points over a 24-hour period. We used siRNA to knock down expression of Rabs of interest in order to elucidate their significance to AIM development and bacterial intracellular survival. Rab GTPases cycle between a soluble GDP-bound inactive state and a vesicular membrane-associated GTP bound active state. To determine if the Rabs of interest are recruited to the AIM in a guanine nucleotide dependent fashion, we assessed their AIM localization using GTPase-deficient and GDP-restricted GFP-Rab fusions. Collectively, these data demonstrate that the A. phagocytophilum-occupied vacuole facilitates selective interactions with host vesicular trafficking pathways by recruiting specific Rab GTPases while excluding others.

B-04 Regulation Of Pre-Mrna Splicing By Group Via Phospholipase A2 (Ipla2)

Bhargavi Emani, Xiaoyong Lei, Sasanka Ramanadham, and Suzanne E. Barbour
Biochemistry and Molecular Biology

Ceramides are bioactive lipids that can promote splicing of apoptosis-related genes, including caspase 9 and Bcl-x. A recent study demonstrated that expression of neutral sphingomyelinase (NSMase), an enzyme that hydrolyzes sphingomyelins to generate ceramide, is regulated by Group VIA phospholipase A2 (iPLA2)-dependent mechanism during β-cell apoptosis. This prompted us to hypothesize that iPLA2 is upstream of ceramide generation in the process regulating splicing of apoptotic genes. To test this, Jurkat T cells were treated with the selective inhibitor of iPLA2, bromoenol lactone (BEL), RNA was isolated and converted to cDNA, and caspase 9 and Bcl-x mRNA species were amplified using RT-PCR. Inhibition of iPLA2 activity with BEL caused a significant shift in splicing favoring variants encoding the anti-apoptotic forms of caspase 9 (caspase 9b) and Bcl-X (Bcl-xL). This shift was consistent with previously reported effects of ceramide and suggested that iPLA2 regulates splicing of these pre-mRNAs. iPLA2 also appears to regulate splicing of its own pre-mRNA, as BEL induced a shift in splicing from the ankyrin iPLA2-1 variant that encodes dominant-negative iPLA2 to the mRNA encoding full length, catalytically active iPLA2. We next determined whether iPLA2 regulates splicing events during a biological response. INS-1 insulinoma cells were treated with thapsigargin to induce ER stress, which can eventually lead to apoptosis. Thapsigarin-treated INS-1 cells exhibited an increase in the ratio of Bcl-xS (pro-apoptotic) to Bcl-xL (anti-apoptotic) but BEL prevented this shift in splicing. Together, these observations indicate that iPLA2 plays an important role in the regulation of pre-mRNA splicing of key apoptotic factors. Our findings therefore suggest a novel role for iPLA2 in determining whether cells survive or undergo apoptosis.

B-05 Microcirculatory Effects Of Hemorhage And Rescucitation On Tissue Oxygenation Using A Hemoglobin-Based Oxygen Carrier

Bjorn K Song, Michael D Connery1, P. Moon-Massat, Aleksander S. Golub, Roland N Pittman.
Physiology and Biophysics

This microcirculatory study compared the effects on oxygen transport of three resuscitation fluids: 5.9% human serum albumin (HSA), an iso-oncotic non-oxygen carrying colloid solution; HBOC-201 (Biopure Corp., Cambridge, MA), a hemoglobin-based oxygen carrier (HBOC); and HBOC-201 with nitroglycerin (NTG). Measurements using intravital microscopy were made on the spinotrapezius muscle of 22 male Sprague-Dawley rats (274 ± 6 g). Interstitial PO2 was measured using phosphorescence quenching microscopy, and recorded before and after hemorrhage, 20 (R20), 60 (R60), and 120 (R120) minutes after resuscitation. Baseline interstitial PO2 (60 ± 2 mmHg) decreased significantly during hemorrhage (to 2 ± 1 mmHg). Upon resuscitation, the resuscitation fluids improved tissue oxygenation to values near baseline. However, the PO2 decreased over the following two-hour interval; although, the group resuscitated with both HBOC-201 and NTG had a significantly higher PO2 than either the HSA or HBOC groups. Arteriolar diameters decreased with hemorrhage and, even though they were restored toward baseline with any of the resuscitation fluids, there were no significant differences among the three fluids used. Mean arterial pressure (MAP) decreased significantly from 99 ± 3 mmHg to 21 ± 1 mmHg with hemorrhage. During R20 the HSA group had a MAP of 114 ± 4 mmHg, while the HBOC and the HBOC + NTG groups had an elevated MAP at 164 ± 5 and 131 ± 6, respectively. Over time, MAP was restored to near baseline values with any of the fluids, i.e., HSA (89 ± 10 mmHg), HBOC (122 ± 8 mmHg), and HBOC + NTG (97 ± 11 mmHg).

B-06 ADAM10 Critically Regulates B Cell Development By Activating Notch2 Signaling

David R. Gibb, Mohey El Shikh, Dae-Joong Kang, Warren J. Rowe, Rania El Sayed, Joanna Cichy, Hideo Yagita, John G. Tew, Peter J. Dempsey*, Howard C. Crawford*, Daniel H. Conrad*
Microbiology and Immunology

The proteolytic activity of a disintegrin and metalloproteinase 10 (ADAM10) regulates cell fate decisions in drosophila and mouse embryos. However, in utero lethality of ADAM10 knockout mice has prevented examination of ADAM10 cleavage events in lymphocytes. To investigate their role in B cell development, we generated B cell-specific ADAM10 knockout and transgenic (Tg) mice. Intriguingly, deletion of ADAM10 prevented development of the entire marginal zone B cell (MZB) lineage. Additionally, cleavage of the low affinity IgE receptor, CD23, was profoundly impaired, but subsequent experiments demonstrated that ADAM10 regulates CD23 cleavage and MZB development by independent mechanisms. Development of MZBs is dependent upon Notch2 signaling, which requires proteolysis of the Notch2 receptor by a previously unidentified proteinase. Further experiments revealed that Notch2 signaling is severely impaired in ADAM10-null B cells. Thus, ADAM10 critically regulates MZB development by initiating Notch2 signaling. In addition, Notch signaling in the bone marrow prevents stem cell commitment to the B cell lineage. Thus, overexpression of ADAM10 on B cell progenitors in ADAM10 Tg mice caused a complete block in B-2 cell development, mimicking the phenotype of Notch (NICD) Tg mice. This study identifies ADAM10 as the in vivo CD23 sheddase and an important regulator of B cell development. Moreover, it has important implications for the treatment of numerous CD23 and Notch mediated pathologies, ranging from allergy to cancer.

B-07 Opioid Tapering In Children: A Critical Review Of The Literature

Deborah Fisher
Pediatric Nursing

Purpose: To synthesize and critically analyze literature related to pediatric opioid withdrawal Design: Critical review of literature related to pediatric opioid tapering and withdrawal Methods: Studies published in peer-reviewed journals were systematically searched using Pubmed, CINAHL, and PsychINFO. Findings: The majority of published research has focused on the episodic nature of withdrawal symptoms during opioid tapering. Only one study produced a valid and reliable pediatric opioid withdrawal symptom assessment instrument, and one study produced a valid and reliable pediatric opioid and benzodiazepine symptom assessment instrument. One study conducted in an adult and pediatric population analyzed the effect of use of an opioid taper algorithm on occurrence and nature of opioid withdrawal symptoms. Conclusion: The scope of research on pediatric opioid withdrawal is limited. Studies examining the effect of an opioid taper algorithm on incidence of withdrawal symptoms in children are sorely needed. Further validation of the two withdrawal assessment tools for children is warranted.:

B-08 Bacterial Cpgs Synergize With Il-15 To Enhance Cd8+ T Cell Function

Derek Hambright, Dustin Cobb, Siqi Guo, and Ronald B. Smeltz
Microbiology and Immunology

CD8+ T cell exposure to the cytokine IL-15 typically results in the formation of T cell memory. Paradoxically, we previously reported that IL-15 can enhance CD8+ effector functions by increasing T cell sensitivity to IL-12. To determine the clinical relevance of our findings we examined the efficacy of bacterial CpGs, which have potent immunomodulatory effects on antigen presenting cells (APC), including induction of proinflamatory cytokines (ie. IL-12). In addition, CpGs can directly stimulate T cells. To determine if IL-15 could synergize with CpG to enhance CD8+ T cell functions, we co-cultured naïve CD8+ T cells with anti-CD3 as well as CpG and/or IL-15. Strikingly, we observed that CD8+ T cells exposed to CpG and IL-15 caused a significant increase in IFN-g production. The effect of CpG+IL-15 was synergistic, not merely additive since addition of IL-15 alone produced only modest levels of IFN-g. Importantly, the observed synergy required IL-12, as T cell responses were diminished in the presence of a neutralizing antibody to IL-12. Further experiments revealed that CpG acted primarily by stimulating IL-12 production by APC, and that T cell expression of the transcription factor T-bet was required. These data suggest that the synergy between CpG and IL-15 involves both APC and T cell-dependent effects. We propose that the synergistic combination of bacterial CpG and IL-15, a feature of lymphopenia/lymphodepletion, could be exploited for effective adoptive cellular immunotherapy in the treatment/regression of solid tumors.

B-09 T-Bet Dependent Regulation Of Cd4 Th17 Cells During Trypanosoma Cruzi Infection

Drew Cobb, Derek Hambright, and Ronald B. Smeltz
Microbiology and Immunology

The T-box transcription factor T-bet is an important regulator of T cell differentiation and effector functions. Investigation of the role of T-bet in immunity to the intracellular parasite Trypanosoma cruzi revealed that T-bet is a critical regulator of antigen-specific Th17 development. CD4 Th17 responses have been implicated in many inflammatory processes which include infectious diseases, asthma, and various autoimmune disorders such as experimental autoimmune encephalomyelitis (EAE) and arthritis. In the context of T. cruzi infection, the absence of T-bet results in a potent Th17 response that is detrimental to host resistance despite normal levels of the Th1 cytokine IFN-gamma. This result prompted us to further investigate the molecular mechanisms by which T-bet regulates the development of Th17 CD4 T cells. We propose several approaches to elucidate the mechanism of T-bet dependent suppression of the Th17 phenotype. First, we will utilize retroviral mediated gene delivery to determine the effect of various mutations of T-bet on the regulation of Th17 differentiation. In addition, we will explore the potential interaction between T-bet and the transcription factor Runx3 and their ability to regulate both Th1 and Th17 differentiation during T. cruzi infection. These studies will be accomplished using a combination of retrovirus-mediated delivery and Cre-mediated deletion of Runx3 from CD4 T cells. These proposed studies will contribute to our understanding of Th17 development at the molecular level, as well as T cell responses to infection.

B-10 Computational Studies: Binding Mode Of Alpha2A-Adrenoceptors

Genevieve S. Alley, Philip D. Mosier, Malgorzata Dukat
Medicinal Chemistry

m-Chlorophenylguanidine (MD-354) binds at low- and high-affinity states of the alapha2A-adrenoceptors (ARs) (Ki = 110 and 825 nM, respectively) and behaves as a weak partial agonist. 3-D homology models of the alpha2A-AR inactive and active state were constructed using the beta2-AR X-ray crystal structure as the template. To validate the models, the endogenous ligands were docked. The docked poses of (R)-epinephrine and norepinephrine showed favorable ligand-receptor interactions: N+ - D3.32, beta-OH - D3.32, m-OH - S5.42, and p-OH - S5.46, while the beta-OH of the lower affinity (S)-isomers were unable to interact with D3.32. These findings are in agreement with mutagenesis data. Four low-energy rotamers of MD-354 were identified in a systematic search and then docked in both models. In the active model, two rotamers docked in a similar pose as the endogenous ligands, in which the guanidinium moiety formed an ionic bond with D3.32 and the m-Cl group formed a H-bond (HB) with S5.46. In the inactive model, three MD-354 rotamers formed an ionic bond with D3.32, but formed no HB with S5.42 or S5.46. However, there were additional favorable interactions: i) hydrophobic: chlorophenyl moiety with F6.52, ii) HB: amidine N with Y6.55. In the alpha2A-AR active state model, MD-354 forms a HB between the m-Cl group and S5.46 (similar to the p-OH in the endogenous ligands). The decreased affinity of MD-354 for the high-affinity state compared to the endogenous ligands can be explained by its lack of interaction with S5.42 and a weaker halogen HB. In the inactive model, MD-354 is shifted closer to D3.32 which optimizes the ionic interaction and increases hydrophobic interactions, which could explain the increased affinity of MD-354 at the alpha2A-AR low-affinity state. MD-354 might be a weak partial agonist due to no interaction with S5.42 and the weaker halogen HB. The binding mode of MD-354 in the alpha2A-AR models is consistent with its binding and functional activity.

B-11 Evidence For Genes On Chromosome 2 Contributing To A Variety Of Psychiatric Outcomes

Jacquelyn Meyers, Danielle M. Dick, Fazil Aliev, John Nurnberger Jr., John Kramer, Sam Kuperman, Bernice Porjesz, Jay Tischfield, Howard Edenberg, Tatiana Foroud, Marc Schuckit, Alison Goate, Victor Hesselbrock & Laura Bierut
Human and Molecular Genetics

Twin studies provide strong evidence of shared genetic liability across a number of different psychiatric conditions. Data from the Collaborative Study on the Genetics of Alcoholism suggest that chromosome 2 may be one region containing genes with pleiotropic effects on a variety of related psychiatric conditions. Chromosome 2 first emerged as a region of interest in the COGA project with linkage to alcohol dependence, near the marker D2S379. Subsequently, linkage to the same region was identified with the phenotypes of suicide attempts and conduct disorder. Interestingly, each of these phenotypes is characterized by elements of impulsivity and behavioral undercontrol. In the present study, we report linkage analyses that jointly consider the phenotypes that have previously been linked in the region in the COGA sample: alcohol dependence, conduct disorder, and suicide attempts. In addition, we followed-up on the linkage signal in the region by testing for association with a systematic screen of Single Nucleotide Polymorphisms across the region. Combining these phenotypes in a joint analysis tests the hypothesis that the phenotypes are alternative manifestations of a shared underlying susceptibility.

B-12 Adjuvant Potential Of Double Stranded Rna

James D. Marion and Jessica K. Bell
Biochemistry and Molecular Biology

Adjuvants trigger a specific immune response in the presence of a target antigen. Currently, the only FDA-approved vaccine adjuvant is alum. To develop an alternative to alum that enhances the immune response, work has focused on the ligands that initiate the innate immune response via pattern recognition receptors (PRRs). Toll-like receptor 3 (TLR3), a PRR, is stimulated by the viral genomic material or replicative intermediate, double stranded RNA (dsRNA). Previous studies have shown that TLR3 activation in vivo requires ≥90bp of dsRNA (Leonard et al. PNAS (2008) 105:258-63). The objective of this study was to determine the adjuvant potential of an ~139bp dsRNA molecule. Large-scale synthesis of 139bp dsRNA from a T7 RNA polymerase-based in vitro system produced ~1.4 mg of material. To measure adjuvant potential, immature dendritic cells were stimulated with the 139bp dsRNA and assessed for maturation markers. Controls included no stimulation and stimulation with positive controls, lipopolysaccharide (LPS) or polyinosinic:polycytidylic acid (pI:pC). To obtain immature dendritic cells, monocytes were cultured with granulocyte/macrophage colony-stimulating factor (GM-CSF) and interleukin 4 (IL-4) for 8 days (Sallusto et al. J. Exp. Med (1994) 179:1109-18). Differentiation into immature DCs was confirmed by loss of CD14 expression and expression of CD1a via FACS analysis. Following 12-16 h of 139bp dsRNA or LPS or pI:pC stimulation, maturation of dendritic cells was assessed by expression of CD80 and CD86 again by FACS analysis. 139bp dsRNA, LPS and pI:pC stimulation resulted in matured DCs. These initial results indicate that 139bp dsRNA is sufficient to initiate an innate immune response. Future studies will define if TLR3 or another dsRNA receptor (RNA-dependent protein kinase receptor-PKR; retinoic acid inducible gene I-RIG-I; melanoma differentiation–associated gene 5-mda5) is essential for the DC maturation observed.

B-13 CB1 Agonist-Like CNS Effects Following Prolonged Inhibition Of Monoacylglycerol Lipase (MAGL) Undergo Tolerance

Joel E. Schlosburg, Divya Ramesh, James J. Burston, Steven G. Kinsey, Lamont Booker, Rehab A. Abdullah, Jonathan Z. Long, Dana E. Selley, Benjamin F. Cravatt and Aron H. Lichtman
Pharmacology and Toxicology

Study of the endocannabinoid system is primarily focused on the two major endogenous ligands, anandamide (AEA) and 2-arachidonoylglycerol (2-AG), and the enzymes largely responsible for their rapid catabolism, fatty acid amide hydrolase (FAAH) and monoacylglycerol lipase (MAGL), respectively. Inhibitors of FAAH, and FAAH (-/-) mice, have allowed researchers to examine the physiologic role and therapeutic potential of elevating endogenous AEA levels. FAAH inhibition has shown promising efficacy in models of pain, emotionality, and various other endocannabinoid modulated systems, with the absence of eliciting CNS side effects commonly associated with CB1 receptor agonists. Specifically, FAAH blockade lacks dependence liability and cannabinoid subjective effects, does not show cross-tolerance to cannabinoid agonists, and does not cause CB1 receptor down-regulation. With the advent of JZL184, a selective and potent MAGL inhibitor, we can now examine the behavioral and physiological consequences of elevating brain 2-AG levels for prolonged periods. In the present study, we investigated the cannabimimetic behavioral effects and biochemical adaptations that occur to the endocannabinoid system following once-daily dosing of JZL184 (40 mg/kg) for six days. FAAH (+/+) and (-/-) mice treated with repeated vehicle, acute JZL184, or repeated JZL184 were evaluated for behavioral cannabimimetic tetrad tolerance, cross-tolerance to THC in tetrad, and somatic signs of CB1 receptor antagonist precipitated withdrawal. Acute JZL184 showed mild analgesia in the tail immersion test, with both FAAH genotypes showing complete tolerance to the drug's analgesic effects with repeated dosing. Mice treated with repeated JZL184, regardless of FAAH genotype, did not exhibit THC-induced antinociceptive or hypothermic effects, suggesting substantial behavioral cross-tolerance. Mice treated with repeated JZL184 also exhibited mild cannabinoid precipitated withdrawal signs similar in magnitude to mild THC dosing regimens. These data provide insight into the respective functional adaptations resulting from prolonged elevation of AEA and 2-AG.

B-14 Faah Inhibition Reverses Lipopolysaccharide-Induced Mechanical Allodynia

Lamont Booker1, Steven G. Kinsey1, Kay Ahn2, Benjamin F. Cravatt3, Aron H. Lichtman1
1Department of Pharmacology and Toxicology, 2Pfizer Global Research and Development, Groton, CT,
3The Skaggs Institute, The Scripps Research Institute, La Jolla, CA

Inflammatory pain is generally a secondary response to an infection or wound healing. The onset of inflammatory pain is often characterized by edema and allodynia to mechanical stimuli. New treatments for hyperalgesia are needed. The endocannabinoid system (ECS) has been implicated in a variety of acute pain models. The ECS is comprised of two primary ligands, anandamide (AEA) and 2-arachidonoylglycerol (2-AG), two receptors (CB1 and CB2) that bind these endocannabinoids, and the enzymes responsible for the biosynthesis and degradation of the endocannabinoids. AEA signaling is short-lived, due to its rapid degradation by the enzyme fatty acid amide hydrolase (FAAH). Additionally, genetic deletion or pharmacological inhibition of FAAH increases AEA levels in the brain and reduces nociception in a wide range of preclinical pain models. In the present study, we investigated whether genetic deletion or pharmacological inhibition of FAAH reverses inflammatory pain induced by intraplantar (ip.l) lipopolysaccharide (LPS) into a hind paw. LPS elicited a concentration-dependent increase in mechanical allodynia with significant differences at 2.5 μg and 25 μg of LPS per paw. Gabapentin dose-responsively reversed the mechanical allodynia, ED50 (95% Confidence Interval)= 8.3 mg/kg (4.8-14.4). To determine the involvement of neuronal and non-neuronal FAAH, we used genetically modified mice which express FAAH only in neuronal tissue (FAAH-NS), mice with no substantial FAAH expression (FAAH (-/-)), and mice with normal functioning FAAH levels (FAAH (+/-)). FAAH (-/-) and not FAAH-NS mice showed an anti-allodynic phenotype to LPS. Using a pharmacological approach to block FAAH, we treated mice with PF-3845, an irreversible FAAH inhibitor. PF-3845 significantly reduced mechanical allodynia elicited by LPS up to 3-fold. Rimonabant completely blocked the anti-allodynic effects of PF-3845, indicating that its effects were mediated through a CB1 receptor mechanism of action. In addition, the saline injected paw responses of FAAH (-/-) mice as well as PF-3845 treated mice were not affected by drug treatments. Taken together, these data suggest that neuronal FAAH is a key regulator involved in inflammatory pain, which actions are mediated through the CB1 receptor.

B-15 Adenovirus Infection Alters Metabolism In Adipose And Hepatic Tissues

Marianna Sukholutsky, W. Palmer Wilkins III, and Suzanne E. Barbour
Biochemistry and Molecular Biology

Recent studies have shown a link between adenovirus infection and obesity. This prompted the hypothesis that adenovirus-5 (Ad-5) infection might augment hepatic and/or adipose tissue lipid metabolism. To test our hypothesis, mice were infected with Ad-5 and screened for changes in lipogenesis and plasma markers associated with the metabolic syndrome. We observed increased expression of sterol regulatory element binding protein 1 (SREBP1) in infected liver tissues, but not in adipose tissues and this correlated with elevated plasma and hepatic triglyceride levels. Elevated expression of adiponectin was seen in Ad-5 infected adipose tissues and this correlated with phosphorylated AMPK in infected liver tissues, suggesting that the AMPK pathway was activated in livers of Ad-5 infected mice. We observed elevated levels of phosphorylated ACC and reduced expression of PEPCK, both downstream targets of AMPK, in livers of Ad-5 infected mice. As PEPCK is an enzyme essential for gluconeogenesis, we hypothesized that Ad-5 infection would reduce blood sugar. Indeed, infected mice exhibited a transient decline in plasma glucose. We next performed experiments to delineate the mechanism whereby Ad-5 induced SREBP1 and used Ad-5 infected HepG2 cells for this purpose. Ad-5 and insulin activate similar signaling pathways, therefore we hypothesized that Ad5-induced SREBP1 was mediated through PI 3-kinase and its target PKCι. Ad-5 infected HepG2 cells exhibited phosphorylation of PKCι and a myristoylated PKC peptide inhibitor suppressed Ad-5-mediated induction of SREBP1 and its downstream target acetyl CoA carboxylase (ACC). These studies demonstrate that Ad-5 infection induces changes in gene expression, glucose, and lipid metabolism and prompt the novel hypothesis that this common respiratory pathogen may be associated with the Metabolic Syndrome.

B-16 Properties Of The Icp0 Tegument Protein Of Hsv-1

Mark G. Delboy, Carlos R. Siekavizza-Robles, and Anthony V. Nicola
Microbiology and Immunology

Herpes simplex virus (HSV) immediate-early (IE) protein ICP0 is a multi-functional regulator of HSV infection. ICP0 that is a present in the tegument layer has not been well-characterized. Protein composition of wild type and ICP0-null virions was similar, suggesting that absence of ICP0 does not grossly impair virion assembly. ICP0 has a RING finger domain with E3 ubiquitin ligase activity that is necessary for IE functions. Virions with mutations in this domain contained greatly reduced levels of tegument ICP0, suggesting that it influences tegument incorporation of virion ICP0. Virus-cell fusion is not influenced by ICP0, but the role of tegument ICP0 in delivery of capsids to the nucleus has not been investigated. The efficiency of incoming capsid arrival at the nucleus at 2.5 hours was dependent on ICP0. ICP0 thus appears to regulate the efficiency of HSV capsid transport to the nucleus in addition to influencing HSV replication. We recently identified a novel role for the host proteasome in a pre-immediate early event in HSV infection. Incoming HSV is inhibited by the proteasome inhibitor MG132 at a post-penetration step. The relationship of HSV ICP0 to the ubiquitin-proteasome system prompted us to investigate its role in entry of HSV. In virions with ICP0 deletions or RING finger domain mutations, entry was resistant to inhibition by MG132 as determined by beta-galactosidase gene expression and confocal microscopy. These results demonstrate new properties of tegument ICP0 including the regulation of HSV pre-immediate early events.

B-17 Inside-Out Signaling Of Estradiol-Mediated S1p Export From Breast Cancer Cells

Masayuki Nagahashi(1,2), Roger H. Kim(1), Jeremy C. Allegood(2), Poulami Mitra(2), Subramaniam Ramachandran(1,2), Kuzhuvelil B. Harikumar(2), Nitai C. Hait(2), Sheldon Milstien(2), Sarah Spiegel(2) and Kazuaki Takabe(1,2)
(1) Division of Surgical Oncology, (2) Department of Biochemistry and Molecular Biology and the Massey Cancer Center, VCU

Sphingosine-1-phosphate (S1P), a potent sphingolipid mediator, regulates diverse cellular processes important for breast cancer progression, including cell proliferation, survival, migration, and angiogenesis. Two specific sphingosine kinase isoenzmes, SphK1 and SphK2, which have different subcellular localizations and distinct functions, produce S1P that mainly acts in autocrine and/or paracrine manners by binding to five specific cell surface G protein-coupled receptors, S1P1-5. SphK1 is overexpressed in breast cancers and promotes estradiol (E2)-dependent xenograft tumorigenesis of MCF7 breast cancer cells, yet it is not known how intracellularly generated S1P is secreted by tumor cells. In this work, we show that overexpression of SphK1, but not SphK2, increased S1P export from MCF7 cells, although both similarly increased its intracellular levels. Conversely, downregulation of SphK1, but not SphK2, with specific small interfering RNAs decreased export of S1P. Both E2 and epidermal growth factor (EGF) activated SphK1 and production of S1P but only E2 stimulated rapid release of S1P from MCF7 cells, as determined by labeling with [3H]sphingosine and differential extraction of [3H]S1P and by direct mass measurements using ESI-MS/MS. E2-induced S1P and dihydro-S1P export required ER-alpha, not GPR30, and was suppressed either by pharmacological inhibitors or gene silencing of ABCC1 (multi-drug resistant protein 1) or ABCG2 (breast cancer resistance protein). Inhibiting these transporters also blocked E2-induced activation of ERK1/2, indicating that E2 activates ERK via downstream signaling of S1P. Taken together, our findings suggest that E2-induced export of S1P mediated by ABCC1 and ABCG2 transporters and consequent activation of S1P receptors may contribute to nongenomic signaling of E2 important for breast cancer pathophysiology.

B-18 Effect Of Serum On Staphylococcus Aureus Biofilm Formation

Nabil Abraham, Kimberly Jefferson
Microbiology and Immunology

Chronic wounds including diabetic foot ulcers, pressure ulcers, and venous leg ulcers are a grave worldwide health problem. The basis for their failure to heal is multifactorial and involves both host-related factors such as poor perfusion and external factors such as bacterial colonization. Recent evidence implicates bacterial biofilm formation in the etiology of these wounds. Because they are exposed to the environment, wounds are invariably colonized by multiple bacterial species. Staphylococcus aureus is a frequent isolate from chronic, non-healing wounds. Our goal is to determine the effect of innate immune defenses on the establishment of a biofilm by bacteria such as S. aureus so that we can understand how biofilms become established in chronic wounds and how to prevent them. We found that a heat-stable serum component with a molecular weight less than 3000 inhibits biofilm formation. The component resulted in a 5 and 7 fold increase in the transcription of the negative regulators of biofilm formation icaR and codY, respectively. Our efforts are currently geared at the identification of this serum component.

B-19 The Application Of Luminescent In Vivo Imaging Using 4t1-Luc2 Cells To Determine The Best Model For Breast Cancer Progression And Metastasis

Omar Rashid1, Masayuki Nagahashi1,2, Subramaniam Ramachandran1,2, Sheldon Milstien2, Sarah Spiegel2, and Kazuaki Takabe1,2
1Division of Surgical Oncology, 2Department of Biochemistry and Molecular Biology and the Massey Cancer Center

Sphingosine-1-phosphate (S1P) is an important target for cancer treatment because it regulates cell proliferation, survival, migration, and angiogenesis, mechanisms necessary for cancer progression and metastasis. It has been previously shown that sphingosine kinase 1 (SphK1) is important for production of S1P, and many breast cancers have been shown to overexpress SphK1, which also correlates with poor prognosis clinically. To investigate SphK1's role in vivo in breast cancer progression, metastasis and treatment, requires an animal model that loyally mimics tumor biology in human. In this study, we compared subcutaneous, intra-mammary and tail vein injections of cancer cells to immunologically intact mice, in order to investigate which approach produces the best model of breast cancer progression and metastasis. 4T1-luc2 cells, a murine breast cancer cell line that stably expresses luciferase and high levels of SphK1, were used. The cells were injected into Balb/c mice subcutaneously, in the mammary fat pad, or intravenously via the tail vein. In vivo cancer progression and metastasis were monitored using Xenogen imaging. When compared with intra-mammary injection, subcutaneously injected cancer cells had diminished primary tumor growth, a decreased rate of metastasis, and histological features clinically different than that seen in breast cancer tumor growth, while tail vein injection produced a high rate of tail tumors. Our results suggest that the intra-mammary fat pad implantation most faithfully mimics breast cancer proliferative and metastatic behavior and therefore serves as an appropriate in vivo model to explore the therapeutic implications of targeting SphK1 for treatment of breast cancer.

B-20 Quantitative Structure - Pharmacokinetic Relationships (Qspkr) Of Beta-Adrenergic Receptor Ligands (Barl) In Humans

Prajakta Badri, Ph.D. Candidate, Jürgen Venitz, MD, Ph.D.
Pharmaceutics

BARL are quite diverse in their human PK characteristics. This study was to develop and validate QSPKR models for biologically relevant PK properties of BARL. Methods: A final dataset of 49 BARL (42 antagonists, 7 agonists) was compiled with systemic PK data in humans: PK variables included in-vitro fraction unbound (fu), in-vivo steady-state volume of distribution (Vdss), total, renal and nonrenal clearance (CLtot, CLren, CLnonren), and their unbound counterparts along with in-vitro β-receptor affinity (Ki). Molecular descriptors (i.e., log(D), molar volume, polar surface area, dipole moment, hydrogen bond acceptors/donors) were obtained from SYBYL and SciFinder. Linear/multiple linear regression was used to construct QSPKR models on two datasets: complete and reduced (excluding BARLs known/suspected to undergo extrahepatic metabolism, e.g., ester hydrolysis). The final models were assessed by r2 ($p<0.05$), and their predictive performance was cross-validated using the leave-one-out method (q2). Results: Log(D) was the most important molecular property affecting the systemic PK of BARL. Log(D) showed a significant effect on fu (n=34, r2=0.62), Vdssu(n=34,r2= 0.53), CLtotu(n=34,r2=0.35),CLnonrenu(n=29,r2=0.36) and CLren(n=39,r2= 0.36). Molar volume, dipole moment and log(D) showed a significant effect on log(Ki) for β1 and β3 receptors (n =15, r2 >0.60, q2>0.40). Conclusions: Plasma protein binding increases strongly with log(D), as do Vdssu, CLtotu, and CLnonrenu. As net result, CLtot, Vdss and CLnonren are not affected by log(D). Secondary to fu, CLren decreases as log(D) increases. QSPKR models using log(D) showed good predictive performance (q2>0.40) during cross-validation for fu, Vdssu and log(Ki). For CLnonrenu and CLtotu, using the reduced dataset showed improved r2 and q2, indicating the importance of extrahepatic clearance on QPKR predictions.

B-21 In Vitro Prediction Of Regional Drug Deposition From Dry Powder Inhalers

Renish R Delvadia1, Peter R Byron1, P. Worth Longest2, and Michael Hindle1
Pharmaceutics

The study sought to develop and evaluate a method to characterize the drug deposition from a powder inhaler in a realistic in vitro model of the mouth-throat (MT), and upper conducting airways (TB) during simulated inhalations. A geometrically realistic physical model of the MT and TB was constructed and installed in an airtight housing. Novolizer, a dry powder inhaler, was primed to deliver 120µg of albuterol sulfate and inserted into the mouth of the model. Air was drawn through the inhaler and model via a filter connected to a breath simulator. A multi-factorial design was implemented to investigate the effects of peak inhalation flow rate (PIFR), time to reach the peak inhalation flow rate (TPIFR) and inhalation volume (V). After each simulated inhalation, drug deposited in the inhaler mouthpiece and various regions of the model was recovered and analyzed by an HPLC method. Using an inhalation with a rapid acceleration (TPIFR = 0.15s) together with a shallow inhalation (V = 2L), there was a clear trend of increasing peripherally (beyond TB) deposited drug and decreasing drug remaining in the mouthpiece with increasing PIFR. When these experiments were repeated using a slow acceleration (TPIFR = 0.9s), this trend was less obvious. When inhalation was deep (V = 4L), inhaler emptying was unaffected by the PIFR or acceleration to PIFR. In all cases at 4L inhalation volume, increasing the PIFR, decreased MT retention and increased the drug reaching to the periphery of the model; TB was unchanged. Surprisingly, the use of a 4L inhalation volume produced no greater peripheral drug deposition when compared to a 2L inhalation volume. From this study we were able to conclude that for Novolizer, peripheral albuterol delivery mainly depends upon the PFIR.

B-22 On The Association Of Body Mass Index And Depression In A Population Based Sample Of Twins.

Roseann E. Peterson, B.A., Hermine H. Maes, Ph.D., Lindon J. Eaves, Ph.D., D.Sc.
Human and Molecular Genetics

PURPOSE: Examine phenotypic associations of body mass index(BMI) and depression and perform bivariate twin analysis to detect genetic and environmental contributions to the covariance between traits. **METHOD:** Participants were n=14,177 twins (63.9% were female) from the Virginia Twin Registry. Univariate and bivariate analyses were performed using the statistical platform Mx. **RESULTS**: Female respondents were found to have significantly lower BMI and significantly higher depression scores than males. A small negative correlation was found for males ($r=-0.069$, $p<0.05$) but not for females. However, a significant quadratic relationship was found between BMI and depression ($p<0.01$), indicating that those with the highest and the lowest BMI's were more likely to have higher depression scores. Univariate analyses of BMI estimated the additive genetic effect to be 75% in females and males, common environment 0% in males and 1% in females, and unique environment 25% in males and 24% in females. Univariate analyses of depression scores estimated the additive genetic effect to be 28%, common environment 6%, and unique environment 66%. A significant genetic correlation was found in females ($rg=0.055$) but not males. Since the relationship between BMI and depression was not linear bivariate methods will be developed to accurately reflect this relationship and depression symptom profiles will also be analyzed.

B-23 Fullerene C70 Derivatives Inhibit Mast Cell Mediated Airway Inflammation And Eosinophilia Associated With Chronic Asthma

Sarah K. Norton*, Anthony Dellinger#, Robert Lenk#, Zhiguo Zhou#, Daniel H. Conrad*, Christopher L. Kepley# *Microbiology and Immunology,, #Luna Innovations Incorporated, Danville, VA

Fullerenes are nanospheres of carbon that are extremely stable and highly reactive with oxygen free radicals. While native fullerenes are insoluble in water, the carbon cage can be derivatized by the addition of polar chemical groups, thus generating water soluble molecules. Water soluble fullerene derivatives have been shown to inhibit mast cell degranulation and cytokine release (J. Immunol. 179: 665-672), demonstrating a potential role in controlling mast cell diseases such as allergic asthma. In order to observe the effects of derivatized fullerenes on chronic features of asthma in vivo, we used a murine model of asthma pathogenesis. Mice were sensitized to ovalbumin by intraperitoneal injection and then challenged by directly introducing the protein into the lungs. Fullerene treated mice did not exhibit any acute toxicity, and when compared to PBS or vehicle treated controls, showed a significant reduction in airway eosinophilia and total airway inflammation. The data also suggest reductions of IL-4, IL-5, and TNF-α in the bronchoalveolar lavage fluid of fullerene treated mice. Together, these results suggest that fullerenes can control chronic inflammation characteristic of asthma pathogenesis, indicating the potential for their use in the treatment of chronic asthma.

B-24 Molecular Basis Of Reduced Pyridoxine 5'-Phosphate Oxidase Catalytic Activity In Neonatal Epileptic Encephalopathy Disorder

Sayali S. Karve, Faik N. Musayev, Mohini S. Ghatge, Martin K. Safo
Medicinal Chemistry

Inborn errors in pyridoxine metabolism that leads to deficiency of the active form of vitamin B6, pyridoxal 5'-phosphate (PLP) in the cell have been found to be a cause for many neurological and non-neurological disorders. PLP is an important cofactor for majority of vitamin B6 (PLP-dependent) enzymes, which catalyze more than 140 essential biochemical reactions in human metabolism, including glucose and lipid metabolism, amino acid and homocysteine metabolism, heme and DNA/RNA synthesis, and neurotransmitter synthesis. Pyridoxine 5'-phosphate oxidase (PNPO) and pyridoxal kinase (PL kinase) are the two key enzymes that metabolize and supply PLP to these vitamin B6 enzymes by both the salvage pathway and the conversion of nutritional sources of vitamin B6. Several pathogenic mutations, including homozygous missense (R229W or R95C), splice site (IVS3-1g > a), nonsense (A174X), or stop codon (X262Q) mutations in PNP oxidase cause neonatal epileptic encephalopathy. This disorder has no cure or effective treatment, and is often fatal. Our aim is to elucidate the molecular basis of reduced PNPO activity as a result of the homozygous missense mutation, R95C in human PNPO. The mutant (R95C), cloned into the expression vector pET28a(+), was transformed in Rosetta cells and expressed at 18 C overnight and at 0.05 mM IPTG concentration. Purification was carried out using Ni-NTA column resulting in about 95% pure protein (48 mg/ml). To determine the effect of the mutation on the enzyme activity, the mutant was compared with the wild type hPNPO in a kinetic assay that determined formation of PLP as an indicator of the enzyme activity. About 80% decrease in the activity of the wild type enzyme was observed. In future, we plan to study the structure of the mutant, its affinity towards FMN (a cofactor required for enzyme activity) and also the mutational effect on the enzyme stability.

B-25 Novel Substrates For The Human Serotonin Transporter: Search For A New Class Of Antidepressants Based On The Channel Properties Of Hsert.

Stefania Averaimo, Hideki Iwamoto, Ernesto Solis, Lynette Daws and Louis J DeFelice
Physiology and Biophysics

Serotonin transporters (SERT) are part of a family of neurotransmitter transporters that function by coupling the transport of the neurotransmitter to the electrochemical gradient of Na+, although Cl- and other ions may be implicated. Depolarization of the pre-synaptic neurons leads to the fusion of vesicles with the cell membrane, causing a release of the neurotransmitter into the synaptic cleft. After the neurotransmitter binds to the receptor on the post synaptic membrane, the cleft is cleared to terminate transmission. Serotonin is taken up into the pre-synaptic neuron by serotonin transporters, reloaded into the vesicles, stored and ready for the next release. Disorders of serotonergic system are among the main causes for the pathogenesis of depression, and serotonin transporters play a main role in this mechanism. In the last two decades new experiments with more advanced technologies have led to a revision of the classical model that posit an electroneutral transport cycle that couples the transport of serotonin to 1 Na+ and 1 Cl- influx to 1 K+ efflux. The new model proposes an authentic ion channel in the transporter. The transporter-channel randomly passes from its closed state to an open state, generating a leak current that can be measured by electrophysiology. The binding of serotonin leads to an increased open probability of the channel and the flow of serotonin and Na+, according to their electrochemical gradient. Flux coupling in the channel allows for the movement of serotonin against its gradient. An appreciable inward depolarizing current is generated whose amplitude can be explained only with the transporter-channel model. In addition to triciclic antidepressants, like imipramine, which also blocks other transporters, specific serotonin reuptake inhibitors (SSRI) have been developed and successfully used to treat depression (e.g., Prozac); however, due to extensive serotonergic projections, SSRIs may cause side effects. Focusing on the ion channel features of serotonin transporters, we have identified two compounds (derivatives of MPP+) that interact with serotonin transporters and could be considered as alternatives for the treatment of depression. The interaction of 5HT, MPP+ and its derivatives (called 15 and 16) elicits an increase of a depolarizing current, and the depolarizing SERT-mediated current causes an increase of excitability in mammalian cells. The effect of this current on cell excitability affects the rate of release and clearance in the rat raphe nucleus. Thus, the new compounds show major effects in controlling the concentration of 5HT in the synaptic cleft and reduced cell toxicity compared with MPP+, making them good candidates for new in vivo experiments in the search of new antidepressants.

B-26 Scribble As A Possible Map Kinase Binding Partner

Steven Christofakis, Hiroshi Miyazaki, M.D., Ph.D.
Philips Institute, School of Dentistry

Extracellular signal-regulated kinases (ERKS; mitogen-activated protein kinases, MAPKs) are known to modulate many cellular activities in response to specific extracellular stimuli and play important biological roles. Thus, perturbed kinase pathways induce pathological conditions, such as tumor development. Ras is a small GTPase that plays a crucial role in the ERK signaling pathways. We reported previously that Ras-like protein in tissue (Rit), a member of the Ras family GTPases, exclusively activates ERK6, and its over-expression confers tumorigenicity. We hypothesized that ERK6 may form a protein complex with other scaffolding molecules, similar to other known MAP kinases. We performed yeast two-hybrid assays using ERK6 as bait, where Scribble was identified as a binding partner. Scribble was originally found as a cell polarity regulating protein in Drosophila. Scribble contains 19 leucine rich repeat (LRR) domains and four tandem repeated PDZ domains. We further confirmed Scribble-ERK6 binding through immunoprecipitation (IP) assays together with other MAP kinases and detected ERK2 as another binding partner. To our surprise, no interaction was observed with the highly homologous MAP kinase ERK1 to Scribble by IP. Other kinases, including JNK, p38-alpha, -beta, -delta and ERK5 showed any binding capabilities with Scribble. IP data revealed that both ERK2 and ERK6 bind to Scribble through its LRR and PDZ domains. By deleting five amino acids from the C-terminus of ERK2 and ERK6, binding was abolished. Although, no homologous sequence is shared in these two kinases at the C-terminus. By co-transfecting kinase plasmids with or without Scribble in MDCK and NIH3T3 cells, in vitro kinase assays with ERK1, ERK2, ERK6 indicated the ability of Scribble to decrease their kinase activities, but not ERK1. This observation suggested that binding of Scribble to these kinases is fundamental for the downregulation of its kinase activity. Furthermore, focus formation assays (FFA) were performed to determine if the activated Rit signaling pathway is suppressed continuously by Scribble in NIH3T3 cells. We used RitQ79L and RasV12, constitutive activators of ERK6 and ERK2, respectively. Results suggested a role of Scribble as a tumor suppressor.

B-27 Lpa-Induced Gastric Cancer Cell Proliferation Is Mediated By Sphingosine Kinase-1

Subramaniam Ramachandran[1,2], Dai Shida[2], Masayuki Nagahashi[1,2], Sheldon Milstien[2], Sarah Spiegel[2] and Kazuaki Takabe[1,2]
Surgery

The lysophospholipids, lysophosphatidic acid (LPA) and sphingosine-1 phosphate (S1P) are important mediators of a variety of biological processes important for maintenance and progression of cancer. Autotaxin and sphingosine kinase 1 (SphK1), responsible for synthesis of LPA and S1P, respectively, are elevated in many cancer types. We previously reported that LPA markedly enhanced SphK1 and S1P3 receptor mRNA levels and transactivated EGFR in MKN-1 gastric cancer cells [Shida et al., Cancer Res. 68:6569, 2008]. We have now shown that downregulation of SphK1 or treatment with the isozyme-specific SphK1 inhibitor, SK1-I, markedly reduced LPA-mediated proliferation of MKN-1 cells. The signaling pathways responsible for LPA-induced SphK1 activation were also investigated. LY294002, an inhibitor of PI3 kinase, and U0126, a MEK1/2 inhibitor, completely abrogated LPA-induced increases in SphK1 mRNA, while inhibitors of protein kinase C, p38, or JNK did not have any effects. These results uncover PI3 kinase and ERK MAPK pathways as mediators of LPA signaling and additionally, implicate SphK1 and S1P production as potential therapeutic targets in gastric cancer.

B-28 Restoration Of Chemo/Radioresistance And Double-Strand Break Repair Proficiency By Wild-Type But Not Endonuclease-Deficient Artemis

Susovan Mohapatra, Lawrence F. Povirk, Imran Khan, Misako Kawahara-Stillion and Steven M. Yannone
Pharmacology and Toxicology

Mutations in the nonhomologous end joining (NHEJ) factor Artemis have been implicated in radiosensitive severe combined immunodeficiency or Athabascan SCID in humans as well as an increased risk of lymphoma in some settings. Artemis is an SNM1 family phospho-protein, which has been shown to have roles in V(D)J recombination, double-strand break repair and DNA damage-induced G2/M cell cycle checkpoint. Prior in vitro studies showed that Artemis has constitutive 5'-3' exonuclease activity, as well as structure-specific DNAPK-dependent endonuclease activity at DNA ends. To assess the possible role of this endonuclease activity in chemo/radioresistance, patient-derived Artemis-deficient CJ179 fibroblasts were complemented with lentiviral vectors expressing either wild-type or D165N Artemis, a mutation that eliminates its endonuclease but not its exonuclease activity. Western blotting showed that wild-type and mutant proteins were expressed at similar levels. As determined by clonogenic survival assays, expression of wild-type Artemis in CJ179 cells conferred approximately twofold resistance to ionizing radiation, as well to the radiomimetic agent bleomycin. However, CJ179 cells expressing the endonuclease-deficient mutant remained as sensitive to all three agents as cells infected with an empty vector. Measurements by γ-H2AX, 53BP1 focus formation and pulsed-field gel electrophoresis assays suggested a repair defect (10-20%) in Artemis-deficient and D165N Artemis mutant cell lines, but not in Artemis-complemented cells, particularly at 6-18 hr post-irradiation. These results, combined with previous in vitro studies, suggest that resolution of terminally blocked DNA ends by the endonuclease activity of Artemis during double strand break repair by NHEJ, may be the biologically relevant function of Artemis in conferring radioresistance.

B-29 Investigation Of A Solvent/Anti-Solvent Crystallization Process For Albuterol Sulfate

Swati Agrawal, Michael Hindle
Pharmaceutics

The purpose of this work was to investigate a solvent/anti-solvent crystallization process for albuterol sulfate (AS) focusing on the effect of critical processing variables. The method involved addition of a supersaturated AS aqueous solution (solvent) into ethyl acetate (anti-solvent). The variables investigated were the solvent/anti-solvent ratio (Ra ratio; 1:200, 1:500 or 1:1000 (w/w)). Solutions were stirred for 30 minutes at different stirring speeds (100, 200, 500, 800 rpm) and then allowed to crystallize in the solution upto 24h. Particles were characterized at various intervals during the crystallization process using different solid state characterization techniques. Particle formation was observed to occur following stirring for 30 min for all crystallization conditions. Particle size was not dependent on crystallization time with similar results immediately following stirring and at 24h ($p>0.05$, one-way ANOVA). Statistical analysis of the mass median diameter revealed a significant interaction between Ra ratio and agitation speed ($p<0.0001$) with significantly larger particles obtained at higher stirring speeds for 1:500 and 1:1000 Ra ratios. Partially crystalline particles were obtained following stirring for 30min for all conditions. Increasing the crystallization time produced an increase in crystallinity reaching 100% at 24h except for Ra ratio 1:1000 particles produced at 500 and 800 rpm. Solution crystallization of the particles was significantly correlated with a decrease in their water content. TGA analysis during the crystallization process revealed that fully crystalline particles at 24h exhibited rapid water desorption at 25 C. The water desorption for incompletely crystalline particles at 24h was much slower. Strongly bound water may induce a lower plasticizing efficiency and result in incomplete solution crystallization. Analysis of the crystallinity data revealed a significant interaction between Ra ratio, agitation speed and crystallization time ($p<0.0001$). A significant role of moisture in solution crystallization with hydrodynamic conditions influencing the particle size was revealed.

B-30 Association Of Chromosome 20 Loci With Categorical Diagnoses And Clinical Dimensions Of Schizophrenia In The Irish Study Of High Density Schizophrenia Families

Bigdeli TB et al
Human and Molecular Genetics

*Bigdeli TB1,3,‡, Maher BS1,2,3, Zhao Z1,2,3, van den Oord EJ3,4, Webb BT3,4, Amdur RL6, Bergen SE1,3, O'Neill FA7, Walsh D8, Riley BP1,2,3, Kendler KS1,2,3, Fanous AH2,3,5,6 Departments of 1Human and Molecular Genetics and 2Psychiatry, 3Virginia Institute for Psychiatric and Behavioral Genetics, and 4Center for Biomarker Research and Personalized Medicine, Virginia Commonwealth University, Richmond, VA, USA; 5Department of Psychiatry, Georgetown University School of Medicine, Washington DC; 6Mental Health Service Line, Washington VA Medical Center, Washington DC; 7Department of Psychiatry, Queens University, Belfast, UK; 8The Health Research Board, Dublin, Ireland. **Background:** Prior genomewide scans of schizophrenia support evidence of linkage to regions of chromosome 20. However, association analyses have yet to provide support for any etiologically relevant variants. Methods: We analyzed 2988 LD-tagging single nucleotide polymorphisms (SNPs) in 327 genes on chromosome 20, to test for association with schizophrenia in 270 Irish high-density families (ISHDSF, N=270 families, 1408 subjects). These SNPs were genotyped using an Illumina iSelect genotyping array which employs the Infinium assay. Given a previous report of novel linkage with chromosome 20p using latent classes of psychotic illness, association analysis was also conducted for each of five factor-derived scores based on the Operational Criteria Checklist for Psychotic Illness (delusions, hallucinations, mania, depression, and negative symptoms). Tests of association were conducted using the PDTPHASE and QPDTPHASE packages of UNPHASED. **Results**: While no single variant was significant after Bonferroni-correction, initial gene-dropping simulations identified loci which exceeded empirical significance criteria for minimum genewise P value or the truncated product of P values. In particular, TOX2 shows association with both intermediate and broad diagnoses of schizophrenia. Additionally, R3HDML and C20orf39 appear to be associated with depressive symptoms of schizophrenia**. Conclusions:** Preliminary results overall provide evidence that chromosome 20 may harbor schizophrenia susceptibility or modifier loci. Ongoing gene-dropping analyses aim to assess the empiric significance of these associations:

B-31 Tie1-Tie2 Interactions Mediate Functional Differences Between Angiopoietin Ligands

Tom C.M. Seegar, Becca Eller, Dorothea Tzvetkova-Robev, Momchil V. Kolev, Scott C. Henderson, Dimitar B. Nikolov, and William A. Barton
Biochemistry and Molecular Biology

The endothelial specific receptor tyrosine kinase Tie2, and the orphan receptor tyrosine kinase, Tie1, are essential for endothelial cell proliferation, migration, and survival during angiogenesis. Despite their considerable similarity, experiments with Tie1 or Tie2 deficient mice highlight distinct functions of these two receptors in vivo. Tie1, however, cooperates with Tie2 during Angiopoietin signaling, demonstrating a degree of functional overlap between the two receptor-systems. Tie2 is further unique among receptor tyrosine kinases with respect to its structurally homologous ligands. Angiopoietin-2 and -3 can function as agonists or antagonists depending upon the local environment, while Angiopoietin-1 and -4, are constitutive agonists. To address the role of Tie1 in Angiopoietin-mediated Tie2 signaling, and determine the basis for the unique behavior of the individual Angiopoietins, we used an in vivo FRET-based proximity assay to monitor Tie1 and Tie2 localization and association in the presence and absence of ligands. Here, we provide direct evidence for Tie1-Tie2 complex formation on the endothelial cell surface and identify molecular surface areas essential for receptor-receptor recognition. We further demonstrate that the Tie1-Tie2 interactions are dynamic, inhibitory, and differentially modulated by Angiopoietin-1 and -2, thereby providing a discrete molecular mechanism for the observed variations in Angiopoietin function. Based upon the available data, we propose a unified model for Angiopoietin-induced Tie2 signaling which highlights the essential role of Tie1 in vascular homeostasis.

B-32 Elucidating The Sources Of Enhanced Oxygen Consumption During Early Reperfusion Following Skeletal Muscle Ischemia In The Rat Spinotrapezius Muscle

William Nugent, Aleksander Golub, and Roland Pittman
Physiology and Biophysis

Prolonged skeletal muscle ischemia is disruptive to the mechanics of cellular respiration. Upon reperfusion, the metabolic rate of the affected tissue is altered in a fashion dependent on the duration and totality of ischemia and this can be used as an indicator of the changes the cellular metabolism has undergone. We have employed Phosphorescence Quenching Microscopy (PQM) in conjunction with a flow-arrest technique to assess the influences of external, pressure-induced 1 to 30 minute focal ischemic durations on the interstitial oxygenation (PO2) and the consumption of oxygen (VO2) in the spinotrapezius muscles of Sprague-Dawley rats. VO2 is assessed by the rate of PO2 decline during brief flow-arrest compressions during reperfusion. Our tests of this intermittent compression technique have indicated that 5 seconds of flow-arrest followed by 15 seconds of flow restoration allow for measurement of VO2 without compromising the baseline or reperfusion recovery of interstitial PO2. Our preliminary studies have confirmed that there is a spike in VO2 during early reperfusion whose magnitude is dependent on the duration of ischemia. This enhanced oxygen consumption, which we found to be ~7 times higher than baseline following a 30 minute ischemic insult, then returns to baseline levels with a exponential decay over the course of several minutes. Since oxygen deprivation is central to many of the problems associated with ischemia and reperfusion, it is important to describe how this increased VO2 relates to the tissue's post-ischemic metabolism in terms of changes in the electron transport chain, nitric oxide levels and reactive oxygen species production. It is our goal to systematically assess the changes in baseline PO2 and VO2 with chemical modification of mitochondrial function and interstitial nitric oxide levels during a range of ischemic durations, up to and including 30 minutes, to determine what processes are responsible for the elevated oxygen consumption during the first few minutes of reperfusion.

B-33 Roles Of Krüppel Like Factors Klf1, Klf2, And Klf4 In Embryonic Beta-Globin Gene Expression

Yousef Alhashem, Divya Vinjamur, Gabriel Eades, Joyce Lloyd
Human and Molecular Genetics

Krüppel like factors (KLFs) are a family of 17 proteins whose main function is gene regulation by binding to DNA elements in the promoters of various genes. KLF transcription factors recognize CACCC-elements and act as activators or repressors. Among the KLF proteins, KLF1, KLF2, and KLF4 share high homology. KLF1 is the founding member of the family and is an erythroid-specific transcription factor. KLF2 is expressed in erythroid, endothelial, and other cells. KLF4 is expressed in erythroid, endothelial, smooth muscle, and other cells. A mouse model lacking KLF1, KLF2, and KLF4 was used to investigate whether these genes have overlapping functions in regulating the embryonic β-globin genes during early embryogenesis. Quantitative RT-PCR assays were used to measure the expression level of Ey- and βh1- globin mRNA at embryonic day 9.5 (E9.5). It was found that KLF1-/-KLF2-/- and KLF1-/-KLF2-/-KLF4-/- embryos express significantly decreased amounts of Ey- and βh1-globin mRNAs when compared to those in WT and KLF4-/- embryos. There were no significant changes in the levels of Ey- and βh1-globin mRNAs between KLF1-/-KLF2-/- and KLF1-/-KLF2-/-KLF4-/- embryos. Preliminary data from other genotypes show that KLF1 might be the only KLF that affect the level of embryonic β-globin gene expression at E9.5. Further investigation is required to elucidate the mechanism of KLF1 function on the expression of the embryonic β-globin genes.

B-34 Single Neucleotide Polymorphism In The Pdxk Gene Coding For Pyridoxal Kinase: Studying Its Effect On The Protein Structure And Its Possible Implications In Human Health

Jigar V. Desai, Faik Musayev, Mohini Ghatge, Martin K. Safo
Medicinal Chemistry

Vitamin B6, in its active form, pyridoxal 5'-phosphate (PLP), is a very important co-factor for over 140 vitamin B6 (PLP-dependent) enzymes, serving vital roles in various transamination, decarboxylation, and synthesis pathways involving glucose and lipid metabolism, amino acid and homocysteine metabolism, heme and DNA/RNA synthesis, and neurotransmitter production. Pyridoxine 5'-phosphate oxidase (PNP oxidase) and pyridoxal kinase (PL kinase) are the two key vitamin B6 salvage enzymes involved in metabolizing inactive B6 vitamers (including pyridoxine, pyridoxal and pyridoxamine) into PLP. The deficiency of PLP is quite rare, but it is implicated in several neurological disorders, steroidal hormone related cancers, pancreatic cancer and neuropathy. Generally dietary insufficiency contributes very less to clinical deficiency. Genetic factors, especially pathogenic mutations in either PNP oxidase or PL kinase are mostly responsible for the deficiency, resulting in null or significant reduction in the enzymatic activity. We report the study of one such mutation in PL kinase, involving the replacement of Ser261 with Phe. The S261F mutant form was made on a cDNA coding for human PL kinase, which was cloned into the expression vector pET28a(+). Site-directed mutagenesis was undertaken using the QuickChange kit from Stratagene. Following, the mutant was expressed from the E. coli HMS 174 and purified using NiNTA column. Preliminary kinetic studies show the S261F mutant to be ~10% active compared to the wild type enzyme. This drastic reduction in activity may be responsible for PLP deficiency in about 1% population, as per the definition of single nucleotide polymorphism. Visual analysis of the wild-type crystal structure suggests that the mutation could lead to drastic tertiary conformational change. Crystallization attempts to elucidate the structure of the mutant have produced small but diffractible crystals to 3.5 Å in an orthorhombic cell with parameters of a=53 b=91, c= 109 Å. Our studies should help unravel the molecular basis for the reduced PL kinase catalytic activity due to the S261F mutation.

B-35 Crystal Structure Of E. Coli L-Threonine Aldolase (Eta): Evidentiary Support For Mechanism Of Reactions Catalyzed By The (E Ta) And Comparison With Other Plp-Dependent Enzymes

Soumya G. Remesh
Medicinal Chemistry

Purpose: To determine the crystal structure of E. coli L-threonine aldolase (L-TA) in the presence and absence of its product or substrate to understand the specificity and selectivity of the reaction catalyzed by the enzyme. The long-term goal is to elucidate the evolutionary relationships amongst vitamin B6-dependent enzymes. **Methods:** Crystallization: Pure protein obtained from our collaborators in University of Rome was used for crystallizing the protein in the absence or presence of Glycine. The native L-TA protein (22 mg/mL) was crystallized using 30% v/v PEG 400 with 0.2 M MgCl2 in 0.1 M HEPES buffer, pH 7.5 (Condition A). Co-crystallization of L-TA (22 mg/mL) with glycine (5 mM) was also attempted using 20% v/v 2-propanol, 20% w/v PEG 4000 in 0.1 M sodium citrate tribasic dehydrate pH 5.6 (Condition B). **Data Collection**: For diffraction data collection, the native L-TA crystals were cryoprotected in condition A, whereas the complex crystals were cryoprotected in a mixture of condition B (40 ul) and 100 % glycerin (5ul). The crystals were flash cooled in a nitrogen stream and diffraction data collected at 100K using a Molecular Structure Corporation (MSC) X-Stream Cryogenic Crystal Cooler, a Rigaku IV ++ image plate detector, and a Rigaku MicroMax-007 X-Ray source (copper) fitted with MSC Varimax Confocal optics operating at 40 kV and 20 mA. **Results:** Crystallization: Thin plate crystals of native L-TA were obtained in orthorhombic cell by hanging drop vapor diffusion method at room temperature with space group C2221, and cell dimensions a=76.82, b=101.45, c=176.85 Ao. L-TA in complex with glycine also gave thin plate crystals in monoclinic cell with space group P21, and cell parameters a=77.09, b=104.84, c=84.86 Ao; β=92.46 deg. **Structure Determination**: The crystal structures for the native and complex L-TA were determined using the WEB-based molecular replacement program, CASPR, and independently with Phenix. Refinements of the two structures are currently ongoing. Preliminary analysis of the L-TA complex structure with the already known crystal structures of the following PLP-dependent enzymes, Thermatoga maritime L-TA (TTA), E. coli serinehydroxymethyl tranferase (SHMT) and rabbit SHMT resulted in root mean square deviations of 0.9, 1.6, and 2.4 Ao, respectively.**Conclusion:** The tertiary structures of E.coli L-TA and TTA are very similar, but show significant differences from the SHMT structures. The active site structures also show some significant differences that could explain the differences in their catalytic function, especially between L-TA and SHMT. The detailed reaction specificity and selectivity will be better understood after completing the refinement of the structure.

B-36 Camk-Ii Mediates Non-Canonical Wnt-Dependent Morphogenic Events During Zebrafish Gastrulation

Jamie McLeod, Sarah C. Rothschild, Ludmila Francescatto, Alexandra Myers and Robert M. Tombes
Biology

Non-canonical Wnts have been shown to influence cell movements during gastrulation. In developing zebrafish embryos, elongation of the anterior-posterior body axis depends on convergent extension, a process that involves alterations in cell adhesion and polarized cell movements and is regulated by Wnt/Ca2+ signaling pathways. Zebrafish encode seven CaMK-II genes (camk2a, camk2b1, camk2b2, camk2d1, camk2d2, camk2g1 and camk2g2) each with specific expression patterns during development. Several of these CaMK-II genes are expressed during the first 12hpf; including camk2b1, camk2b2, camk2g1 and camk2g2. Morpholino antisense oligonucleotide knockdown of camk2b1 results in undulation of the notochord, while camk2g1 knockdown results in somite compression and abnormal tail curvature. These phenotypes are similar to the Wnt5 and Wnt11 morphants, respectively. Wnt5 and Wnt11 are core members of the non-canonical Wnt/PCP pathway and have been shown to regulate convergent extension. These results suggest an interaction between CaMK-II and the non-canonical Wnt pathway. In order to evaluate the role of camk2b1 and camk2g1 during early development, three different approaches were used. First, the actin cytoskeleton was visualized using Alexa488-Phalloidin and revealed that stereotypical cell shapes were reapportioned in camk2b1 and camk2g1 morphants. Second, in situ hybridization analysis of the notochord and somite markers ntl and myoD showed a truncated anterior-posterior body axis with compressed and distorted somites. These effects are not due to altered cell fate specification. Finally, injection of a dominant negative CaMK-II construct results in duplicated and shortened trunks. These results are consistent with a role for specific CaMK-II genes during convergent extension supporting their linkage with the non-canonical Wnt pathways. We propose that Wnt11 signaling acts on camk2g1 to affect the posterior region of the developing embryo including yolk plug closure, somite formation and separation, whereas Wnt5 may signal to camk2b1 to affect the more anterior portion of the developing body axis.

B-37 HIV Protease Inhibitors Activate The ER Stress Response And Disrupt The Lipid Metabolism In 3T3-L1 Adipocytes.

Beth S Pecora, Lixin Sun, Xudong Wu, Weibin Zha, Emily Gurley, Elaine Studer, Phillip B Hylemon, William M. Pandak, Luyong Zhang, Guangji Wang, Huiping Zhou.
Microbiology and Immunology

HIV protease inhibitor-induced lipodystrophic syndrome is a major side effect of current anti-HIV therapy. However, the underlying molecular mechanism remains unclear. We have recently shown that HIV PI-induced ER stress and activation of the unfolded protein response (UPR) represents an important cellular mechanism by which HIV PIs disrupt lipid metabolism and induce inflammation in hepatocytes and macrophages. The aim of this study was to determine if HIV PIs also induce ER stress, activate the UPR, and affect the lipid metabolism and differentiation in adipocytes. Methods: Mouse 3T3-L1 adipocytes were used in this study. The effect of individual HIV PI on differentiation and lipid accumulation was examined by Oil red O staining. Activation of the UPR was determined by real time RT-PCR and Western Blot analysis. The expression of adipokines/cytokines was determined by real-time PCR and ELISA. Results: Different HIV PIs had different effects on the UPR activation, cell differentiation, and lipid metabolism in adipocytes. Both lopinavir and ritonavir dosedependently activated the UPR, increased IL-6 expression, reduced adiponectin expression, and induced cell apoptosis. But amprenavir had less effect. Conclusions: HIV PI-induced ER stress response and activation of the UPR may represent a critical molecular mechanism underlying HIV PI-associated lipodystrophy and metabolic syndrome.

C-01 The Impact Of Lack Of Access To Health Care On Health Status

Allison A. Wellman
Epidemiology and Community Health

In light of current discussions concerning health care reform it was of interest to determine the extent to which poor health status is associated with lack of health care coverage. According to the Centers for Disease Control and Prevention, chronic disease is the leading cause of death in the U.S. and results in decreased quality of life and trillions of dollars per year in health care expenses. In 2007, 18.2% of Americans were uninsured for at least part of the year. Uninsured Americans are more likely to die during hospitalization, suffer premature death, fail to receive preventive services, lack a primary care physician, and often must pay more for medical services. Conflicting reports exist on the association between health insurance status and health outcomes. For this analysis, data from the 2007 Behavioral Risk Factor Surveillance System (BRFSS) health survey was used to evaluate this relationship. Adult participants were considered to lack access to health care if the respondent did not have any kind of health care coverage (including health insurance, HMO, or government plan such as Medicare) and "poor health" was classified as self-reported fair or poor health. Logistic regression analysis was performed using SAS to provide crude and adjusted estimates of the association between lack of access to health care and poor health. Of those surveyed, 15% reported lack of any type of heath care coverage, and 16% reported poor health. After adjusting for confounders (income, age, education, and employment status), those without access to health care were 24% more likely to have poor health than those who had access to health care. Poorer health and lack of access to health care was also seen to be more prevalent among adults of lower socioeconomic status and minorities. 32% of Hispanics and 20% of Blacks reported lack of access to care. This study suggests that lack of health care coverage may result in poor health. Improving the health of individuals will likely result from a combination of improving access to health care and preventive services, promoting and enabling healthy behaviors, and improving socioeconomic conditions.

C-02 Analysis Of Microrna Data

Andre Williams, MS Kellie Archer, PhD
Biostatistics

MicroRNAs (miRNA) are small single stranded RNA molecules, found in eukaryotes, responsible for the regulation of gene expression at the level of translation. Herein we describe analytical steps undertaken for processing Luminex MicroRNA (miRNA) data. This platform uses a bead-based technology where a random number of beads per miRNA are used to assess miRNA abundance. Background correction and normalization were found to be important procedures needed to remove technical variation from the data. Further, replicate hybridizations are an important means for assessing quality. Similar to other technologies, significance testing can be performed using standard hypothesis testing procedures with resulting p-values used for estimating the false discovery rates (FDR). Results comparing normal, cirrhotic, and hepatocellular carcinoma tissues will be presented.

C-03 Fabrication Of 3-D Nerve Guides Using Electrospinning For Nerve Reconstruction

Balendu Shekhar Jha, Raymond J. Colello and David G. Simpson
Anatomy and Neurobiology

We describe the structural and functional properties of 3D, "semi-solid" cylindrical nerve guide produced by air gap electrospinning of polycaprolactone (PCL) polymer. It is well documented that on 2D scaffolds, an aligned array of electrospun fibers provide the guidance cues such that the nerve fibers grow preferentially in the direction of orientation of these fibers. Air gap electrospinning makes it possible to produce three dimensional, macroscopic, cylindrical constructs composed of dense anisotropic arrays of nano-to-micron scale diameter fibers. These fibers are aligned in parallel with the long axis of the constructs; an architectural feature that provides thousands of individual channels to direct axon growth. We fabricated aligned scaffolds from PCL polymer at a concentration of 200 mg/mL using air gap electrospinning. In vitro experimentation demonstrates that axons of the rat dorsal root ganglion can penetrate in between the PCL fibers, and can be induced to align with the 3D arrays of these fibers which range from 400 to 1,500 nm in cross sectional diameter. We next used the electrospun PCL nerve guides (fibers nominally 1 micron in diameter) to reconstruct a 10 mm lesion in the rodent sciatic nerve. After 7 weeks, the implant retained its structure with minimal fibrosis. The proximal domains of the guides contained dense, parallel arrays of myelinated and non-myelinated axons and Schwann cells. In distal domains, the axons were bundled together in structures reminiscent of the perineurium. The density of the regenerating myelinated axons decreased as we moved from the proximal end of the implant towards the distal end. This decrease in the density was accompanied with the decrease of the size of the axons. There was no axon located outside the periphery of the nerve guide confirming the fact that the implanted nerve guide did provide directionality and guidance to the regenerating axons from the proximal stump towards the distal stump. Quantitative analysis of the number and size of the axons at various sites of the implant versus the number and size of axons in a normal rodent sciatic nerve will be used to predict the extent of nerve regeneration mediated by these electrospun 3D guides. Functional blood vessels were found to be scattered throughout the implant. We speculate that end organ targeting might be improved if axons can be directed to regenerate along specific tissue planes by a nerve guide composed of 3D fiber arrays.

C-04 Novel Cinnamic Acid-Based Dehydropolymers For Emphysema: Triple Inhibitors Of Elastase, Inflammation And Oxidation

B. Saluja1, J. Thakkar2, U.R. Desai2, M. Sakagami1
Pharmaceutics

Novel cinnamic acid-based dehydropolymers were assessed in vitro as triple inhibitors of neutrophil elastase (NE), lung inflammation and oxidation, and then tested for in vivo protective effects in a rat model of emphysema. Sulfated or unsulfated dehydropolymers of caffeic, ferulic or sinapic acid were synthesized and assessed in the chromogenic NE substrate hydrolysis assay, inflammatory transcription factor (NFkB) assessment in Calu-3 cells and chemical anti-oxidant assay in well-plate format. The most potent inhibitor was then administered to the lungs at 30 μg/kg in the elastase-induced rat model of emphysema, and its protective effects on the airway luminal neutrophilia and the airspace enlargement were determined from differential cell count of the bronchoalveolar lavage fluid (BALF) and mean linear intercept (MLI) of the alveolar airspace 48 h and 28th day post-elastase induction, respectively. All the dehydropolymers exhibited concentration-dependent inhibitory activities to NE hydrolysis, induced Calu-3 inflammatory NFkB activity and chemical oxidation in a range of 0.01-100 μM. Among them, the sulfated caffeic acid dehydropolymer, CDS, was shown to be the most potent, yielding the half-maximal inhibitory or anti-oxidative concentrations of 0.40□0.04, 10-15 and 3.51□0.18 μM, respectively. In the elastase-induced emphysema rats, CDS at 30 μg/kg was shown to protect from the 6.7- and 170-fold increased total and neutrophil cell counts in the BALF by 34.3□20.7 and 65.3□3.7 %, respectively. Moreover, the 1.4-fold airspace enlargement (MLI = 75.3□11.8 μm) in this emphysema model appeared to be confined by CDS, leaving the MLI value near normal at 55.2□5.6 μm. These data provided a strong support to the therapeutic potential of CDS for the use in emphysema treatment, specifically when administered to the lung.

C-05 Development Of A Second Generation, Canine Lyme Vaccine: Identification Of The Predominant Ospc Types Found In Canine Lyme Borreliosis

DeLacy V. LeBlanc, Christopher G. Earnhart, and Richard T. Marconi
Microbiology and Immunology

Lyme disease is the most common vector-borne disease in North America and Europe. In North America, Lyme disease is caused by the pathogenic spirochete Borrelia burgdorferi while in Europe and Asia the species Borrelia garinii and Borrelia afzelii are responsible for this infection. Lyme disease causes significant morbidity in canines, underscoring the importance for better understanding of borrelial infection in dogs and the need for a canine vaccine. In this study, ten dogs were infected with Borrelia burgdorferi though the bites of Ixodes scapularis ticks collected from the environment. Tissue biopsies from the infected canines were used to characterize Borrelia burgdorferi infection in dogs in order to allow for targeted vaccine development. A polyvalent, chimeric vaccine based on the borrelial protein outer surface protein C (OspC) is being developed in our lab. OspC is a critical virulence factor for the Lyme Borrelia and has been shown to be required for establishment of mammalian infection. While ospC is stable during infection, multiple antigentically distinct types exist within the Borrelia population, driving the need for a polyvalent vaccine. In order to determine the OspC types most commonly found during canine infection, DNA was extracted from tissue biopsies and ospC was amplified, cloned, sequenced and molecular phylogenetic analyses were performed. This information can be applied towards development of a Lyme disease vaccine for canines that would be broadly protective by incorporating the OspC types most commonly found during canine infection.

C-06 Acute Elevation Of Endocannabinoids Attenuates The Precipitated Opioid Withdrawal Syndrome

Divya Ramesh1, Scott T. O'Neal1, Jonathan Z. Long2, Benjamin F. Cravatt2 and Aron H. Lichtman1 1 Department of Pharmacology and Toxicology, 2The Skaggs Institute for Chemical Biology and Department of Chemical Physiology, The Scripps Research Institute, La Jolla, CA
Pharmacology and Toxicology

It has long been known that cannabis sativa and its primary active constituent, □9-tetrahydrocannbinol (THC), reduce opioid withdrawal symptoms. In the nervous system, THC produces its pharmacological actions predominantly on CB1 cannabinoid receptors. The endogenous cannabinoids, anandamide (AEA) and 2-arachidonyl glycerol (2-AG), also activate CB1 receptors, but they are rapidly metabolized by their respective enzymes, fatty acid amide hydrolase (FAAH) and monoacyl glycerol lipase (MAGL). Inhibiting these catabolic enzymes results in elevations of AEA and 2-AG and they produce far fewer pharmacological effects than THC. The recent development of selective inhibitors of FAAH and MAGL provides important pharmacological tools to investigate the role of endocannabinoids in modulating opioid dependence. The objective of this study was to determine whether elevating AEA or 2-AG, via inhibition of their respective metabolizing enzymes, would reduce precipitated morphine withdrawal symptoms. Male ICR mice were implanted subcutaneously with a morphine pellet, which is a well established model of opioid dependence. Mice were challenged 72 h later with the opioid receptor antagonist, naloxone, to precipitate withdrawal. The withdrawal signs included number of jumping incidences, number of paw tremors, number of head twitches, body weight loss during withdrawal and the occurrence of diarrhea. Pretreatment with the MAGL inhibitor JZL184 significantly reduced the intensity of all naloxone-precipitated withdrawal measures to a similar magnitude as THC treatment. These effects of JZL184 were reversed by the CB1 receptor antagonist rimonabant but not by the CB2 receptor antagonist SR144528, suggesting a CB1 receptor specific mechanism of action. The FAAH inhibitor PF-3845 reduced the intensity of jumps during opiate withdrawal through a CB1 receptor mechanism but did not affect other withdrawal signs. The results from the present study are the first to show that elevating endogenous cannabinoid levels ameliorate the expression of opioid withdrawal. Thus, the enzymes responsible for endocannabinoid degradation offer promising targets for possible new treatments for opioid dependence.

C-07 The Absence Of Synaptically Evoked Plateau Potentials In Dlgn Relay Cells Leads To A Failure In Retinogeniculate Refinement

Dilger, E.K., Morhardt, D. R., Shin, H. S. and Guido, W
Anatomy and Neurobiology

In developing relay cells of the dLGN, repetitive stimulation of the optic tract in a manner that mimics the temporal features of spontaneous retinal waves evokes long lasting, high amplitude depolarizations (plateau potentials) that are mediated by L-type calcium channels. The large Ca2+ influx generated by plateau activity could potentially initiate signaling cascades to activate the transcription of plasticity related genes and retinogeniculate remodeling. We sought to determine whether synaptically evoked plateau potentials in LGN relay cells are necessary for the refinement of the retinogeniculate connections. To address this, we examined retinal wave activity, the synaptic responses of relay cells, and the eye-specific patterning of retinogeniculate projections in a transgenic mouse that lacks the □3 subunit of the L-type Ca2+ channel. These mutants have far fewer membrane bound L-type Ca2+ channels and greatly attenuated L-type activity. In □3 nulls, L-type plateau potentials are rarely observed in the LGN, even at young ages and when repetitive pulses of optic tract stimulation are used. The few that do occur have different kinetics and seem to rely more on the NMDA receptor than L-type channel activation. In vitro multi-electrode array recordings of peripheral retina reveal pharmacologically normal stage II (cholinergic) and stage III (glutamatergic) spontaneous retinal waves in □3 null mice. However, the retinogeniculate projections of □3 null mice fail to segregate properly. In vitro thalamic slice recordings reveal that LGN relay cells in □3 nulls also show less functional pruning than wild type mice, and continue to receive as many as 8-10 inputs even as late as P21, a time when a wild-type relay cell might receive 1-2 inputs. Thus, these results suggest that postsynaptic L-type Ca2+ channel activity is necessary to implement the activity dependent refinement of the retinogeniculate pathway.

C-08 Functional Effects Of Fluorescent Hsert Ligands Validated By Homology-Based Docking Studies

Ernesto Solís, Jr., Igor Zdravkovic, Ian D. Tomlinson, Sergei Y. Noskov, and Louis J. De Felice
Physiology and Biophysics

We employ several techniques including fluorescence microscopy, electrophysiology, and molecular modeling to compare fluorescent analogs of 1-methyl-4-phenylpyridinium (MPP+). MPP+ is a known monoamine transporter substrate with high transport affinity. Adding an electron donating dimethyl amine group to the phenyl ring of MPP+ results in a fluorescent compound, called 4-(4-(dimethylamino) phenyl)-1-methylpyridinium (APP+). This study compares the functional effect of fluorescent MPP+ analogs on the human serotonin (5HT) transporter (hSERT). In previous studies, we took advantage of the fluorescent compound 4-(4-diethylaminostyryl)-N-methylpyridinium (ASP+) to study biophysical properties of the human norepinephrine transporter (hNET). While ASP+ was well-transported by both hNET and the human dopamine transporter, it was poorly transported by hSERT. Therefore, we synthesized APP+ as a novel fluorescent substrate for hSERT. APP+ fluorescence accumulation competes with 5HT, is inhibited by the hSERT inhibitor paroxetine, and is Na+ and Cl- dependent, suggesting APP+ is a substrate for hSERT. Recent experiments indicate ASP+ is not transported specifically by hSERT. ASP+ is still transported in parental cells and in hSERT-expressing cells pretreated with paroxetine. Interestingly, electrophysiology recordings of hSERT-expressing oocytes show that while APP+ induced an hSERT-mediated inward-current, ASP+ induced a small hSERT-mediated outward-current. To understand these opposing effects by similar compounds, we are using a homology model of hSERT based on the recently crystallized bacterial leucine transporter, and employ in silico rigid docking methods to determine how well the ligands dock within the active region of the hSERT model. The goal is to relate the structure of transporter ligands to their functional effect and interaction with hSERT.

C-09 Snon Regulates Transcriptional Activation Or Repression Of TGF-Beta Signaling By Preventing Recruitment Of CBP And HDAC1 In Esophageal Cancer Cells

Eugene Y. Kim, Anna V. Miller, Amy C. Ladd, Catherine I. Dumur, David C. Williams, and Deborah A. Lebman
Biochemistry and Molecular Biology

The development of esophageal cancer is associated with altered regulation of expression of the SnoN oncoprotein. It is well established that SnoN exerts its effects by binding to Smad proteins which are the major effectors of transforming growth factor-beta (TGF-b) signaling, but the extent to which deregulation of SnoN expression modulates responses to TGF-b remains unclear. Furthermore, it is not clear how SnoN can block both Smad-mediated transcriptional activation and repression in the context of different promoter elements in vivo. To address this, we analyzed the genetic and molecular responses to TGF-b in an esophageal cancer cell line in which TGF-b induces degradation of SnoN and in a derivative of this cell line engineered to express a form of SnoN that cannot be degraded in response to TGF-b. Deregulation of SnoN expression abrogated the majority of early gene responses associated with both TGF-b induced growth arrest and epithelial mesenchymal transition, including repression of c-myc and activation of both PAI and Slug, respectively. In addition, chromatin immunoprecipitation (ChIP) analysis of occupancy of Smad binding elements (SBE) or TGF-b inhibitory elements (TIE) in vivo indicated that while Smad3, Smad4, and SnoN occupied all the promoters that were tested, SnoN prevented CBP binding to SBEs within PAI and slug promoters. Furthermore, when SnoN was present, histone deacetylase 1 (HDAC1) could not bind the c-myc TIE. Thus, our results show that SnoN regulates both transcriptional activation and repression by interfering with recruitment of co-regulatory factors to Smad3-Smad4 complexes.

C-10 Entry Of Herpes Simplex Virus Requires Cholesterol In The Virion Envelope And Plasma Membrane Of Host Cells

Frances M. Saccoccio and Anthony V. Nicola
Microbiology and Immunology

Herpes simplex virus (HSV) is the most common cause of sporadic viral encephalitis. HSV is a large, enveloped, DNA virus that infects cells via different entry pathways in a cell type dependent manner. HSV enters epithelial cells via pH-dependent endocytosis. In contrast, neurons are infected in a pH-independent manner by fusion between the viral envelope and plasma membrane. Both of these pathways require the viral glycoproteins gB, gD, and gH-gL, and one of several known cellular receptors for gD. Cholesterol depletion of Vero cells, which support pH-independent fusion at the plasma membrane, was previously shown to inhibit HSV infection. Depletion of cholesterol from the virion envelope is also known to inhibit HSV entry into Vero cells. To better understand the mechanism of HSV entry, the plan is to define the precise step in viral entry that requires cholesterol. HSV entry into cholesterol-depleted Vero cells was blocked at a post-binding step. These data suggest that for entry into Vero cells, cholesterol is required for fusion between the viral envelope and the plasma membrane. HSV entry into cholesterol-depleted CHO-nectin-1 cells, which support pH-dependent endocytosis, was blocked at a post-binding step. These data suggest that HSV entry into CHO-nectin 1 cells requires cholesterol for endocytic uptake. When the viral envelope was depleted of cholesterol, HSV was unable to enter CHO-nectin 1 cells, suggesting that envelope cholesterol also plays a role in viral entry into these cells. Thus, plasma membrane cholesterol is required for HSV entry via both pH-dependent and pH-independent pathways at different steps in the entry pathway.

C-11 New Cellular Accumulation Pathway For Tri-Platinum Compounds Using Heparan Sulfate

Heveline Silva, John B. Mangrum, John J. Ryan and Nicholas P. Farrell
Chemistry

Cancer is a significant health problem, particularly due to drug resistance. Cisplatin is the most commonly used platinum compound in cancer chemotherapy. Cisplatin resistance is often attributed to reduced cellular accumulation, which allows for cancer recurrence. Triplatinum compounds have higher cytotoxicity than cisplatin and higher cellular accumulation, which is unusual given their high charge (+4, +6 and +8 for BBR3464, AH44 and AH78, respectively). We are examining the mechanism of cellular accumulation of charged platinum compounds. Based on analogy with the charged compound polyarginine, first deduced from X-ray crystallography with DNA, we have begun to examine the interactions with glycosaminoglycans (GAG) from the cell surface. These GAGs, such as heparan sulfate (HS) and chondroitin sulfate (CS), are known to mediate the binding of many charged ions to cels. Their internalization could allow for the uptake of interacting molecules. We used CHO cell variants lacking HS or HS and CS to investigate the influence of GAGs in the internalization of charged triplatinum compounds. A nona-arginine peptide labeled with TAMRA dye (TAMRA-R9) was used to measure cellular interactions altered by the presence of platinum compounds. Fluorescence microscopy images were obtained from CHO cells exposed to Hoescht 33342 (1.0 μM) and TAMRA-R9 (1.0 μM) for 1h, with or without triplatinum compound pre-treatment. Differences observed in microscopy assay were quantified by flow cytometry. We found that TAMRA- R9 entry into CHO cells was greatly reduced by the absence of HS and CS, demonstrating the importance of these GAGs in its cellular interaction. Triplatinum compounds, but not uncharged, mono-nuclear cisplatin, blocked TAMRA-R9 entry. These data indicate that triplatinum compounds can compete for GAG binding, demonstrating a novel mechanism of cellular entry for tri-nuclear versus mono-nuclear platinum chemotherapeutics. Our findings offer a potentially new avenue to overcome chemotherapy resistance in cancer.

C-12 Anaplasma Phagocytophilum Infects Murine Mast Cells In Vitro

I. Nore Ojogun, Bernice Huang, Daniel Miller, Brian Barnstein, John J. Ryan, and Jason A. Carlyon
Microbiology and Immunology

Anaplasma phagocytophilum is an ixodid tick-transmitted obligate intracellular bacterium that infects neutrophils to cause granulocytic anaplasmosis in humans, a variety of wild and domestic animals, and laboratory mice. Infection of human and murine neutrophils is dependent on bacterial recognition of sialylated glycans. Mast cells are present in connective tissue, where they play a sentinel role in immunological survery and host defense. Mast cells have been documented at the ixodid tick bite site; and neutrophil recruitment to sites of bacterial infection is partially dependent on mast cell derived cytokines and chemokines. We hypothesized that A. phagocytophilum initially infects mast cells following tick transmission and infected mast cells recruit naïve neutrophils. As a requisite first step towards addressing this question, we assessed bacterial binding and infection of murine bone marrow-derived mast cells (BMDMCs) in vitro. A. phagocytophilum bound with equal efficiencies to mock- and sialidase-treated BMDMCs, which indicates that the bacterium utilizes a novel non-sialylated receptor on mast cells. A. phagocytophilum effectively invaded BMDMCs and intracytoplasmic bacterial inclusions were visualized within BMDMCs at 72 h. However, the percentage of infected BMDMCs declined considerably throughout the time course. To determine if A. phagocytophilum survival within mast cells is impaired, we visualized the integrity of A. phagocytophilum organisms within BMDMCs by electron microscopy. Lastly, we assessed the profile of cytokines and chemokines elicited following by BMDMCs exposure to A. phagocytophilum. These data provide the first evidence that mast cells are susceptible to A. phagocytophilum infection and represent the foundation for further exploring the relevance of this phenomenon in vivo.

C-13 Platelet Function Is Impaired Immediately Following Resuscitation From Cardiac Arrest In A Swine Model

Jessica Brueckner, Nathan White MD, Erika J. Martin MT, Donald Brophy PharmD, Kevin Ward MD, Robert Diegelmann PhD
Departments of Emergency Medicine, Pharmacy, and Biochemistry

The presence of coagulopathy is associated with increased risk of multiple organ failure and death in patients successfully resuscitated from cardiac arrest. However, the coagulopathy produced is poorly understood. We examined coagulation during the post-cardiac arrest syndrome in order to better characterize its timing and function. Methods: Domestic swine (N=6) were subjected to electrically-induced cardiac arrest for 12 minutes and resuscitated using standard normothermic American Heart Association advanced cardiac life support. Coagulation function was measured by PT, PTT, and fibrinogen from plasma and Thrombelastography (TEG), platelet contractile force (PCF), and clot elastic modulus (CEM) from whole blood. Tests were compared at baseline prior to arrest, during arrest, and then serially during the post-resuscitation period. Results: PCF and CEM were significantly reduced by 15 minutes post-resuscitation ($p<0.04$). TEG displayed prolonged clot initiation times immediately after ROSC compared to the intra-arrest measurement ($p<0.03$). PT, PTT, fibrinogen, platelet counts were not abnormal and did not change significantly ($p>0.12$). Conclusion: Whole blood clotting function is significantly impaired immediately upon resuscitation from cardiac arrest. This coagulopathy may be primarily associated with altered platelet function.

C-14 Analysis Of The Diguanylate Cyclase Rrp1 And Its Role In Borrelia Burgdorferi Pathogenesis

Jessica L. Kostick, Elizabeth A. Rogers, & Richard T. Marconi
Microbiology and Immunology

Two-component systems (TCS) are a central component of gene regulation within Borrelia burgdorferi, the causative agent of Lyme disease. Upon activation by phosphorylation, Rrp1 produces cyclic diguanylate (c-di-GMP) via its diguanylate cyclase domain (GGDEF domain). C-di-GMP has been demonstrated to be a significant bacterial secondary messenger and is believed to play a role in the pathogenesis of bacteria including Vibrio, Escherichia, Salmonella, and Pseudomonas. However, the role of the Rrp1-Hpk1 TCS and c-di-GMP signaling in the pathogenesis of Borrelia remains relatively uncharacterized. Previous microarray studies of a non-pathogenic, Δrrp1 B31-5A13 strain confirmed that Rrp1 regulates the core Borrelia genome, including proteins involved in essential metabolic processes and virulence mechanisms. Therefore, the rrp1 deletion in a pathogenic strain is essential to further pursue analysis of infection efficacy, transmission between vector and host, and virulence mechanisms including host immune invasion after the loss of Rrp1. In this study, a Δrrp1 B. burgdorferi mutant and its rrp1 complement was constructed by allelic exchange mutagenesis in a B31-5A4 pathogenic strain and needle inoculated into mice. Murine infection by the Δrrp1-5A4 mutant and rrp1 complement was confirmed by qPCR and spirochete cultivation from infected tissues. In vitro growth analysis revealed delayed growth of the Δrrp1-5A4 strain at 27ºC, the approximate internal temperature of an Ixodes tick. This data suggests that Rrp1 and c-di-GMP may also have a critical role in tick spirochete acquisition. To assess the impact of Rrp1 overexpression on infection, an rrp1-pBSV2 plasmid was constructed and introduced into B31-5A4 B. burgdorferi. Further examination of these pathogenic Δrrp1, rrp1 complement, and overexpressing strains will not only provide invaluable incite concerning the involvement of Rrp1 and c-di-GMP in B. burgdorferi infection and transmission but also enhance the overall understanding of c-di-GMP signaling in bacteria in general.

C-15 Diffuse Axonal Injury Within The Optic Nerve Following Fluid Percussion Brain Injury: A New Approach For The Comprehensive Evaluation Of Diffuse Axonal Injury

Jiaqiong Wang John E. Greer Susan A. Walker John T. Povlishock
Anatomy and Neurobiology

Diffuse axonal injury (DAI) impairs axonal transport and demonstrates progressive axonal swelling and delayed disconnection. However, to date, the full spectrum of DAI associated changes is incompletely understood, due to the fact that majority of previous studies were conducted in highly dispersed and heterogeneous fiber systems where it was difficult to consistently follow axonal changes with a high degree of fidelity, particularly once disconnection occurred and triggered anterograde and retrograde changes. To overcome these challenges, we carried out the study of traumatic axonal injury in the highly organized visual system, using YFP-16 transgenic mice which express a yellow spectral variant of green fluorescent protein (GFP) in the cytosol of retinal ganglia cells and their axonal projections. In the YFP-16 transgenic mouse TBI model, scattered axonal changes can be recognized within discrete loci of the optic nerve following TBI, and progressive axonal change can be evaluated in both the rostral and caudal axonal segments, providing unprecedented insight into the anterograde and retrograde responses to injury. Following the postinjury, delayed axonal disconnection, rostral and distal axonal swellings develop with the numbers of rostral axonal swellings increasing in the initial period following injury, and then decreasing overtime post TBI. In contrast, the caudal axonal swellings continue to increase overtime post TBI. The colocalization of YFP fluorescence with β-amyloid precursor protein (APP) immunofluorescence suggests that APP, which is commonly used to detect both human and animal DAI, is localized only to the proximal axonal segments, which regresses over time. Thus, the APP most likely provides only an incomplete picture of the total progression of DAI. Parallel EM studies confirmed and extended these LM observations. The incorporation of YFP-16 transgenic mice with this TBI model provides new insight into the pathogenesis and progression of DAI, suggesting a potentially unique platform for assessing downstream deafferentation in the visual system, and the subsequent evaluation of neuroplastic reorganization. Lastly, the discrete and consistent localization of the optic nerve injury provides a ready template for rapid therapeutic screening.

C-16 Interaction And Function Of Sphingosine-1-Phosphate And Prohibitin-2 In Mitochondria

Graham M. Strub, Jie Liang, Melanie Paillard, Ludovic Gomez, Nitai C. Hait, Qun Chen, Edward J. Lesnefsky, Sheldon Milstien, Sarah Spiegel
Departments of Biochemistry and Molecular Biology and Medicine, Division of Cardiology

Sphingosine-1-phosphate (S1P) is a potent lipid mediator that regulates diverse physiological and pathological processes acting through five specific cell surface receptors. The majority of research to date has focused on the activation of these receptors, but there is now evidence to suggest that S1P also exerts intracellular functions independent of its receptors. We have now identified prohibitin-2 (PHB2), a transcriptional repressor and mitochondrial chaperone protein, as a novel intracellular S1P binding protein by pull down assays with S1P agarose beads and mass spectrometry. Recent studies identified large assemblies of PHB2 with its homologue PHB1 in the inner membrane of mitochondria which were suggested to be the physiologically active structures that control the functional integrity of mitochondria. We found that sphingosine kinase 2 (SphK2), one of the isoenzymes that forms S1P, was also present in the mitochondria. However, S1P interacted with PHB2 in the mitochondria independently of PHB1. Moreover, the presence of SphK2 was critical for the formation of the complex between cytochrome oxidase subunit IV (COX IV) and PHB2. Depletion of SphK2 in Hela cells resulted in a decrease of oxidative phosphorylation (OXPHOS) with complex I, II and IV substrates. Isolated heart mitochondria from SphK2 knockout mice also displayed reduced OXPHOS activity. These results point to novel actions of intracellular S1P in the mitochondria and provide new insights into the functions of S1P-PHB2-COX IV association in the mitochondria to regulate energy production and mitochondrial oxidant production.

C-17 A Transgenic Approach To The Study Of The Consequences Of Diffuse Axonal Injury

Greer JE, McGinn MJ, Povlishock JT
Anatomy and Neurobiology

Much is known concerning the initiating cascades as well as secondary events related to DAI, yet little is known about the chronic fate of neurons sustaining DAI. Traditional immunohistochemical methods have failed to identify this injured population at late time points. To circumvent these challenges we have utilized a transgenic mouse strain (YFP-H) which expresses fluorescent protein in restricted neuronal populations. Adult mice (25g-30g) were subjected to cFPI and the brain tissue was analyzed with routine fluorescent and confocal microscopy. Through this approach, we noted that scattered axonal projections from lamina V neurons revealed a repertoire of axonal change. Early post injury these axons revealed focal swellings that proceeded to disconnection and dieback, a phenomenon readily identified in the YFP positive fibers. With increasing survival (2d) the YFP positive swellings were no longer observed, yet following image deconvolution the proximal dilated axonal stumps could be identified and subsequently followed. Over time (3d post injury) many of these proximal axonal segments manifested projections, reminiscent of reactive sprouting following injury. In some cases, these axons progressed beyond reactive sprouting, now revealing long proximal axons capped by torpedo shaped swellings, morphologically similar to growth cones. In summary, these observations demonstrate the utility of this transgenic approach in studying the consequences of DAI and, importantly, highlight the potential for regenerative attempts following DAI. Conceivably, studies utilizing this approach will allow for the characterization and manipulation of these regenerative responses.

C-18 Tgf-Beta Suppresses Mast Cell Function In Vivo And In Vitro

Fernando Josephine and Ryan
Biology

Mast cell activation is a critical component of allergic disease, and may be regulated by cytokines present in the microenvironment. We recently described the suppressive effects of TGF-β1 on IgE signaling in mouse and human mast cells. We have furthered this study, demonstrating that TGF–β1 injection or aerosolization reduces mast cell IgE receptor expression in vivo, and suppresses eosinophil recruitment in a model of airway hyperresponsiveness. We find that TGF-β1 inhibits expression of the key signaling molecules Akt, Fyn, and Stat5 employed by the IgE receptor. In contrast, expression or activation of ERK, JNK, GSK and p38 was unaffected. Our data supports the theory that TGF-β1 possesses potent mast cell suppressive activities both in vitro and in vivo.

C-19 An Organotypic Hippocampal Slice Culture Model Of Acquired Seizures

J.M. Ziobro, D.S. Carter, R.E. Blair, L.S. Deshpande, R.J. DeLorenzo
Neurology

Acquired epilepsy (AE) is one of the most common neurological disorders with significant impacts on quality of life. Neuronal insults can induce plasticity changes that lead to AE during the latent period after injury known as epileptogenesis. To more efficiently study the plasticity changes that occur during epileptogenesis, we have developed a model of spontaneous seizures in organotypic hippocampal slice cultures (OHSCs). OHSCs represent an advantageous model to study AE because they maintain neuronal morphology, cellular and anatomical relations, and network connections. To induce plasticity changes, we utilized two separate types of injury. The first injury model involved treatment with 4-aminopyridine (4-AP), while the second injury model induced a stroke-like injury via treatment with 3.5mM glutamate. In both models, long term changes were observed with field potential recordings as a significant number of slice cultures in both treatment groups developed seizure-like activity. In addition, we used propidium iodide (PI) staining to examine cell death in these OHSCs. In both treatment groups, PI staining revealed a significant increase in cell death acutely after injury compared to control slices, however, there was no significant difference at later time points, indicating that there was not additional cell death after the initial injury phase. These data indicate that the initial injury phase is responsible for most of the cell death that occurs, while the surviving, but injured cells remain and undergo the plasticity changes responsible for epileptogenensis. The establishment of this model will allow for future studies to explore the underlying molecular mechanisms and changes that occur during epileptogenensis in an in-tact tissue culture model.

C-20 Identification Of A Novel Mitochondrial Isoform Of DNA Methyltransferase 1

Lisa Sale Shock, Prashant V. Thakkar, Erica J. Peterson, Shirley M. Taylor
Microbiology and Immunology

Methylation of mammalian nuclear DNA occurs in the context of a CpG dinucleotide, and exhibits both specific and dynamic patterns surrounding the promoter regions of key regulatory genes. Aberrant DNA methylation patterns are among the hallmark features of tumor cells, and dysregulation of the most abundant DNA methyltransferase (DNMT1) is at least partly to blame. Methylation of mitochondrial DNA (mtDNA) has also been reported, and features of mtDNA methylation, including a general underrepresentation of CpG dinucleotides and nonrandom CpG methylation, strongly resemble nuclear DNA. Our lab has recently identified a novel isoform of DNMT1 (mtDNMT1) that translocates to the mitochondria by way of a mitochondrial leader peptide. This peptide is conserved across several species for which the full DNMT1 sequence is known. Its presence in the mitochondrial compartment, coupled with evidence of CpG methylation of mtDNA suggests the involvement of DNMT1 in methylating, and potentially regulating, the mitochondrial genome. We hypothesize that mtDNMT1 binds and methylates mtDNA, and that its methylation activity plays a regulatory role in mitochondrial gene expression, replication of mtDNA, and/or the structure of mtDNA. We have generated a tumor cell line in which a tandem affinity purification (TAP) tag has been inserted at the C-terminal end of a single DNMT1 endogenous allele by homologous recombination. The TAP-tagged DNMT1 cell line is a novel tool that will allow us to isolate mtDNMT1 from the mitochondria, so we might begin to understand its function.

C-21 Tissue Oxygenation During Experimental Arterial Gas Embolism Using Intravital Microscopy

Luciana Torres, PhD1,2, Ivo Torres Filho, MD,PhD2,3 and Bruce Spiess, MD1,3
Anesthesiology

Arterial gas embolism (AGE) is clinically important since it can cause ischemia in the tissue in which the air bubbles are trapped, leading to hypoxia and ultimately cell death. Microvascular responses to AGE and local O2 tensions (PO2) have never been evaluated in vivo using intravital microscopy. Perfluorocarbons (PFC) have been advocated as a potential treatment of AGE. We studied the unique O2 delivery properties of PFC emulsion in the ability to salvage injured tissue. We developed a methodology to image and study AGE and PFC action in real time in the microcirculation of living rodents. Cremaster muscle of anesthetized rats was exposed for microscopy. To study bubble reabsorption and tissue oxygenation due to a transitory (mild) AGE, we injected 15 to 60 μL of air into the cremaster arteriolar network. To study severe AGE, we injected 1 mL/kg of air, followed by a treatment with PFC. Intravital videomicroscopy allowed geometric, hemodynamic and PO2 measurements in vivo on the muscle. Repeated microvascular assessments included: bubble reabsorption time, luminal diameter, red blood cell velocity, blood flow, and tissue PO2. In the mild AGE, tissue PO2 decreased following AGE but certain areas, supplied by vessels that later became occluded, did not become fully hypoxic since O2 was supplied by nearby microvessels with blood (or plasma) flow. The in vivo reabsorption time of bubbles about 15 pL in volume was 30 s. Severe AGE induced pronounced muscle ischemia (no blood flow on most studied sites). Tissue PO2 dropped from 18 ± 5 mmHg to 5 ± 3 mmHg in 5 min after air bubble lodging in the arteriolar network. Significant vasoconstriction (30% of control values) was observed in the arterioles after bubble lodging. After PFC injection, arteriolar blood flow increased to 11 ± 1 nL/s while arteriolar and tissue PO2 increased to 31 ± 8 and 17 ± 4 mmHg (compared to 2 ± 1 and 5 ± 3 mmHg during AGE), respectively. Administration of PFC after severe AGE improved tissue oxygenation by providing additional O2 supply in the affected tissue and possibly decreasing bubble dwell time and inflammation

C-22 Sphingosine-1-Phosphate Accelerates The Development Of Functionally Mature Chymase-Expressing Human Mast Cells

Price MM, Kapitonov D, Allegood J, Milstien S, Oskeritzian CA, and Spiegel S.
Biochemistry and Molecular Biology

Developed from bone marrow-derived progenitors, mast cells (MCs) are tissue-resident cells that function as key players in inflammation. MCs circulate in the blood as immature precursors where they likely encounter the serum-borne bioactive metabolite sphingosine-1-phosphate (S1P) during migration to target tissues. MCs developed from cord blood-derived progenitors cultured with stem cell factor (SCF) alone express intragranular tryptase. We found that S1P accelerated the development of cord blood-derived MCs and surprisingly increased the numbers of MCs expressing chymase in addition to tryptase. These MCs have functional FcepsilonRI receptors, and similar to other functionally mature MCs that express both tryptase and chymase, also express CD88 and are activated by anaphylatoxin C5a and the secretagogue compound 48/80. S1P induced release of IL-6, a cytokine known to promote development of functionally mature MCs, from cord blood cultures containing adherent macrophages, and from highly purified macrophages, but not from macrophage-depleted CB-MCs. In contrast, S1P stimulated secretion of the chemokine monocyte chemoattractant protein 1 (MCP-1/CCL2) from macrophage-depleted CB-MCs. These results suggest crucial roles for S1P in regulating development of human MCs and their functions and reveal a complex interplay between macrophages and MC progenitors in the development of mature human MCs.

C-23 Electrochemical Profiling Of The Ascorbic Acid Redox System During Cardiac Arrest

Melissa Rich, Nathan White, Maryanne Collinson, Kevin Ward
Emergency Medicine and Chemistry

Ascorbic Acid (AA) system is an important blood antioxidant system that is linked to red blood cell metabolism. The AA system acts to quench damaging free radicals that have been implicated in ischemia-reperfusion injury but remains poorly understood during critical illness. The goal of this study is to profile the AA redox system during severe global ischemia-reperfusion injury induced by cardiac arrest. Immature domestic swine were subjected to 12 minutes of cardiac arrest with standard cpr and post-resuscitation care. Markers of metabolism including glucose, pH, oxygen content, lactate, and base excess were monitored by blood gas analysis. The behavior of the AA redox system in whole blood was monitored by electrochemical open circuit potential and cyclic voltammetry using a 3-electrode system in order to develop an electrochemical profile of the AA system during each phase of injury. A total of 7 swine were subjected to cardiac arrest of which 2 were successfully resuscitated. AA open circuit potential (overall redox balance), oxidation current voltage (oxidation state) and amplitude (AA concentration) were not different at baseline, during cardiac arrest, or after resuscitation ($p>0.10$) However, the voltage difference between the major AA oxidation and blood reduction peaks increased significantly during the cardiac arrest period ($p=0.041$) and recovered with resuscitation. AA oxidation voltage also correlated negatively with glucose concentration ($r=-0.4$, $p=0.039$). Cardiac arrest and resuscitation are associated with changing AA blood redox profiles that may indicate altered antioxidant activity linked to cellular glucose metabolism

C-24 The Impact Of Low Consumption Of Vegetables And Fruits On Incidence Of Overweight And Obesity In Adults

Dr. Monica R. Gaidhane
Epidemiology and Community Health

Introduction: Obesity is considered to be an epidemic in US with over 66% adults being overweight or obese. It's associated with increased risk of hypertension, diabetes, cardiovascular diseases, certain cancers, shorter life expectancy and is one of the most important medical problems in the United States. Studies have shown that diets high in vegetables and fruits can help lower chronic disease risk and aid in weight management. USDA recommends 5 to 9 servings of fruits & vegetables per day **Objective:** To quantify the effect of Low Consumption of Vegetables & Fruits on Increased incidence of Overweight & Obesity in Adults **Methods:** A cross sectional study was done on 351358 participants over the age of 18. The participants were obtained from the 2007 Behavioral Risk Factor Surveillance System, a population-based list-assisted random-digit-dialed telephone survey of the noninstitutionalized U.S. adults. **Main Determinant measures:** The participants were classified into two groups of Less than 5 or More than 5 servings of vegetables and fruits per day based on their consumption. **Main Outcome Measures**: Based on their BMI, the participants were classified into two groups of Overweight / Obese or Underweight/ Normal weight. A BMI over 25 was classified as Overweight or Obese. **Results:** Using logistic regression, it was observed that people who consumed less than 5 servings of fruits and vegetables per day were 1.28 times more likely to be overweight or obese (Crude odds ratio [OR] = 1.28, 95% confidence interval [CI] = 1.26-1.29). 64% of the participants were overweight or obese and only 25% of the entire sample consumed more than 5 servings of vegetables and fruits. Females were less likely to be overweight or obese and more likely to consume more than 5 servings of vegetables and fruits per. **Conclusion:** This study suggests that consumption of less than 5 servings of vegetables and fruits may have a small impact on the rising incidence of Overweight or obese people. Income levels, education status, gender, exercise, other lifestyle factors and dietary factors can affect the relationship between consumption of vegetables and fruits and BMI. Prospective studies or interventional trials are needed to see the direct impact of low or high intake of vegetables and fruits on incidence and prevalence of overweight/obese people.

C-25 Zeta Potential Measurements For Contact-Antimicrobial Coatings

Murari L. Gupta*, Kennard Brunson*, Asima Chakravorty*, Julio C. Alvarez**, Fernando Luna-Vera**, ThuTrang T. Nguyen** and Kenneth J. Wynne*
Chemical and Life Science Engineering

Co-polyoxetane telechelics based on tetra alkyl ammonium functionality have shown contact-antimicrobial behavior. In order to investigate the relationship of accessible quaternary surface charge density to biocidal efficiency of these contact-antimicrobial coatings based on polyurethanes modified with quaternary surface charge, streaming potential measurements were performed. A conventional base polyurethane HMDI-BD(50)-PTMO(1000) and a P[AB] ran-copolyoxetane soft block polyurethane were chosen for this study. Co-polyoxetane telechelics are represented as P[AB], where A and B are repeat units with differing side chains and were used as polymer surface modifier (PSM). The A repeat has a trifluoroethoxymethyl side chain [CF3CH2O-CH2-] and the B repeat has a C12 quaternary side chain [(CH3)2(C12H25)N-(CH2)4-]. Micro-fluidic capillary channels were fabricated by imbedding a fused-silica capillary between polypropylene flat sheets. Streaming potentials were then measured by sodium bromide solution (1mM/L) as bulk-electrolyte at a neutral pH. Accessible surface charge density was calculated using Gouy equation.

C-26 Activated Neutrophils Enhance Vascular Reactivity To Angiotensin II Via Rhoa Kinase Activation By Reactive Oxygen Species

Nikita Mishra, MBBS Scott W. Walsh, PhD
Physiology and Biophysics

Women with preeclampsia have enhanced vascular reactivity to Angiotensin II (AngII), but the reason for this is not known. Recently, extensive systemic vascular infiltration of activated neutrophils was reported in women with preeclampsia. Activated neutrophils release toxic substances, such as reactive oxygen species (ROS). We hypothesized that neutrophil release of ROS would enhance vessel reactivity to AngII. **Methods:** Resistance arteries (200-500m) were isolated from omental fat biopsies obtained from normal pregnant patients undergoing C-sections (n=20). Endothelium was denuded by passing a fine metal wire through the lumen. Vessels were mounted on a DMT myograph and maintained at constant pressure at 37C in Dulbecco's-PBS with continuous slow flow of D-PBS through the vessel lumen. A video camera connected to an online imaging system was used to record real time changes in the arterial outer wall diameter every 10s. Data were recorded for 10 min at each dose of AngII. Each experimental treatment was preceded by addition of 40mM KCl to confirm vessel viability. Compressed air was used to aerate the vessels. AngII dose response (10-9M to 10-5M) was followed by repeat AngII dose response with activated neutrophils (ANC < 2000; 10-8M IL-8) perfused through the vessel lumen and repeated with addition of SOD (150U/ml)/Catalase (5000U/ml) or a specific Rho kinase inhibitor Y-27632 (3μM). Control experiments were performed with perfusion using IL-8 alone. AngII dose response was also tested with ROS alone (hypoxanthine, 0.36mM + xanthine oxidase, 0.004IU/ml), then ROS with SOD (150U/ml)/Catalase (5000U/ml) or Y-27632 (3μM). Statistical analysis was done using one-way ANOVA and Newman-Keuls. **Results:** AII caused a dose response contraction. Maximum response at 10-6M was (-18.6±2.03m, mean±S.E). In the presence of activated neutrophils (-44.5±5.93m, $p<0.001$) and ROS (-39.5±6.4m, $p<0.001$), the vasoconstrictive response to AII was significantly greater. SOD/Catalase and Y-27632 significantly blocked the enhanced response to AII by activated neutrophils ($p<0.05$) and ROS ($p<0.01$). **Conclusion**: These new data are the first to show that ROS production by activated neutrophils enhance vascular reactivity to a vasoconstrictor via RhoA/Rho kinase mediated calcium sensitization in vascular smooth muscle. This is probably an important mechanism for the development of hypertension in preeclampsia.

C-27 Sphingosine Kinase 2 And S1P In The Nucleus Regulate Histone Acetylation By Inhibition Of Histone Deacetylases

Nitai C. Hait, Jeremy Allegood, Michael Maceyka, Graham M. Strub, Kuzhuvelil B. Harikumar, Tomasz Kordula, Sheldon Milstien, and Sarah Spiegel
Biochemistry and Molecular Biology

The pleiotropic lipid mediator, sphingosine-1-phosphate (S1P), can act intracellularly independently of its cell surface receptors, yet its targets have not been identified. In this work we have shown that sphingosine kinase 2 (SphK2), one of the isoenzymes that generates S1P, is associated with nucleosomal histone H3 and produces S1P that regulates histone acetylation. S1P specifically binds to the histone deacetylases HDAC1 and HDAC2 and inhibits their enzymatic activity preventing the removal of acetyl groups from lysine residues within histone tails. When S1P is added to isolated nuclei or SphK2 is overexpressed, increased acetylation occurs at the same histone lysines. SphK2 associates with HDAC1/2 in repressor complexes and is selectively enriched at the p21 and c-fos promoters, where it enhances local histone H3 acetylation and transcription. Thus, HDACs are direct intracellular targets of S1P, the first identified endogenous small molecule regulator of these enzymes, linking nuclear S1P to remodeling of chromatin and epigenetic regulation of gene expression.

C-28 Adenovirus-5 Infection Induces Hepatic Lipid Synthesis And Hypertriglyceridemia In C57bl/6 Mice

W. Palmer Wilkins III, Rachael Griffiths, Jin-Woo Choi, Richard L. Atkinson, Philip B. Hylemon, Gregorio Gil, and Suzanne E. Barbour
Biochemistry and Molecular Biology

A growing body of literature implicates viral infections in dyslipidemia, fatty liver disease, and obesity. Both wild type and replication-deficient adenovirus-5 have been linked to changes in lipid metabolism. Upon intravenous administration, adenovirus-5 exhibits significant tropism to the liver, a major regulator of systemic lipid metabolism. These observations prompted the hypothesis that adenovirus-5 might augment hepatic lipid synthesis. We demonstrate that first generation adenovirus-5 vectors induce expression of SREBP1 and its target genes in HepG2 cells, rat primary hepatocytes, and livers of C57BL/6 mice. Adenovirus-5 infected mice exhibit increased liver triglyceride and hypertriglcyeridemia, but no changes in SREBP2 expression or plasma cholesterol. These observations are reminiscent of the effects of insulin, another selective inducer of SREBP1. Like insulin, adenovirus-5 activates the PI3K/Akt pathway in cultured hepatocytes and infected livers. PI3K inhibitors suppress induction of SREBP1 in adenovirus-5-infected cultured cells and mouse livers and also suppress adenovirus-5-induced hypertriglyceridemia in C57BL/6 mice. These studies support the emerging concept of virus-induced dyslipidemia and suggest that like hepatitis C, adenovirus-5 infection could be associated with fatty liver disease. Our observations also prompt caution concerning the use of replication-deficient adenovirus-5 to study lipid metabolism in the liver.

C-29 Regulation Of Platelet-Activating Factor Acetylhydrolase By Oxidized Phospholipids

Rachael Griffiths, Minkyeong Son, Muralikrishna Mukkamala, Norbert Leitinger and Suzanne E. Barbour
Biochemistry and Molecular Biology

Objective: Platelet-activating factor acetylhydrolase (PAFAH), the lipoprotein-associated phospholipase A2 (LpPLA2), is elevated in atherosclerosis and has been implicated in the pathogenesis of disease. However, the mechanisms regulating PAFAH expression in atherosclerosis remain unknown. We hypothesize that PAFAH is induced by oxidized phospholipids (oxPL) on mildly oxidized low density lipoprotein (oxLDL) particles in the early atheroma. Methods and Results: PAFAH expression was quantified in THP1 monocytes treated with oxidized 1-palmitoyl-2-arachidonyl-sn-glycero-3-phosphocholine (oxPAPC). OxPAPC increased PAFAH expression and this induction was mediated by long-chain oxPL (LC-oxPAPC) binding to prostaglandin receptors. LC-oxPAPC induced IL-6 and this cytokine was required for optimal PAFAH induction. Together, these data suggested a novel mechanism for PAFAH induction in early atheromas. To determine if oxPL could induce PAFAH under conditions that mimic those in developing atheromas, primary macrophages (Mφ) and dendritic cells (DC) were treated with mildly oxidized LDL, as a source of oxPL. Remarkably, mildly oxLDL significantly induced PAFAH in DC but had no effect on PAFAH in Mφ. Conclusions: These data indicate that oxLDL-activated DC are the source of the high PAFAH levels that characterize atherosclerosis. This study is the first to provide a mechanism for increased PAFAH expression in atherosclerosis.

C-30 Morphologically Distinct Classes Of Relay Neurons Reside In Different Regions Of The Mouse Dorsal Lateral Geniculate Nucleus (Dlgn)

Rana N. Eldanaf, Thomas E. Krahe, Emily K. Dilger, Tania A. Seabrook, And W. Guido
Anatomy and Neurobiology

The mammal visual system consists of parallel pathways designed to analyze aspects of the visual scene. Retinal ganglion cells in the mouse are also comprised of separate channels that have distinct molecular, morphological, and functional features, as well as unique patterns of connectivity. While some of these channels exhibit distinct central projections, it remains unclear whether they are recapitulated onto recipient cells in central target structures. To address this, we used in vitro recordings in thalamic slices and 3-D reconstructions of biocytin filled dLGN relay cells to determine whether classes of thalamic relay cells exist and whether they reside in distinct regions. We examined a number of morphological features and the intrinsic membrane properties of 61 relay cells between postnatal day (P) 2-40. The only distinguishing feature was dendritic architecture. Scholl ring and polar plot analyses revealed that as early as P2 relay cells could be classified into 3 groups (X-, Y-, and W-like). X-like cells had dendrites that radiate in a bi-conical manner. Y-like cells had spherically oriented dendritic trees and W-like cells had dendrites oriented in a hemi-spherical fashion. These morphologically defined cell types appeared to cluster into distinct regions of dLGN. X-like cells were found primarily in the ventral monocular region, and were innervated exclusively by crossed retinal projections. Y-like cells were found to be concentrated in the binocular region, positioned primarily where uncrossed retinal projections terminate. These cells also had dendritic trees that routinely crossed eye specific borders and received binocular input at late postnatal ages. W-like cells were located in an outer shell close to boundaries of dLGN and received input from crossed retinal projections. In contrast to the regional specificity of relay cells, interneurons were distributed throughout the entire nucleus. Whether different morphological types of interneurons exist remains an open question. While it remains unclear whether functionally divergent pathways are present in dLGN, the regional specificity of morphologically distinct subsets of relay cells supports the notion that the mouse visual system, like other higher mammals possess separate channels.

C-31 Prostate Cancer Screening: Addressing Racial And Ethnic Disparities

Sameer Arora
Epidemiology and Community Health

Background: Prostate cancer is the most common cancer diagnosed among men in the U.S. According to the American Cancer Society, an estimated 186,320 men in the U.S. will be diagnosed with prostate cancer in 2008. The incidence rate of prostate cancer is highest for black men, and intermediate for whites, followed by others.PSA screening becomes more relevant for the Afro-American population as they have higher risk and mortality for prostate cancer as compared to other racial groups. **Objective:** The purpose of this study was to quantify the effect of race on the prevalence of self-reported Prostate cancer screening. **Methods:** Cross sectional study of 2006, BRFSS Survey analysis involving 96,991 Males aged 40 years and above who responded to the 2006 Behavioral risk factor Surveillance system (BRFSS). **Main Outcome Measure**: Self-reported Prostate cancer Screening using (Prostate-Specific Antigen) PSA test as indicated on questionnaire for 2006 BRFSS survey. **Results:** Men from Afro-American racial background accounted for approximately eight percent of population screened for prostate cancer. After adjusting for access to a personal physician, PSA Screening rates were found to be higher for Black population (Adjusted OR=1.37{1.30, 1.45}) whereas Hispanic (Adjusted OR=0.80{0.76, 0.84}) and other racial groups (Adjusted OR=0.56{0.53, 0.60}) had a lower PSA screening rate as compared to white. **Conclusions:** Lower educational level, lack of job, health care coverage and access to a personal physician may be directly related to PSA screening rates. Afro-American men are being more screened despite a higher incidence rate probably due to higher awareness and counseling.

C-32 Regulation And Role Of YKL-40, A Novel Molecule, During Astrocyte Differentiation: Implications For Reactive Gliosis And Glioma Invasiveness

Sandeep K Singh, Katarzyna Wilczynska, Lauren Bryan, Catherine Dumur, and Tomasz Kordula
Biochemistry and Molecular Biology

Despite the current therapeutics, the average survival time of Glioblastoma multiforme (GBM) patients is 10-12 months, mainly due to infiltrative nature of GBM cells. GBM cells can be regarded as cells that escaped the astrocyte differentiation program. We have found that the expression of YKL-40, a novel secretory molecule, is activated during the invitro differentiation of astrocytes from neural progenitors (NPs). In primary human astrocytes, the expression of YKL-40 is regulated by the transcription factors NFI-X3 (Nuclear factor I-X3, a splice isoform of NFI-X) and STAT3 which both are critical for gliogenesis. Over-expression of NFI-X3 in GBM cells dramatically activates YKL-40 expression, which is responsible for increased invitro migration and invasion of GBM cells. Moreover, exogenous YKL-40 increased invitro migration of primary human astrocytes. Notably, astrocytes become reactive, proliferate and migrate to the injury site during brain pathological states. Accordingly, the major neuro-inflammatory cytokines IL-1, IL-6 and OSM stimulated the expression of YKL-40 in primary astrocytes. Moreover, NFkB, STAT, and AP-1 elements within the YKL-40 promoter modulate the response to IL-1 and IL-6/OSM. In conclusion, YKL-40, a novel secretory molecule that controls glial cell migration, is regulated by the gliogenic transcription factors. It is also activated by the pro-inflammatory cytokines during reactive astrogliosis. We propose that these mechanisms controlling YKL-40 expression in the normal cells are constitutively active in GBMs, and contribute to its elevated levels and consequent invasive phenotype of GBM cells.

C-33 Regulation Of Vascular Smooth Muscle Contraction

Silvina M. Alvarez, Ph.D., Amy S. Miner and Paul H. Ratz, Ph.D.
Pediatrics, Biochemistry and Molecular Biology

RhoA kinase (ROCK) participates in K+-depolarization (KCl)-induced Ca2+ sensitization of contraction. Whether constitutive, depolarization-activated, or Ca2+-activated ROCK plays the major role in this system remains to be determined. This study was designed to determine whether Bay k 8644 (Bay), a dihydropyridine that promotes Ca2+ channel clusters to operate in a persistent Ca2+ influx mode, can cause ROCK-dependent Ca2+ sensitization. Renal artery rings from New Zealand White rabbits were activated with Bay and tension was continuously measured. Tissues were frozen at 5, 15 and 60 min or at the steady-state of contraction and processed to measure active RhoA, ROCK substrate (myosin phosphatase targeting subunit, MYPT1) and myosin light chain (MLC) phosphorylation (MLCp), or loaded with fura-2 to measure [Ca2+]i. Effects of selective contraction inhibitors were assessed in resting (basal) tissues and those contracted with Bay. Bay increased [Ca2+]i, MLCp and tension, but not MYPT1 phosphorylation. ROCK inhibition by H-1152 reduced basal MYPT1-pT853 and MLCp and the Bay-induced increases in MLCp and tension but not [Ca2+]i. H-1152 had no effect on MYPT1-pT696, but staurosporine inhibited basal MYPT1-pT853, MYPT1-pT696 and MLCp. Active RhoA was increased only at 5 min by Bay even though contraction was maintained for 60 min. Pretreatment with the iPLA2□-specific inhibitor BEL inhibited Bay-induced contraction. These data suggest that constitutive activities of ROCK and a staurosporine-sensitive kinase regulate basal phosphorylation of MYPT1, which in-turn participates with iPLA2, Ca2+ entry and activation of MLCK in producing a Bay-induced contraction. Additional studies are required to determine whether the transient increase of active RhoA is necessary for tension maintenance

C-34 Delineation Of The Critical Region For Brachydactyly-Mental Retardation Syndrome By Array Comparative Hybridization: New Candidate Genes For Sleep Disturbance And Albright's Hereditary Osteodystrophy-Like Phenotypes

Stephen Williams, Santhosh Girirajan, Helga Toriello, Ellen Magenis, David Tegay, Eli Hatchwell, Norma Nowak, and Sarah Elsea
Human and Molecular Genetics

Brachydactyly-mental retardation syndrome or Albright hereditary osteodystrophy-like syndrome, associated with a deletion of chromosome 2q37, is characterized by craniofacial abnormalities, mental retardation, stereotypies, aggressive/self-injurious behaviors, distinct short fingers and toes, short stature, obesity, and eczema. Previous reports have primarily described large deletions, thus compromising the identification of causative genes. Here we describe two subjects identified in an aCGH screen of patients referred for molecular evaluation of Smith-Magenis syndrome (SMS) but who have no 17p11.2 deletion or mutation of RAI1. Both subjects, Case 1 (1.2 Mb deletion) and Case 2 (3.0 Mb deletion), have overlapping deletions and present with the classic phenotype, including mental retardation, brachydactyly, behavioral problems, developmental delays, and self-injury. Interestingly, Case 2 also presents with sleep disturbance, while Case 1 has normal sleep and melatonin secretion. The Case 2 deletion includes the circadian clock gene PERIOD 2 (PER2), which is a critical player in normal circadian processes, while Case 1 is not deleted for PER2. Given the overlap in deletion, we have been able to refine the critical region for this syndrome to ~1.2 Mb, including HDAC4, NDUFA10, and OTOS. We propose that haploinsufficiency of HDAC4 (histone deacetylase 4) is the vital contributor to the del2q37 syndrome, therefore providing a candidate gene for further evaluation in subjects who present with the AHO-like brachydactyly-mental retardation syndrome phenotype but for whom no deletion can be identified.

C-35 Intensity Exercise On Reducing Coronary Artery Disease Among Smokers

Susan Cha
Epidemiology and Community Health

Background: Cardiovascular diseases, such as coronary artery disease (CAD), are the leading causes of death in the United States; in fact, more than 2,600 Americans die every day because of some form of cardiovascular disease. Tobacco smoking is strongly associated with the increased risk for myocardial infarctions and CAD whereas other studies have indicated protective effects of exercise on people from developing CAD. This study evaluates whether good behavioral lifestyle choices such as engaging in moderate intensity exercise moderates the biological effects of smoking in adults. Although many studies have examined the effects of exercise in adults with cardiovascular disease or in healthy individuals, few have demonstrated the effects of exercise among smokers and how it can reverse the negative consequences of smoking. **Objectives:** It is of interest to determine whether moderate intensity exercise reduces the prevalence of CAD among smokers. **Methods:** Data was used from the 2007 Behavioral Risk Factor Surveillance System (BRFSS) results provided by the Center of Disease Control and Prevention (CDC). BRFSS provides surveillance data on health practices and risk behaviors related to diseases among the adult population (aged 18 and older) obtained through a phone survey. This cross-sectional study used data from a random sample of 51,802 eligible adult smokers. **Results:** Separate logistic regression models provided adjusted estimates of the association between moderate physical activity and prevalence of CAD. In 2007, adult smokers who had moderate intensity exercise were 22% less likely to report CAD than smokers with little or no moderate intensity exercise. **Conclusions:** Moderate intensity exercise was associated with a lower prevalence of CAD among adult smokers. A longitudinal cohort study that studies the effects of exercise on incidence of CAD may be appropriate.

C-36 Coordinated Innervation Of Retinogeniculate And Corticogeniculate Porjections In The Dlgn Of The Mouse

T. A. Seabrook, T. E. Krahe, E. K. Dilger, D. R. Morhardt, W. Guido
Anatomy and Neurobiology

Circuit development in the dorsal lateral geniculate nucleus (dLGN) of the mouse has focused on the remodeling of retinogeniculate connections. The bulk of synapses in dLGN are nonretinal in origin, and little is known about how and when these inputs develop. Here we compared the timing and pattern of innervation of retinal projections with those from two nonretinal sources; intrinsic interneurons in dLGN and corticothalamic (CT) cells in layer VI of cortex. At postnatal day (P) 0-1, crossed retinal projections have already formed a dense plexus of terminations throughout dLGN, the intrageniculate leaflet and ventral geniculate nucleus (vLGN). Uncrossed retinal projections begin to innervate geniculate nuclei at P1 and by P3 they form a large rudimentary patch in dLGN. Between P3-10 uncrossed projections recede and eye specific modules emerge. Slice recordings reveal that at early postnatal ages, retinal axons form excitatory synaptic connections with both relay cells and interneurons. Feed-forward inhibitory connections between intrinsic interneurons and relay cells begin to appear between P7-9 but the full complement of inhibitory responses does not fully develop until P14-16. To examine CT projections we made use of the golli-τ-GFP transgenic mouse, which labels cortical layer VI cells (Jacobs et al., 2007). At P2, CT fibers reside at the medial border and by P4 begin to innervate dLGN in a medial to lateral direction. At P10-12 CT fibers reach the lateral boundaries of dLGN and continue to arborize thereafter. To determine when functional CT synapses develop, we used a slice preparation that allows for the separate access of retinogeniculate and CT fibers. Functional CT synapses were not present during the first postnatal week at a time when retinogeniculate responses were routinely recorded. However, at P14 robust postsynaptic CT responses could be evoked. They exhibited paired pulse facilitation and were of sufficient amplitude to activate plateau-like depolarizations. In sum, these results suggest that retinal and nonretinal innervation of dLGN proceeds in a coordinated fashion. Retinal projections are the first to arrive and form functional connections. The innervation and formation of nonretinal connections is delayed and does not fully emerge until the remodeling of retinal connections occurs.

C-37 Cannabinoid Receptor Interacting Protein (Crip1a) Attenuates Constitutive Cb1 Receptor Signaling And Cb1 Downregulation

Tricia H. Smith, Maurice R. Elphick, Deborah L. Lewis, Ching-Kang Jason Chen, Dana E. Selley
Pharmacology and Toxicology

Cannabinoid Receptor Interacting Protein (CRIP1a) interacts with the C-terminal tail of the CB1 receptor (Niehaus et. al., 2007). To examine the effects of CRIP1a on CB1 receptor function, HEK cells stably transfected with CB1 (hCB1-HEK) were compared to cells with a stable co-transfection of CRIP1a (hCB-HEK-CRIP1a). Stoichiometric analysis revealed an under-expression of CRIP1a relative to CB1 receptors in hCB1-HEK cells and a CRIP1a to CB1 receptor molar excess in hCB1-HEK-CRIP1a cells. In [35S]GTPγS binding studies, a measure of CB1 receptor mediated G protein activation, CRIP1a expression lowered Emax values for the agonist WIN 55,212-2 (WIN), but not methanandamide (MethA). The inverse agonism by SR141716A (SR1) was reduced by CRIP1a, indicating a reduction of CB1 receptor constitutive activity by CRIP1a. hCB1-HEK cells (± CRIP1a co-transfection) were pre-incubated with WIN, Δ9-tetrahyrdocannabinol (THC) or vehicle for 4 hours, followed by MethA-stimulated [35S]GTPγS binding to assess receptor desensitization or [3H]SR-141716A binding to assess changes in receptor number. In hCB1-HEK cells, both WIN and THC caused CB1 receptor desensitization that was unaffected by CRIP1a. Both ligands produced downregulation of the CB1 receptor, which CRIP1a attenuated in the presence of WIN but not THC. In conclusion, CRIP1a attenuates constitutive CB1 receptor signaling and decreases CB1 downregulation for the full agonist WIN, but not the partial agonist THC.

C-38 Specific Recruitment Of RNA Pol II By NFI-X3 Induces GFAP Expression In Glial Cells

Sandeep K Singh, Katarzyna Wilczynska, Adrian Grzybowski, Lauren Bryan, Tomasz Kordula
Biochemistry and Molecular Biology

NFI-X knockout mice show severe brain malformations, including agenesis of corpus callosum and hydrocephalus, suggesting that NFI-X is critical for normal brain development. However, the identities of target genes as well as NFI-X splice isoforms expressed in the nervous system are elusive. We cloned a novel human splice isoform NFI-X3, and subsequently characterized its expression and function in primary astrocytes and differentiating neural progenitors. Interestingly, a unique proline rich transcriptional activation domain of NFI-X3 strongly transactivated several astrocyte-specific genes, including GFAP and SPARCL1. Conversly, a specific knockdown of NFI-X3 strongly diminished target gene expression in astrocytes. The relative abundance of NFI-X3 in glioma cells is dramatically lower than in primary human astrocytes. Moreover, NFI-X3 expression is significantly increased during astrocyte maturation, suggesting its critical role during gliogenesis. Activation of glial-specific genes includes demethylation of their promoters and subsequent increase in histone tail acetylation. However, NFI-X3 activates GFAP expression without affecting either promoter methylation or histone tail acetylation. Nevertheless, NFI-X3 significantly increased the recruitment of Pol II and transcription-coupled trimethylation of K4 of histone H3. In conclusion, these novel data unravel a major role of NFI-X3 in regulating astrocytes differentiation, including expression of the astrocyte-specific genes such as GFAP.

C-39 Molecular Pathogenesis Of Wolfram Syndrome Different In Different Causal Genes

Sami S. Amr , Rita Shiang
Human and Molecular Genetics

Wolfram Syndrome (WFS) is a debilitating autosomal recessive neurodegenerative disorder characterized by juvenile onset insulin dependent diabetes mellitus (DM) and optic atrophy (OA) as well as a number of neurological and endocrine complications that result in early death. Previous research has mapped Wolfram syndrome to chromosome 4p16.1 and the disease has been attributed to mutations the WFS1 gene affecting the WFS1 protein (wolframin), an ER membrane glycoprotein that plays a role in intracellular Ca2+ homeostasis. Several studies of WFS1 mutant or knockdown cells revealed increased levels of the unfolded protein response (UPR) markers, increased apoptosis, and decreased proliferation. Furthermore, other research shows an upregulation of WFS1 upon activation of UPR elements. An additional locus for WFS on chromosome 4q22-24 was identified by linkage studies of 4 Jordanian Bedouin families with 16 affected individuals. We identified the responsible gene in the critical region as CISD2, a gene encoding an ER intermembrane small protein (ERIS) with a conserved iron-sulfur binding CDGSH domain. Using the pSUPER RNAi system (oligoengine) to knockdown CISD2, in-vitro models were created in two cell lines; rat pancreatic insulinoma cells (INS1) and mouse neuroblastoma cells (N1E-115). Spliced XBP-1, a marker of the UPR, was not upregulated in CISD2 knockdown cells and CISD2 mutant lymphoblastoid cells taken from a WFS affected individual. Another marker, phosphorylated-eIF2α, also did not show upregulation in the affected lymphoblastoid cells. CISD2 expression in wildtype cells treated with the ER stressor thapsigargin did not change compared with untreated controls. These data suggest that, unlike WFS1, CISD2 does not play a role in the UPR and mutant CISD2 results in WFS in a manner different than that in mutant WFS1.